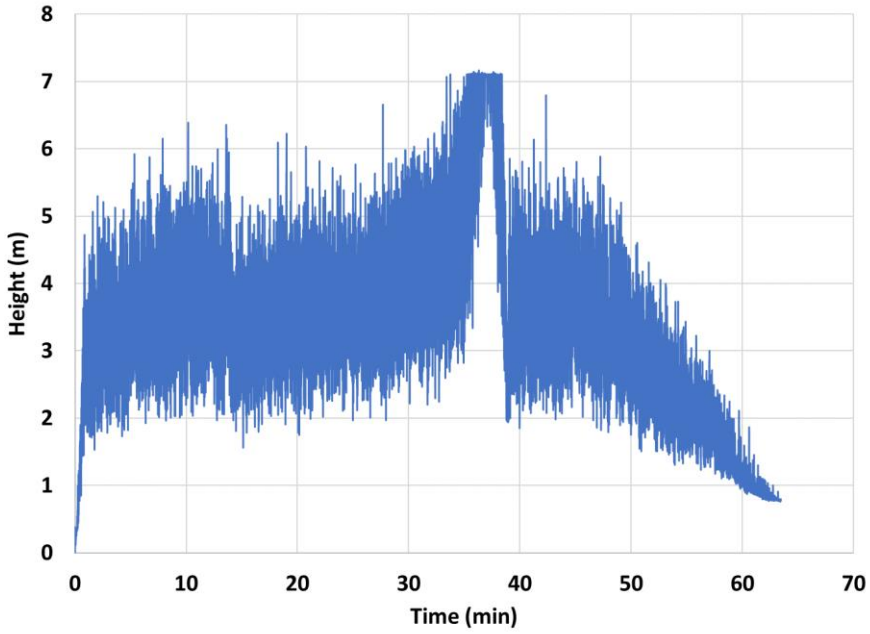

Figure 6-159: Flame height from IR camera measurements (Test 3.2).

6.3.3. Test 3.3

For this test, there was no calorimeter and the Dilbit was maintained at a supply temperature of 20 ± 5°C. The Dilbit fuel was supplied and maintained at a constant fuel level of about 30 mm (1.2 inches) for approximately 30 minutes. After 30 minutes, the Dilbit fuel supply was terminated and Jet-A fuel was introduced for about 7 minutes.

6.3.3.1. Fuel Supply Temperature

Figure 6-160 shows fuel supply temperature over time. The temperature averaged over 0-30 minutes is 17.6 ±0.1°C.

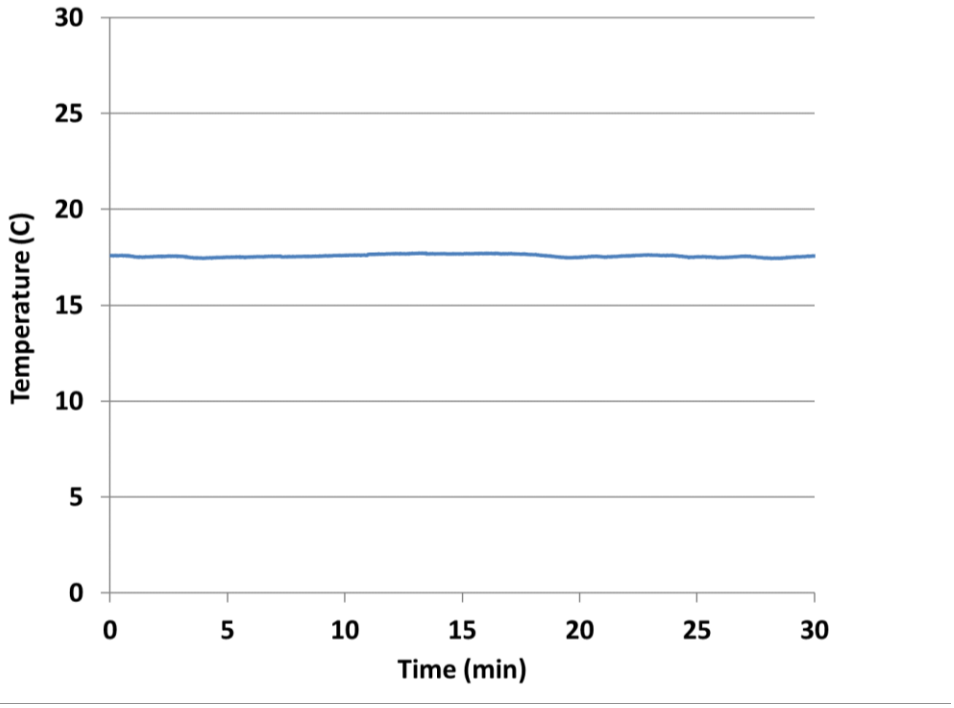

Figure 6-160: Temperature of fuel supply into pan (Test 3.3).

6.3.3.2. Fuel Rake Thermocouple Temperatures

Figure 6-161 shows temperatures from TCs within the liquid fuel. The fuel level at approximately 30 mm (1.2") is indicated at TC16. For this test the pan was filled to this level prior to ignition. At around 9 minutes all thermocouples rapidly increased by about 200°C indicating that heat from the flame was transferred throughout the pool. Thermocouples at locations TC3, TC10, and TC28 indicated faulty readings so are not included in the figure.

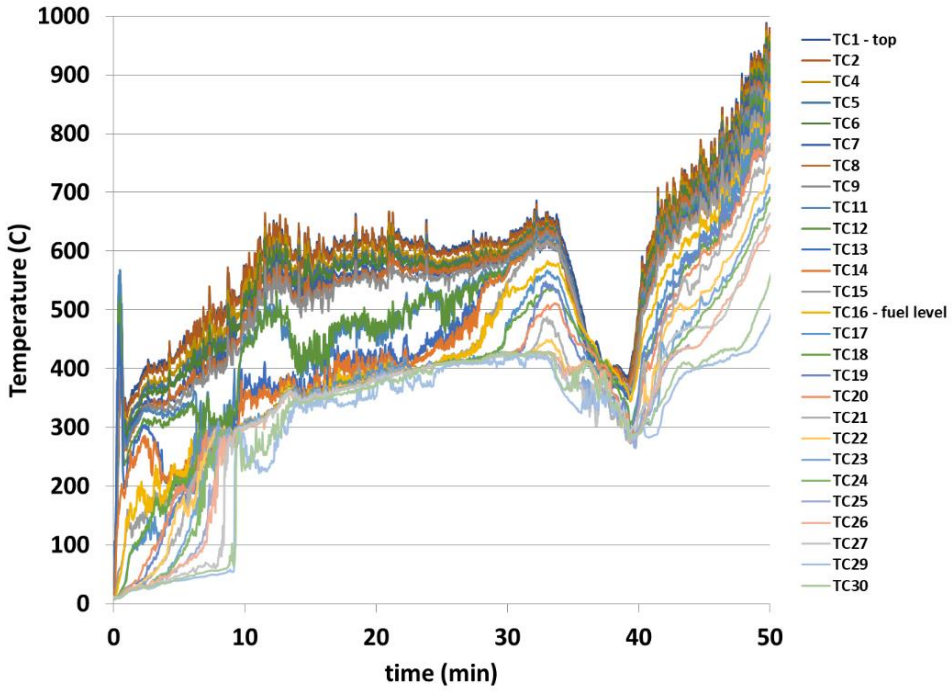

Figure 6-161: Fuel rake thermocouple temperatures (Test 3.3).

6.3.3.3. Burn Rate

The burn rate is determined by identifying a period in which the differential pressure gauge reading is nearly constant and determining the slope of the change in weight of the fuel tank during that period. Two periods were identified in which the dP gauge was nearly constant, namely, from 8.5 to 10 minutes and 16.8 to 18.5 minutes provided the longest duration over which the dP gauge was constant (Figure 6-162 and Figure 6-163, respectively). The slope of the curve over 8.5 to 10 minutes is 3.23 kg/min (r^2 = 99%) which corresponds to a mass flux of 0.017 kg/m^{2}s. The slope of the curve over 16.8 to 18.5 minutes is 2.73 kg/min (r^2 = 99%) which corresponds to a mass flux of 0.014 kg/m^{2}s. The different values for the two periods indicate that the average burn rate changed during the test. After about 20 minutes the dP gauge failed, so the burn rate at later times could not be evaluated. The weight of the post-test residue in the pan was 32.9 kg (72.3 lbs).

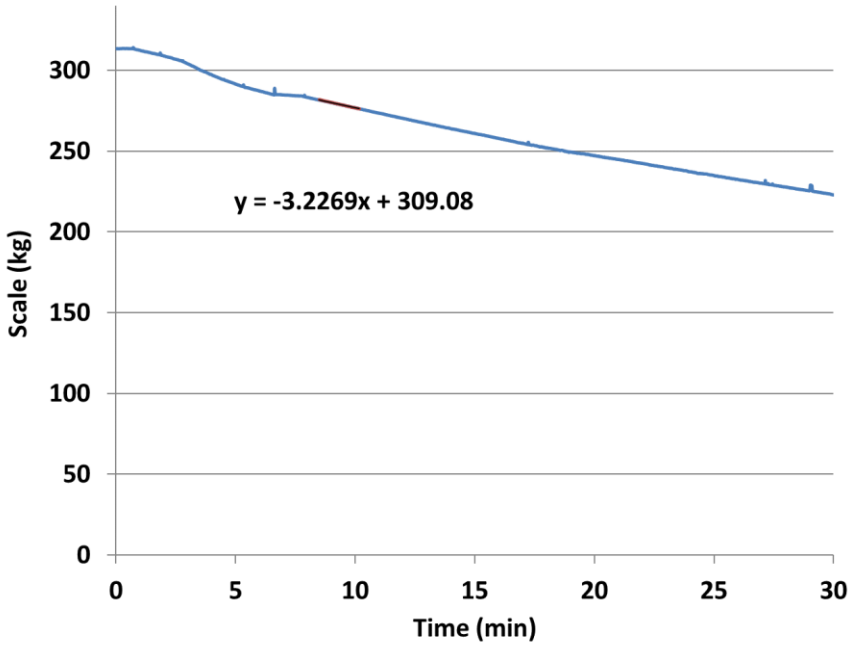

Figure 6-162: Fuel weight over time based on scale measurement (8.5 to 10 minutes) (Test 3.3).

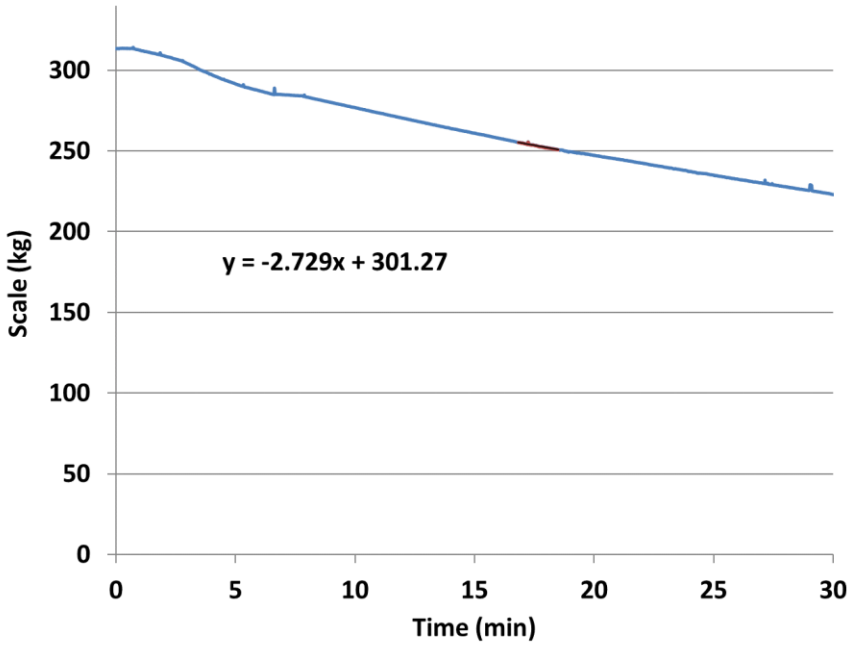

Figure 6-163: Fuel weight over time based on scale measurement (16.8 to 18.5 minutes) (Test 3.3).

6.3.3.4. Radiometers

Figure 6-164 and Figure 6-165 provide the heat flux over time from six narrow-angle and five wide-angle radiometers at the various height locations. The readings decrease until reaching about 10 minutes then are somewhat constant until about 25 minutes. The increase at about 35 minutes is from the introduction of the Jet-A fuel.

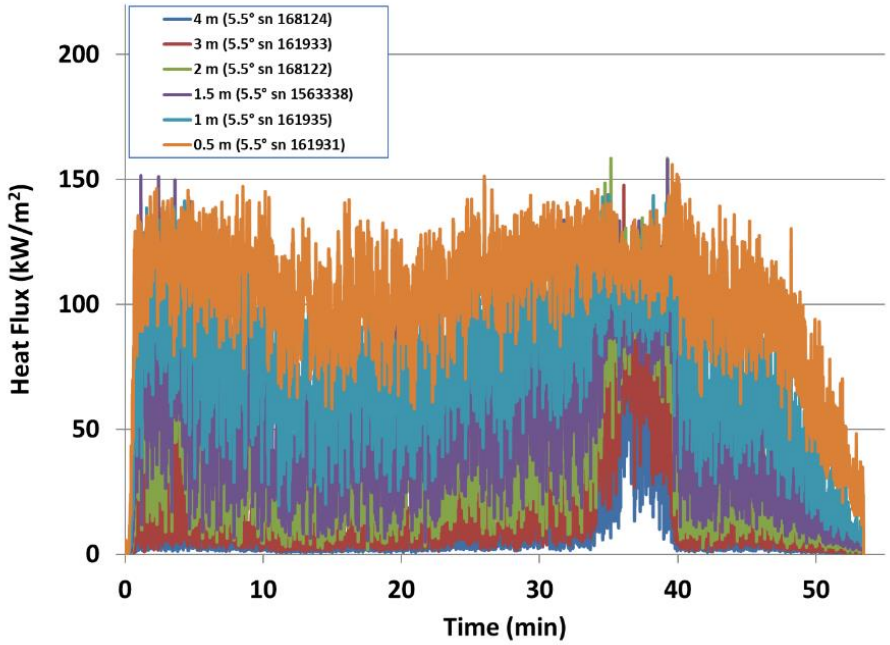

Figure 6-164: Heat flux measurement from narrow view radiometers at different heights (Test 3.3).

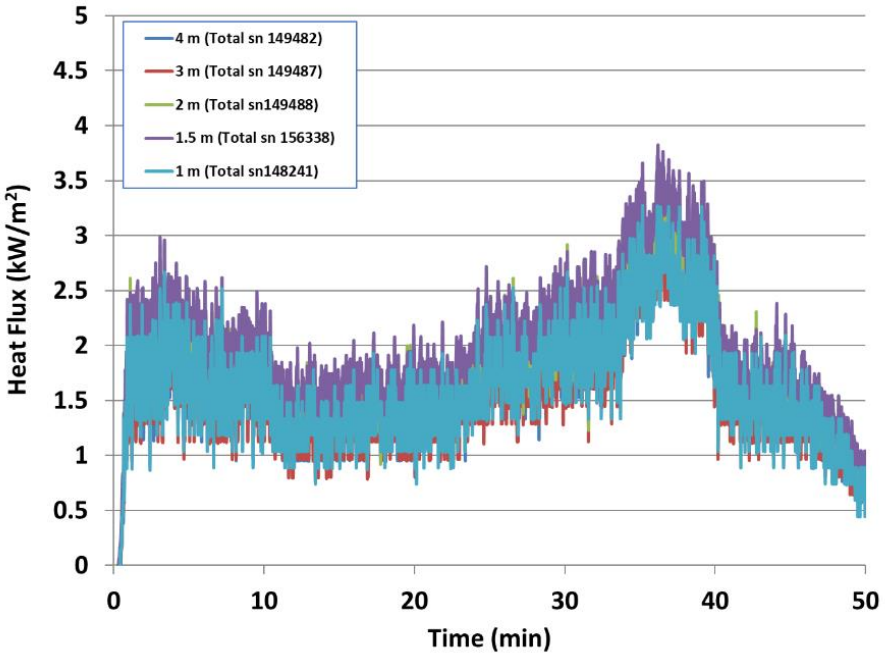

Figure 6-165: Heat flux measurement from wide view radiometers at different heights (Test 3.3).

6.3.3.5. Thermocouple Rake in Fire Plume

Figure 6-166 provides temperature measurements over time from the TCs placed within the fire plume at its vertical centerline. The thermocouple at the location of 0.5 m above the pan was removed since the calorimeter was not present and its stand was used to suspend the thermocouple.

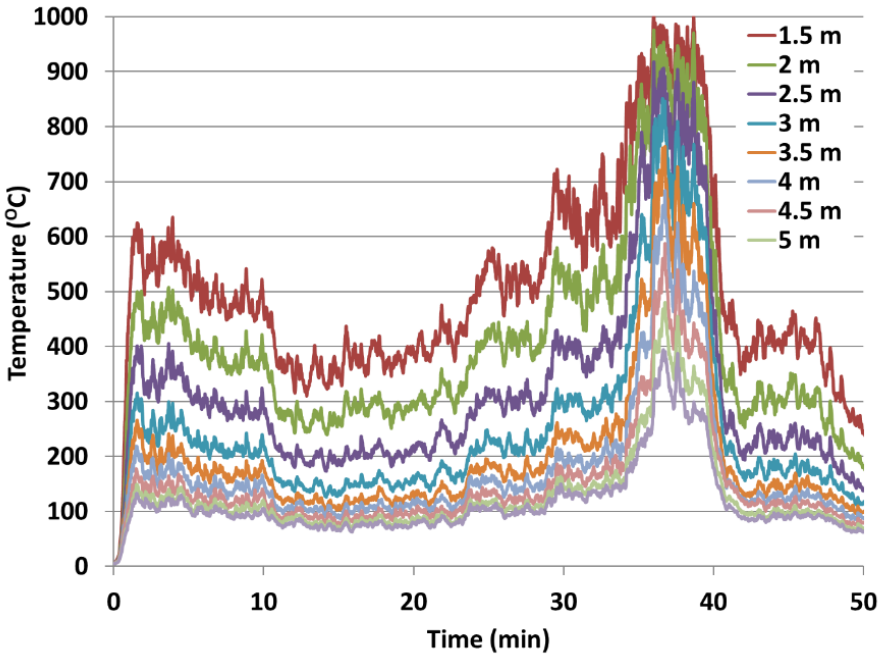

Figure 6-166: Temperature measurements from vertical thermocouple rake in centerline of fire plume (Test 3.3).

6.3.3.6. Plume Temperature and Surface Emissive Power

Figure 6-167 provides IR camera measurements of surface temperatures of the fire plume and surface emissive power averaged over the time during which the Dilbit crude oil was burning. The time and spatially averaged SEP is 71.1 ± 9.6 kW/m^2 and the time-averaged local maximum SEP is 188.5 ± 17.1 kW/m^2.

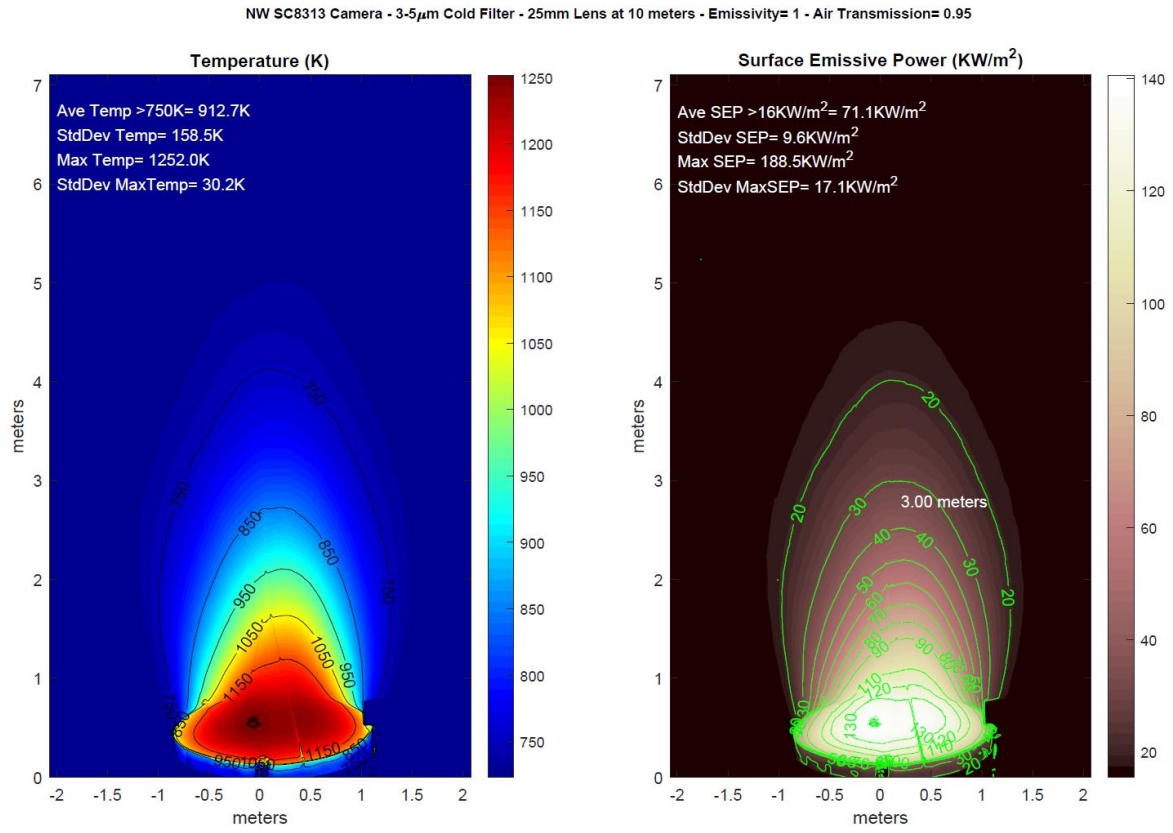

Figure 6-167: Fire plume temperatures and surface emissive power values from IR camera measurements (Test 3.3).

6.3.3.7. DFT TC Temperature and Derived Heat Flux

Figure 6-168 and Figure 6-169 provide DFT temperatures and heat flux, respectively. The term 'front' refers to the thermocouple measurement for the plate closest to the fire, while the term 'back' refers to the thermocouple measurement for the plate furthest from the fire.

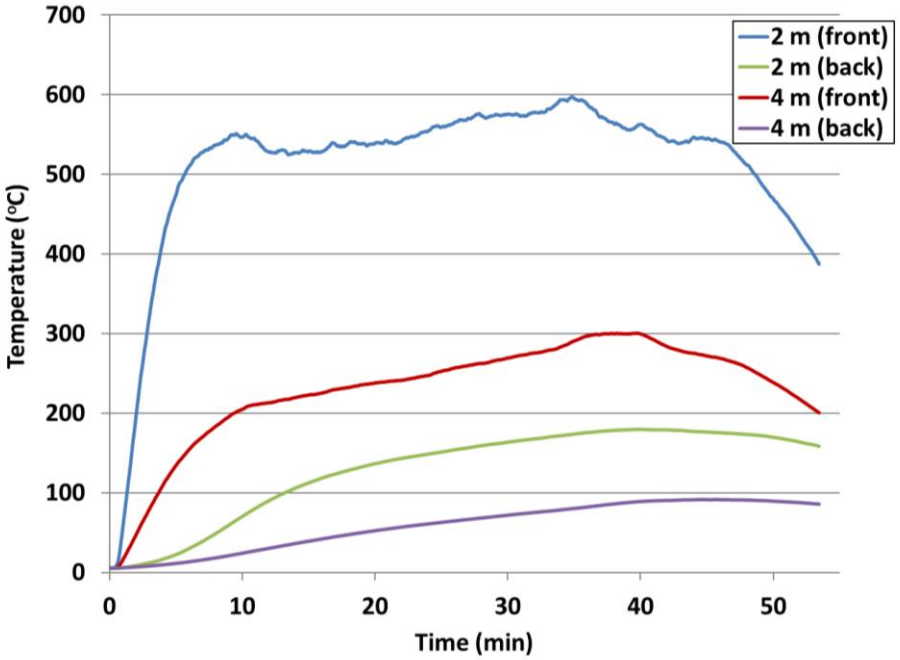

Figure 6-168: Thermocouple temperatures from DFT instruments. Distances are from center of pan (Test 3.3).

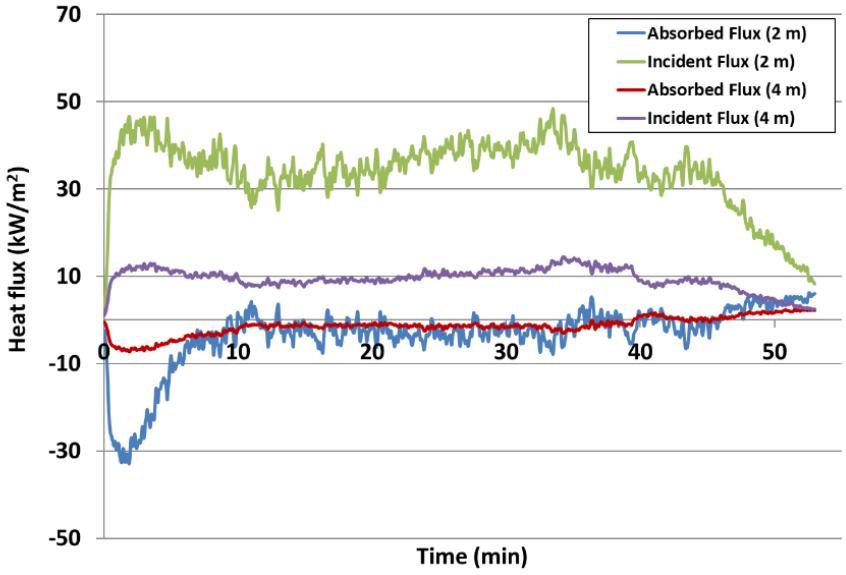

Figure 6-169: Derived heat flux values from DFT instruments. Distances are from center of pan (Test 3.3).

6.3.3.8. Heat release rate

Data from the combustion gas analyzer was collected for this test but provided erroneous readings. The heat release rate based on evaluating the product of the heat of combustion (43.275 MJ/kg), mass flux (0.017 kg/m^{2}s), and pan area (3.14 m^2) is 2.31 MW.

6.3.3.9. Flame Height

Figure 6-170 shows the flame height as measured from the IR camera. The average flame height is 3.4 ± 0.8 m average over 3-30 minutes. Note that when the Jet-A was introduced at approximately 30 minutes the flame height increased to an average of about 5.6 m. The field of view of the camera did not encompass above 7 m due to limitation of the radial distance of the test chamber and the camera lens. Thus, the data is clipped at that height.

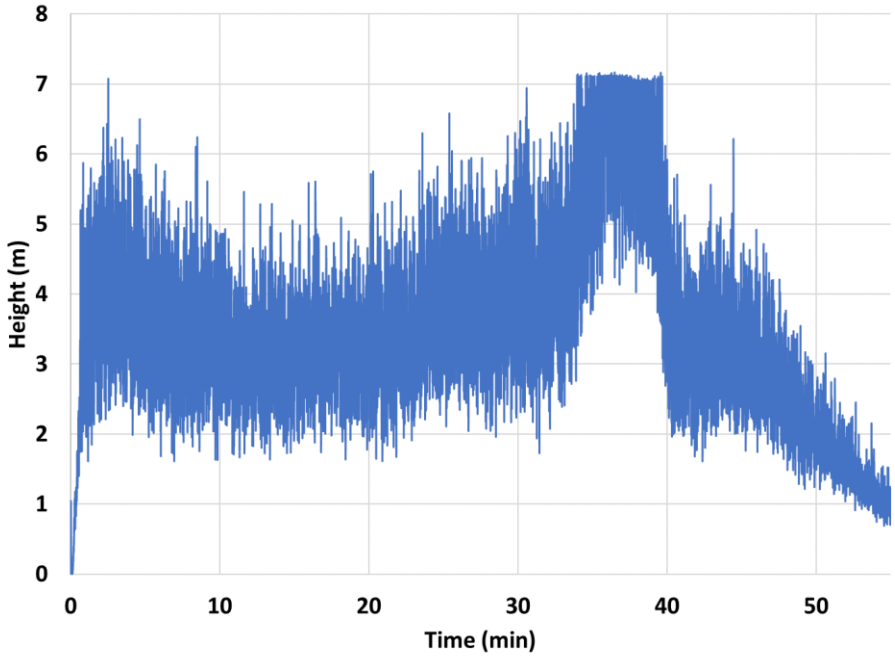

Figure 6-170: Flame height from IR camera measurements (Test 3.3).

6.3.4. Test 3.4

For this test, there was no calorimeter and the Dilbit fuel level was not maintained but allowed to burn down. The pan was filled to a height of 7.6 cm (3 inches) at a supply temperature of 20 ± 5°C. After 54 minutes, when the flame appeared to be nearly extinguished, Jet-A fuel was introduced into the pan for about 7 minutes and then continued to burn for about 40 minutes.

6.3.4.1. Fuel Supply Temperature

Prior to ignition the pan was filled to a level of 7.6 cm (3") with Dilbit fuel at an average temperature of 22.1 ± 1.5°C. Figure 6-171 provides the fuel supply temperature over time. The time required to fill the pan was approximately 24 minutes.

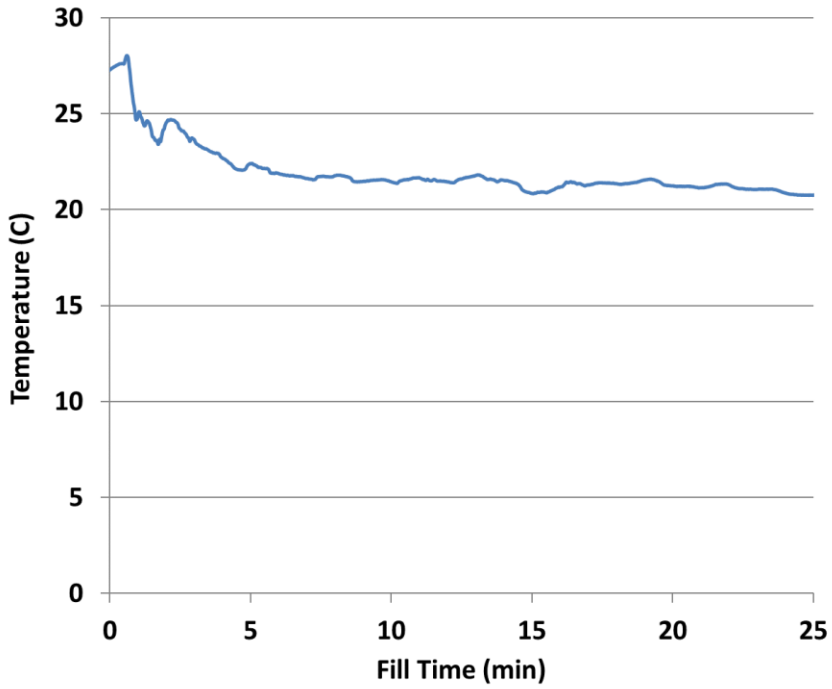

Figure 6-171: Temperature of fuel supply into pan (Test 3.4).

6.3.4.2. Fuel Rake Thermocouple Temperatures

Figure 6-172 shows temperatures from TCs within the liquid fuel. The fuel level prior to ignition was above the 6 cm (2.4") height of the thermocouple rake. For this test the pan was filled to this level prior to ignition. At around 15 minutes all thermocouples rapidly increased by about 200°C indicating that heat from the flame was transferred throughout the pool. Thermocouples at locations TC2, TC9, TC10, TC12, TC13, and TC27 indicated faulty readings so are not included in the figure.

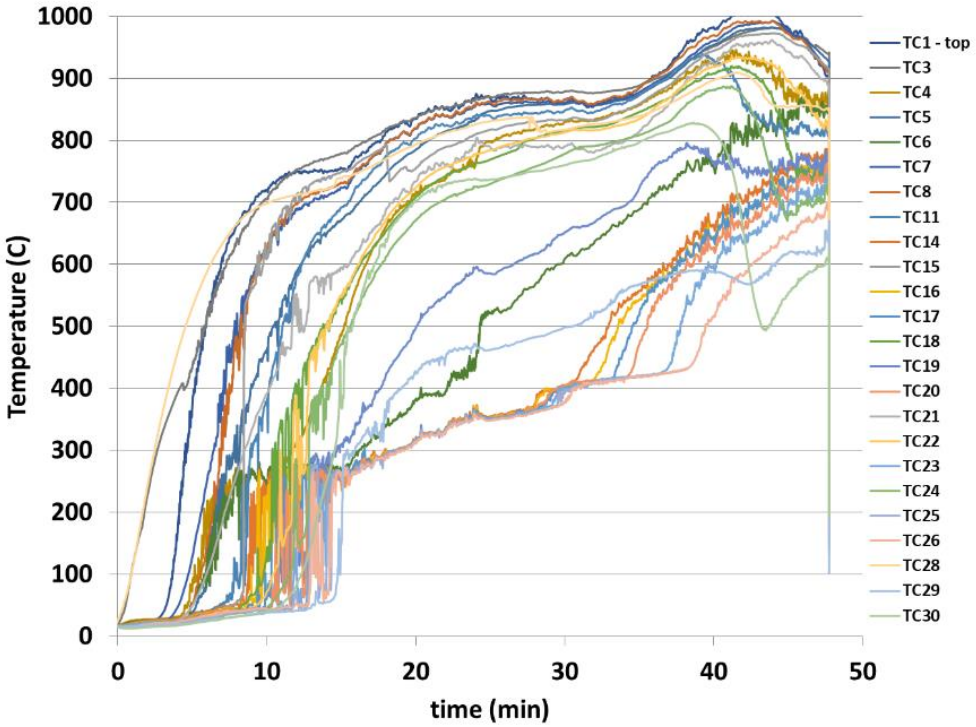

Figure 6-172: Fuel rake thermocouple temperatures (Test 3.4).

6.3.4.3. Burn Rate

The average burn rate is determined by dividing the total mass of fuel burned over the burn time. The mass of Dilbit fuel required to fill the pan to a level of 7.6 cm (3") was approximately 221 kg (487 lbs or 63 gallons). Figure 6-173 shows the total mass supplied from the Dilbit container which is approximately 273 kg (601 lbs). The difference between the total fuel supplied and the mass of fuel in the pan is approximately 52 kg (114 lbs) which indicates the remaining balance was in the fuel transfer line, drain-down valve, and heat exchanger.

The mass of post-test residue in the pan was approximately 39.7 kg (87.3 lbs). Thus, the total mass of Dilbit burned was approximately 181 kg (398 lbs) over a duration of 54 minutes. The average burn rate is then 3.4 kg/min which corresponds to a mass flux of 0.018 kg/m^{2}s.

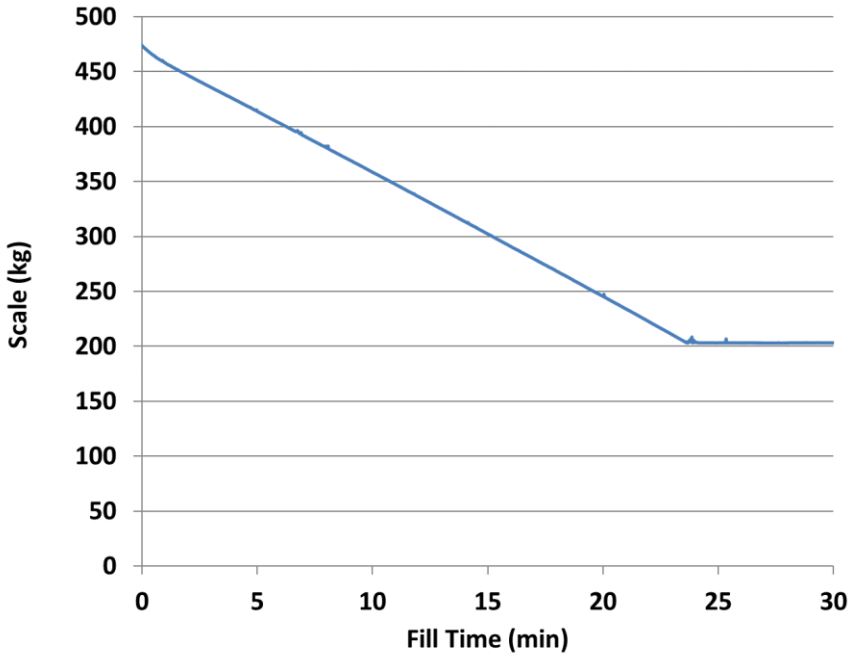

Figure 6-173: Fuel weight over time during filling the pan (Test 3.4).

6.3.4.4. Radiometers

Figure 6-174 and Figure 6-175 provide the heat flux over time from six narrow-angle and five wide-angle radiometers at the various height locations. The increase at about 54 minutes is from the introduction of the Jet-A fuel.

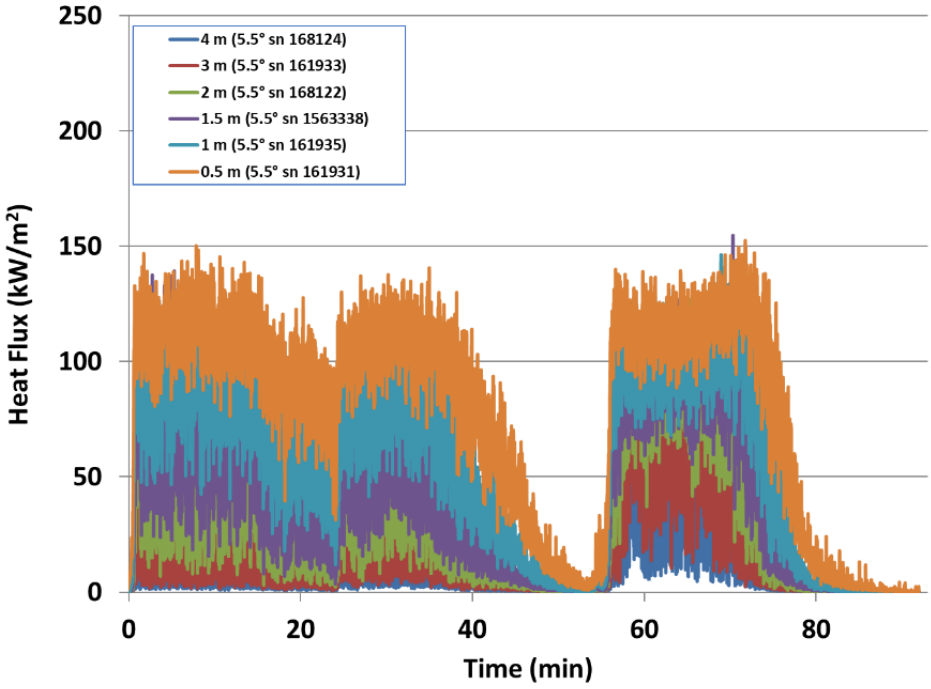

Figure 6-174: Heat flux measurement from narrow view radiometers at different heights (Test 3.4).

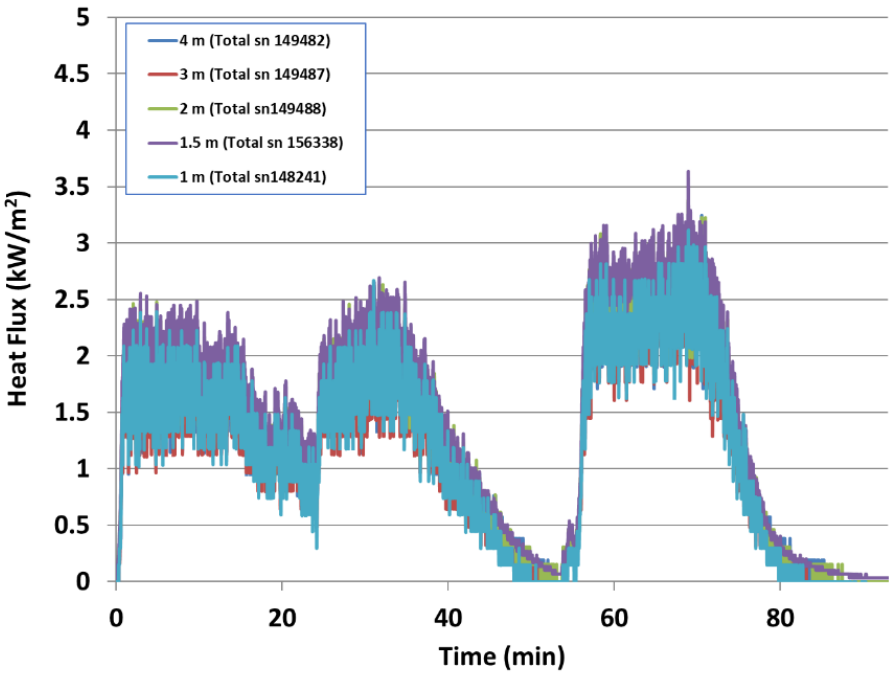

Figure 6-175: Heat flux measurement from wide view radiometers at different heights (Test 3.4).

6.3.4.5. Thermocouple Rake in Fire Plume

Figure 6-176 provides temperature measurements over time from the TCs placed within the fire plume at its vertical centerline. The thermocouple at the location of 0.5 m above the pan was removed since the calorimeter was not present and its stand was used to suspend the thermocouple.

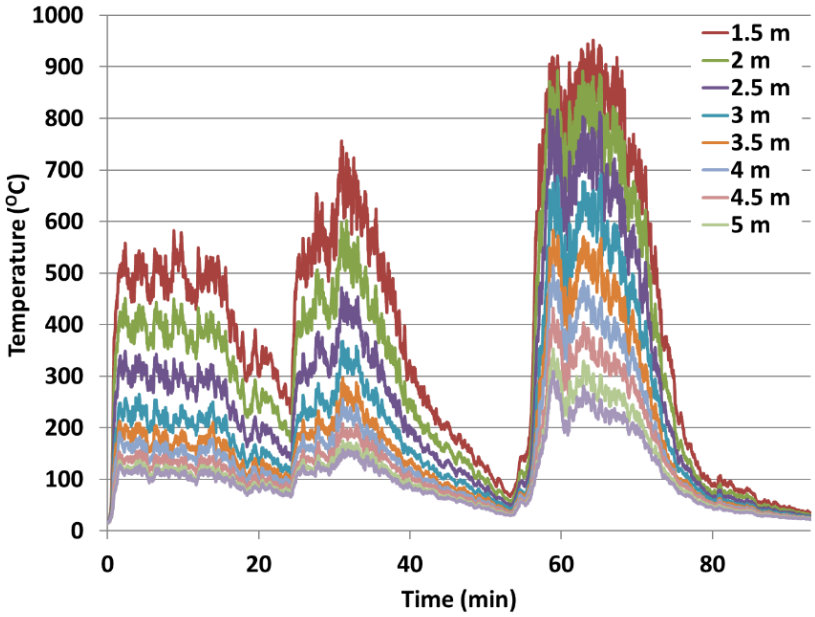

Figure 6-176 Temperature measurements from vertical thermocouple rake in centerline of fire plume (Test 3.4).

6.3.4.6. Plume Temperature and Surface Emissive Power

Figure 6-177 provides IR camera measurements of surface temperatures of the fire plume and surface emissive power averaged over the time during which the Dilbit crude oil was burning. The time and spatially-averaged SEP is 69.8 ± 8.9 kW/m^2 and the time-averaged local maximum SEP is 188.2 ± 19.31 kW/m^2.

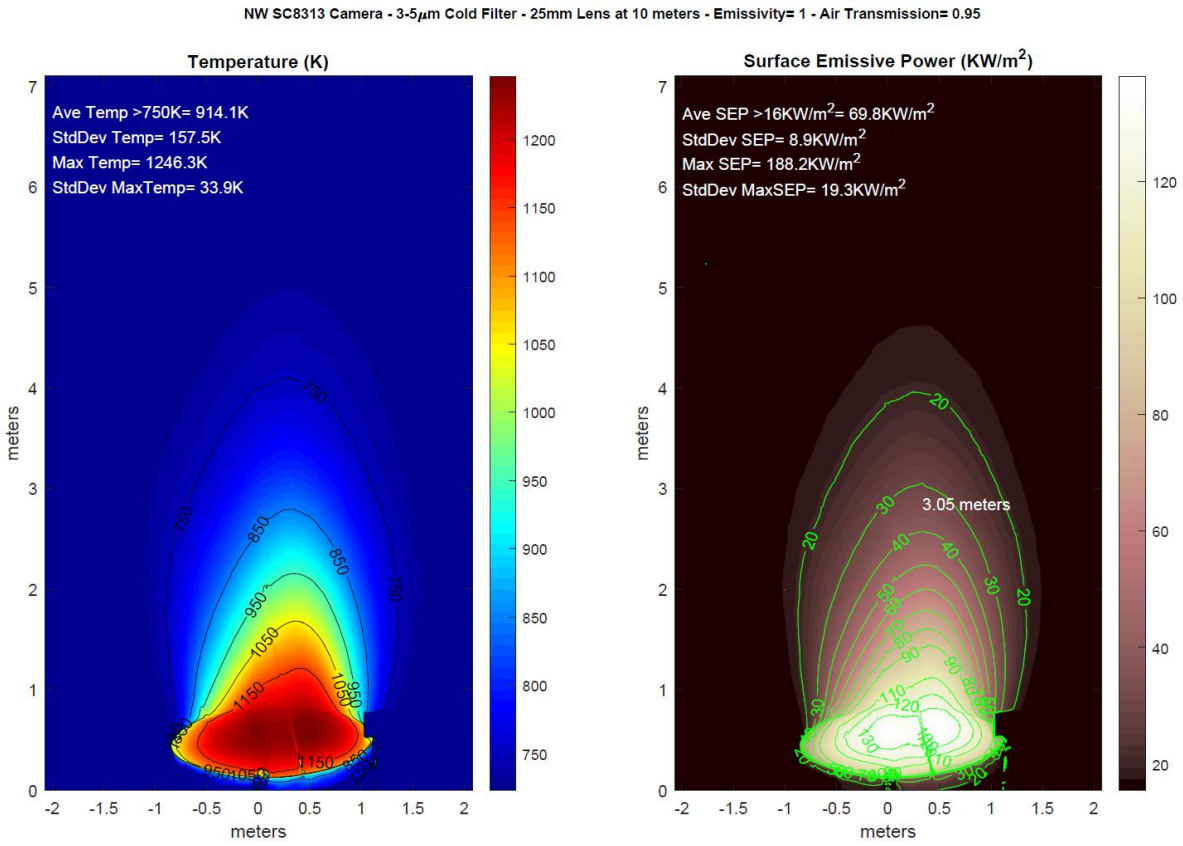

Figure 6-177: Fire plume temperatures and surface emissive power values from IR camera measurements (Test 3.4).

6.3.4.7. DFT TC Temperature and Derived Heat Flux

Figure 6-178 and Figure 6-179 provide DFT temperatures and heat flux, respectively. The term 'front' refers to the thermocouple measurement for the plate closest to the fire, while the term 'back' refers to the thermocouple measurement for the plate furthest from the fire.

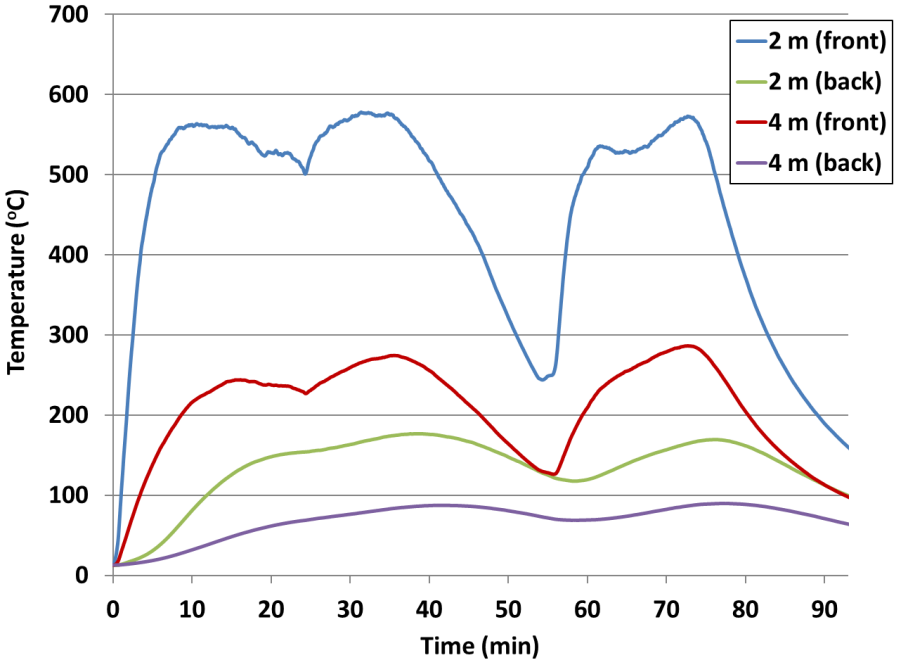

Figure 6-178: Thermocouple temperatures from DFT instruments. Distances are from center of pan (Test 3.4).

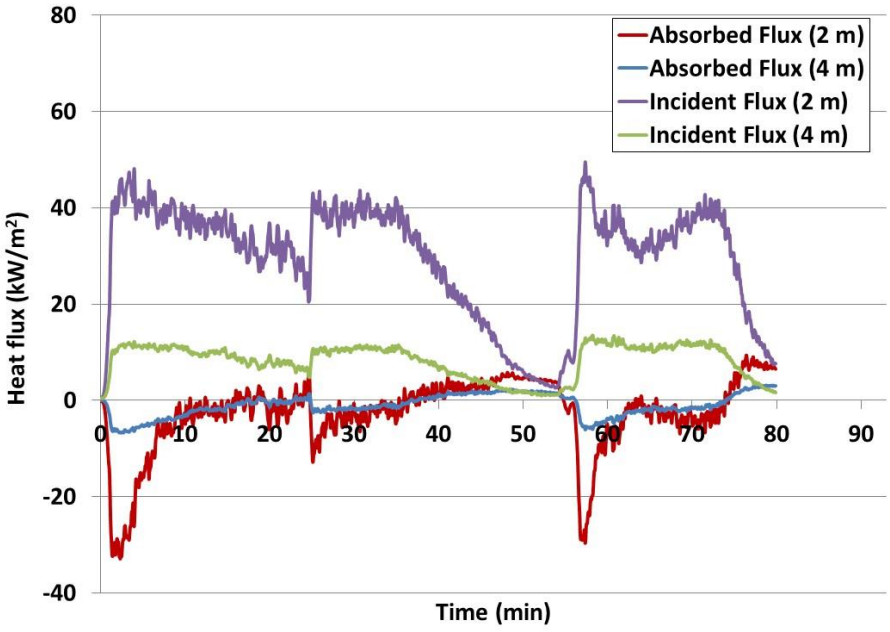

Figure 6-179: Derived heat flux values from DFT instruments. Distances are from center of pan (Test 3.4).

6.3.4.8. Heat release rate

Data from the combustion gas analyzer was collected for this test and results provide a heat release rate of 3.72 ± 1.18 MW. The heat release rate based on evaluating the product of the heat of combustion (43.275 MJ/kg), mass flux (0.018 kg/m^{2}s), and pan area (3.14 m^2) is 2.45 MW.

6.3.4.9. Flame Height

Figure 6-180 shows the flame height as measured from the IR camera. The average flame height is 3.5 ± 0.8 m averaged over 3 to 25 minutes. Note that when the Jet-A was introduced at approximately 54 minutes the flame height increased to an average of about 5.7 m. The field of view of the camera did not encompass above 7 m due to limitation of the radial distance of the test chamber and the camera lens. Thus, the data is clipped at that height.

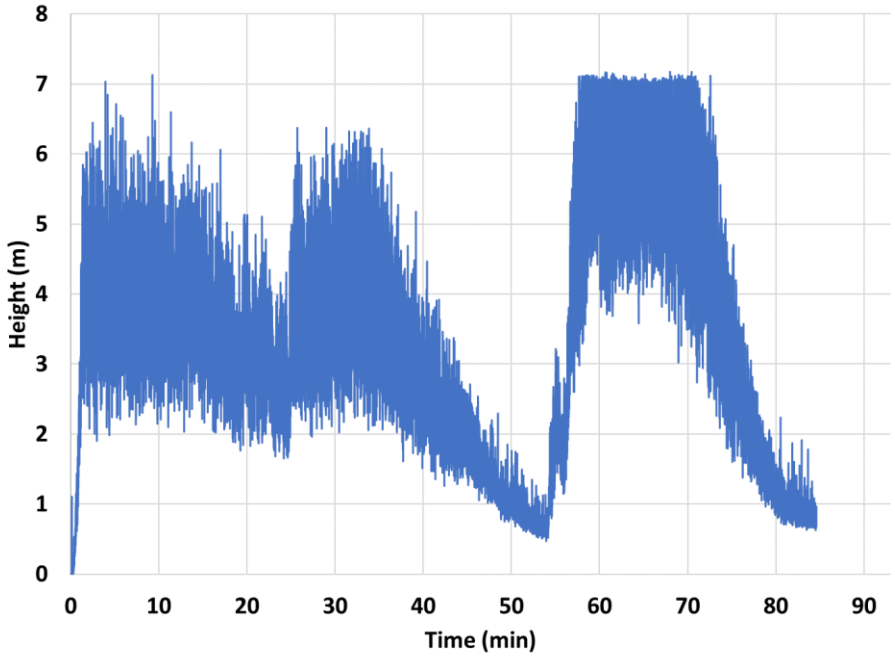

Figure 6-180: Flame height from IR camera measurements (Test 3.4).

6.3.5. Test 3.5

For this test, the calorimeter was elevated 1 m from its centerline to the bottom of the fuel pan and is a repeat of test 3.1. The Dilbit fuel was supplied and maintained at a constant fuel level of about 30 mm (1.2 inches) for about 30 minutes. After 30 minutes, the Dilbit fuel supply was terminated and Jet-A fuel was introduced for approximately 7 minutes.

6.3.5.1. Fuel Supply Temperature

Figure 6-181 provides the fuel supply temperature over time. The temperature averaged over 5-30 minutes is 24.9 ± 0.4°C.

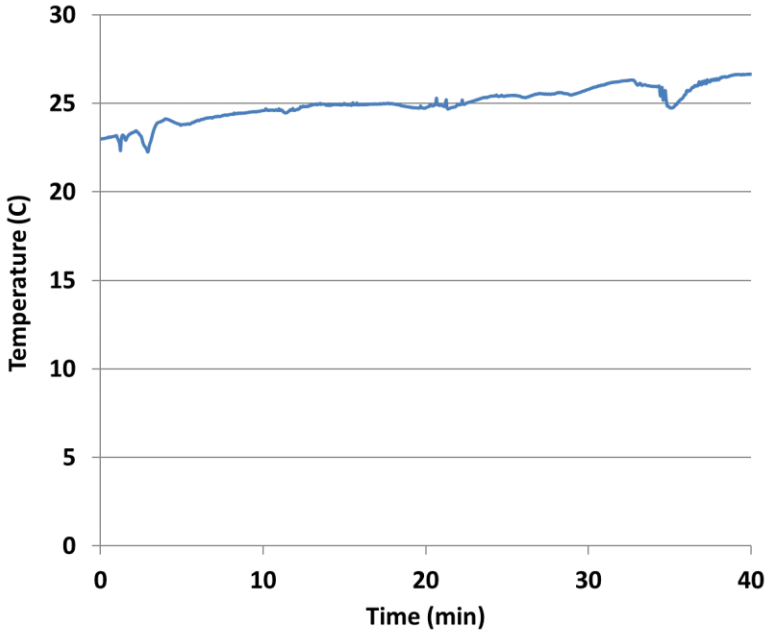

Figure 6-181: Temperature of fuel supply into pan (Test 3.5).

6.3.5.2. Fuel Rake Thermocouple Temperatures

The pan was filled to a level of approximately 30 mm (1.2”). Figure 6-182 shows temperatures from TCs within the liquid fuel which indicates that the thermocouples failed. The cause of the failure is unknown.

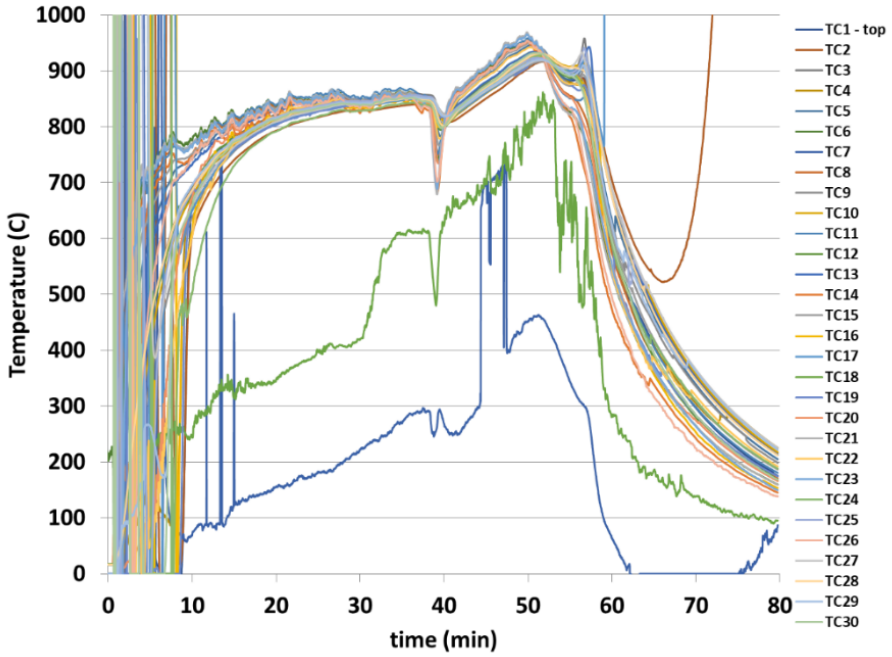

Figure 6-182: Fuel rake thermocouple temperatures (Test 3.5).

6.3.5.3. Burn Rate

The burn rate is determined by identifying a period in which the differential pressure gauge reading is nearly constant and determining the slope of the change in weight of the fuel tank during that period. This test had the longest period over which the dP gauge was nearly constant (2 to 20 minutes). The slope of the curve shown in Figure 6-183 of fuel mass over time varied. Thus, a polynomial curve fit (r^2 = 99%) was differentiated to determine the burn rate as it varied over this duration (Figure 6-184). The results indicate that the burn rate varied between 2.9 kg/min (0.015 kg/m^{2}s) to 3.7 kg/min (0.019 kg/m^{2}s). The weight of the post-test residue in the pan was 29.3 kg (64.5 lbs).

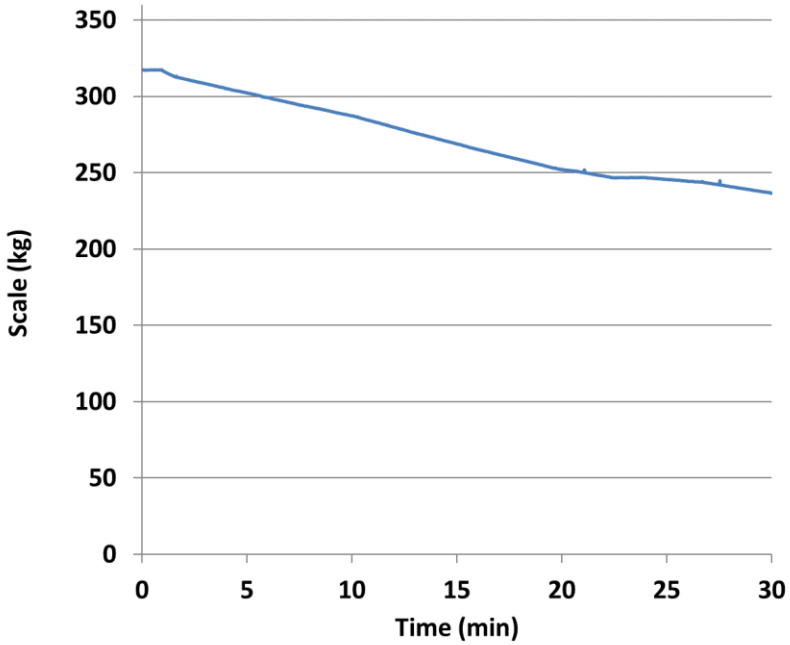

Figure 6-183: Fuel weight over time during filling the pan (Test 3.5).

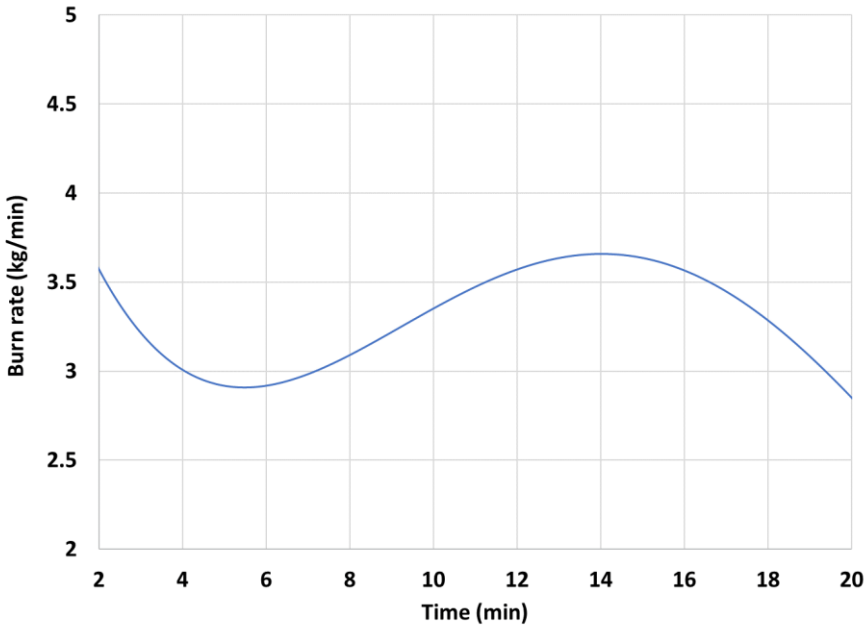

Figure 6-184: Burn rate (kg/min) versus time (test 3.5).

6.3.5.4. Radiometers

Figure 6-185 and Figure 6-186 provide the heat flux over time from six narrow-angle and five wide-angle radiometers at the various height locations. The increase at about 30 minutes is from the introduction of the Jet-A fuel.

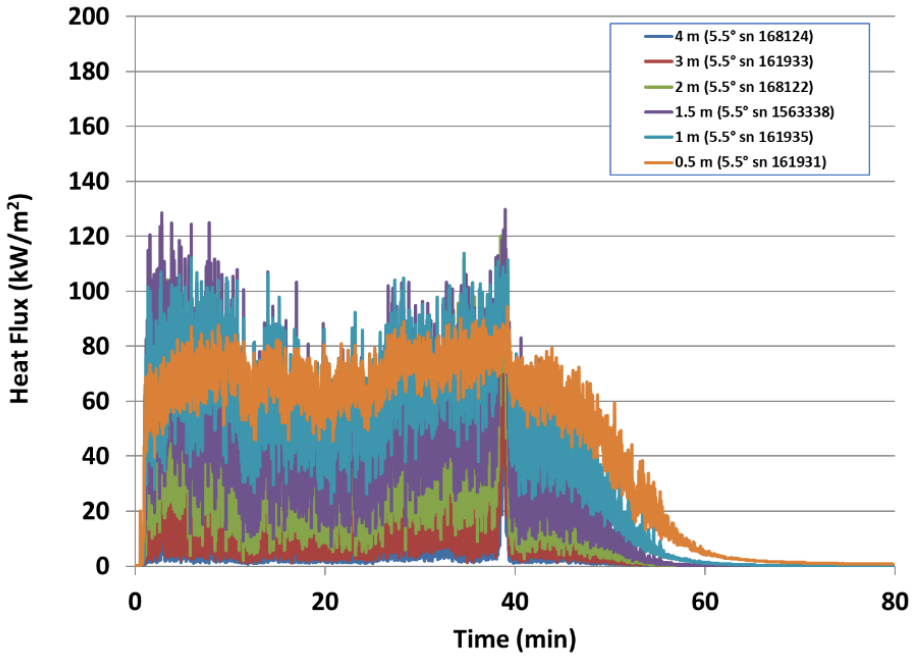

Figure 6-185: Heat flux measurement from narrow view radiometers at different heights (Test 3.5).

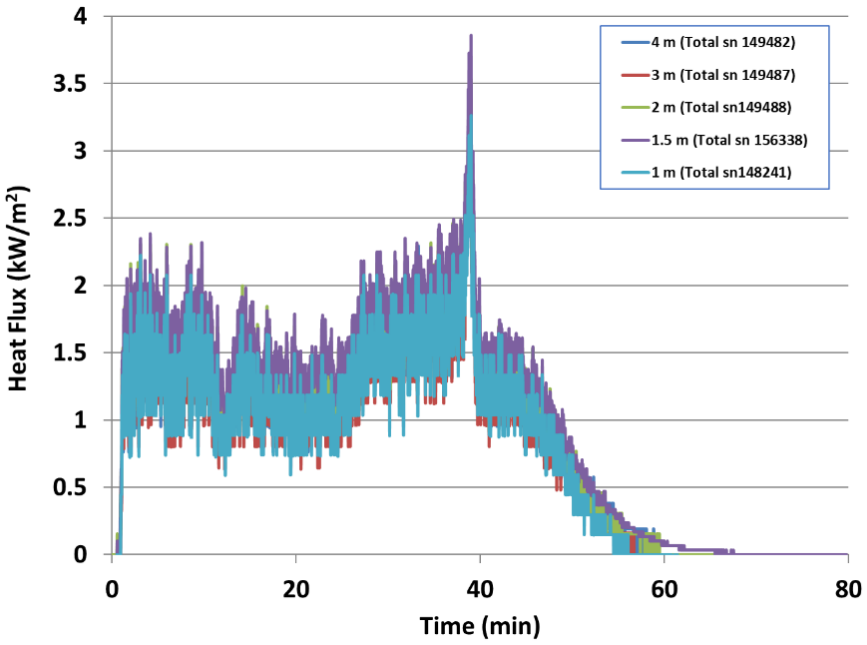

Figure 6-186: Heat flux measurement from wide view radiometers at different heights (Test 3.5).

6.3.5.5. Thermocouple Rake in Fire Plume

Figure 6-187 provides temperature measurements over time from the TCs placed within the fire plume at its vertical centerline.

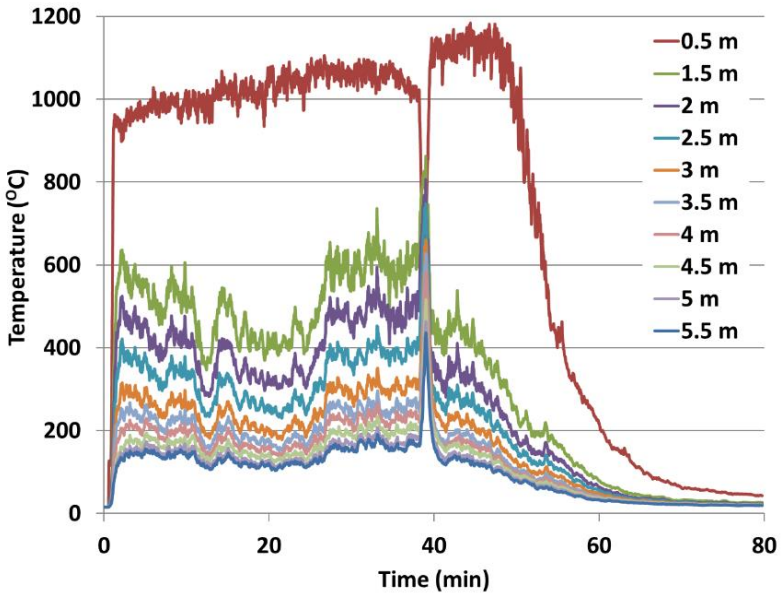

Figure 6-187: Temperature measurements from vertical thermocouple rake in centerline of fire plume (Test 3.5).

6.3.5.6. Plume Temperature and Surface Emissive Power

Figure 6-188 provides IR camera measurements of surface temperatures of the fire plume and surface emissive power averaged over the time during which the Dilbit crude oil was burning. The time and spatially averaged SEP is 72.6 ± 7.4 kW/m^2 and the time-averaged local maximum SEP is 191.5 ± 16.5 kW/m^2.

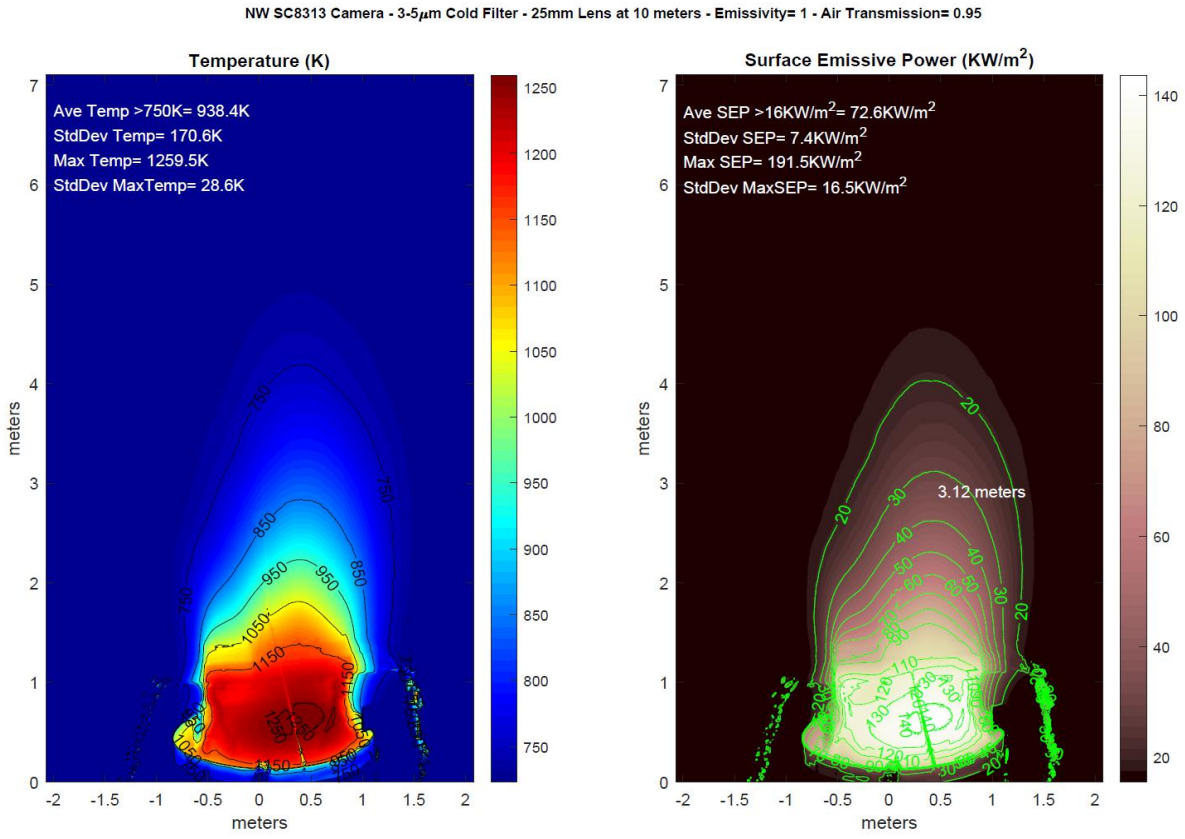

Figure 6-188: Fire plume temperatures and surface emissive power values from IR camera measurements (Test 3.5).

6.3.5.7. DFT TC Temperature and Derived Heat Flux

Figure 6-189 and Figure 6-190 provide DFT temperatures and heat flux, respectively. The term 'front' refers to the thermocouple measurement for the plate closest to the fire, while the term 'back' refers to the thermocouple measurement for the plate furthest from the fire.

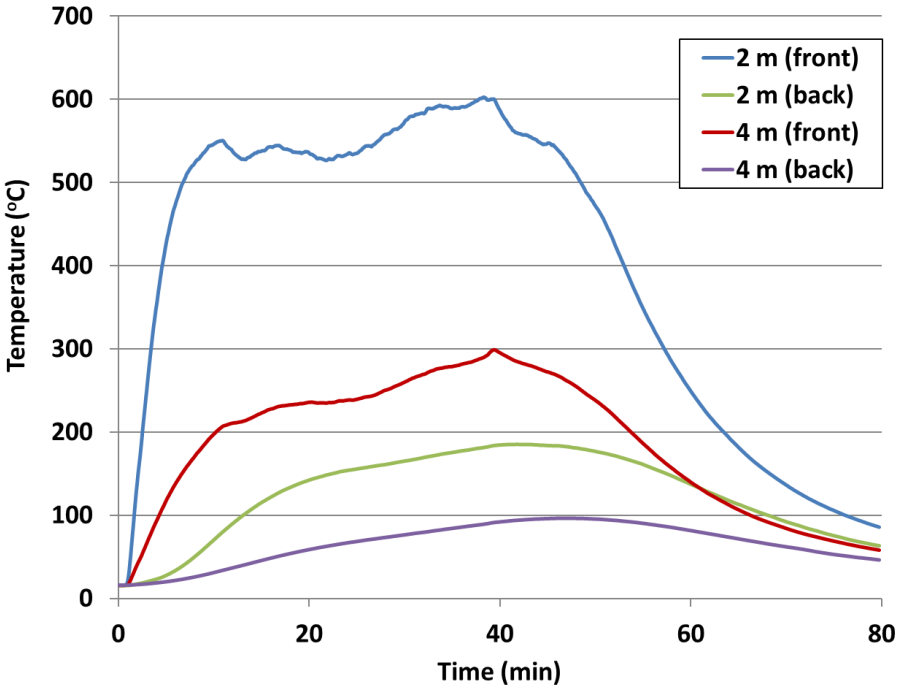

Figure 6-189: Thermocouple temperatures from DFT instruments. Distances are from center of pan (Test 3.5).

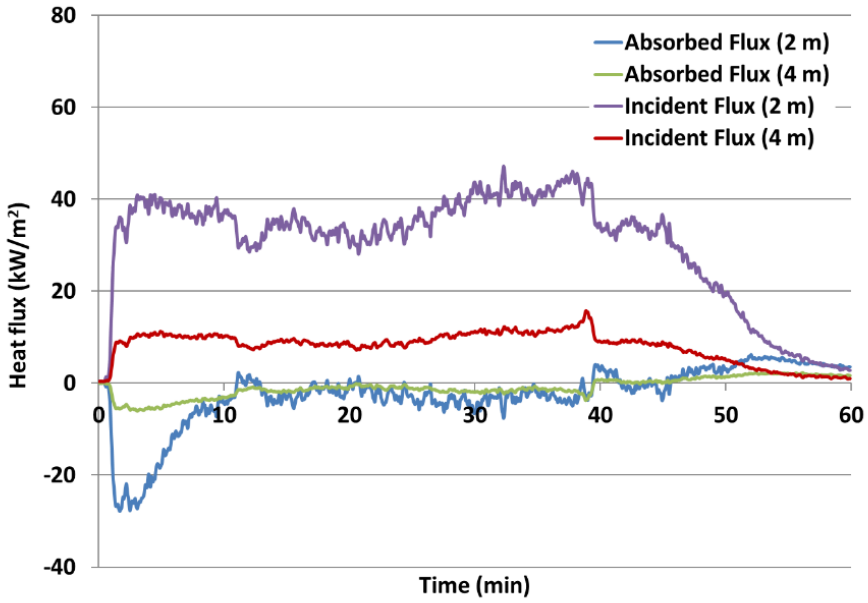

Figure 6-190: Derived heat flux values from DFT instruments. Distances are from center of pan (Test 3.5).

6.3.5.8. Calorimeter TC Temperature and Derived Heat Flux

Figure 6-191 through Figure 6-193 provide temperatures over time from TC measurements placed on the inner and outer cylinders, as well as external to the calorimeter. Figure 6-191 provides thermocouple temperatures on the outer surface of the inner cylinder. None of the inner thermocouples failed. Figure 6-192 provides thermocouple temperatures from the inner surface of the outer shell (midcase) of the calorimeter. The thermocouples at location 2L135°, 2L270°, 2C45°, 2C90°, 2C270°, and 2R270° failed. Figure 6-193 provides thermocouple temperatures on the exterior of the outer cylinder. None of the exterior thermocouples failed.

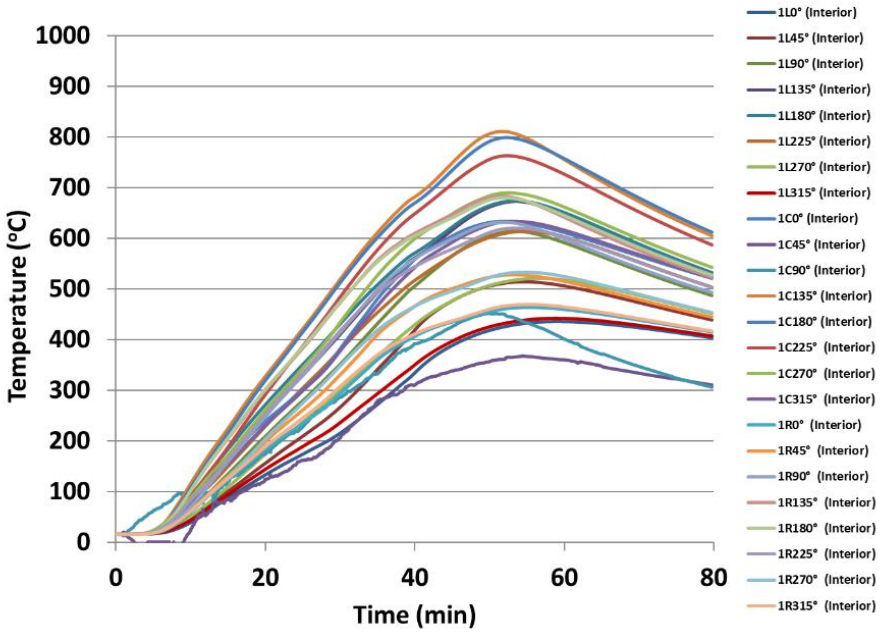

Figure 6-191: Thermocouple temperatures at inner cylinder stations (Test 3.5).

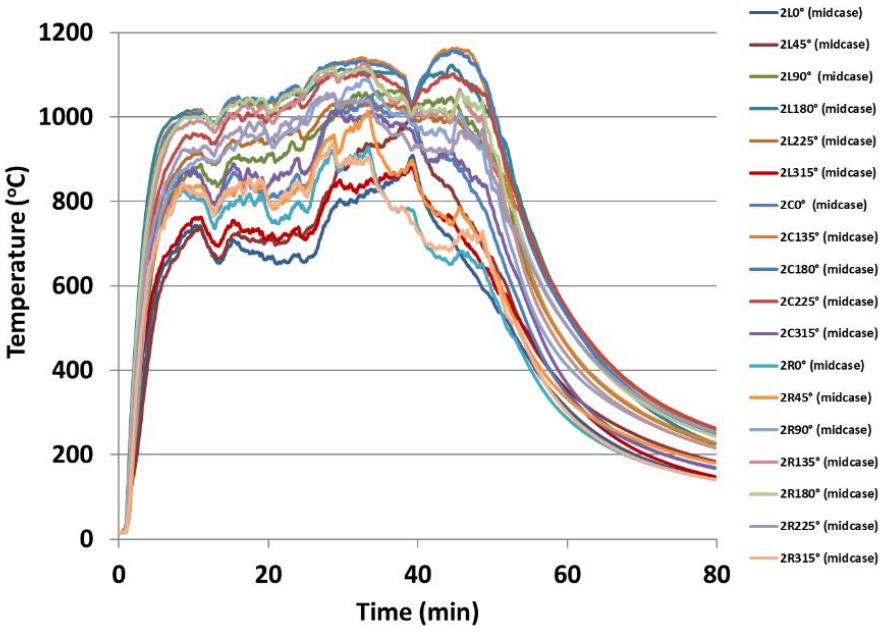

Figure 6-192: Thermocouple temperatures at outer cylinder stations (Test 3.5).

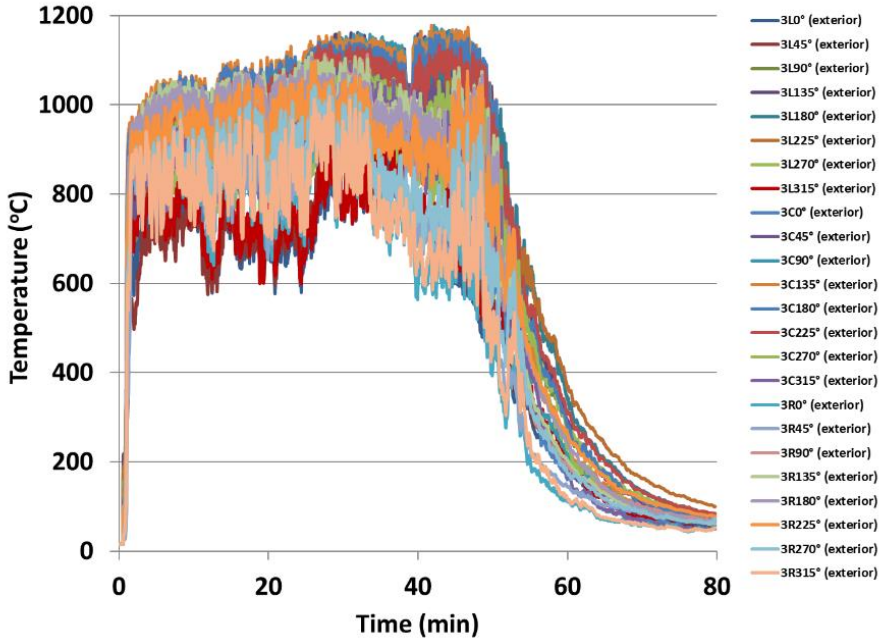

Figure 6-193: Thermocouple temperatures at exterior cylinder stations (Test 3.5).

6.3.5.8.1. Heat Flux to Calorimeter

Figure 6-194 and Figure 6-195 provide the absorbed and total heat flux to the calorimeter, respectively.

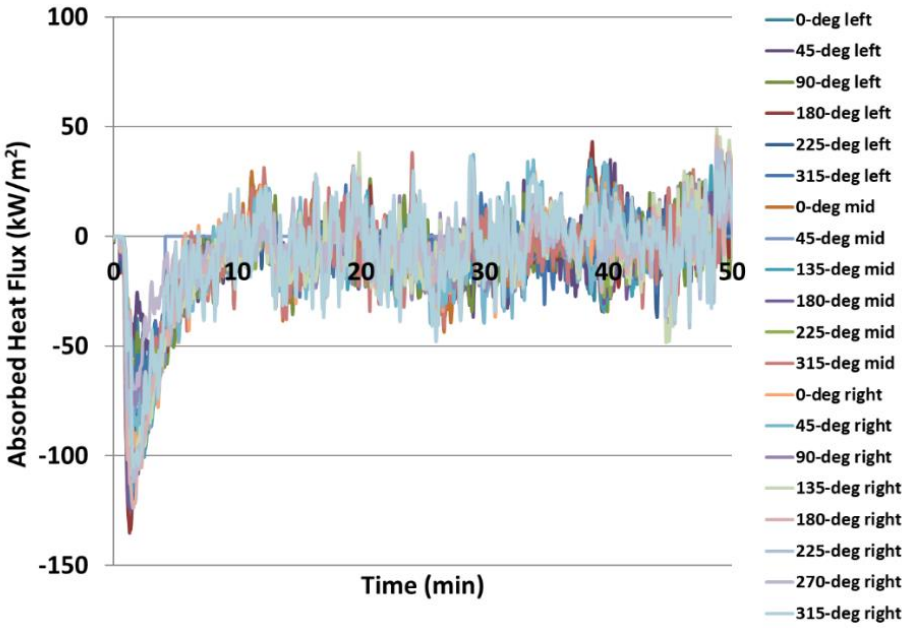

Figure 6-194: Absorbed heat flux to calorimeter (Test 3.5).

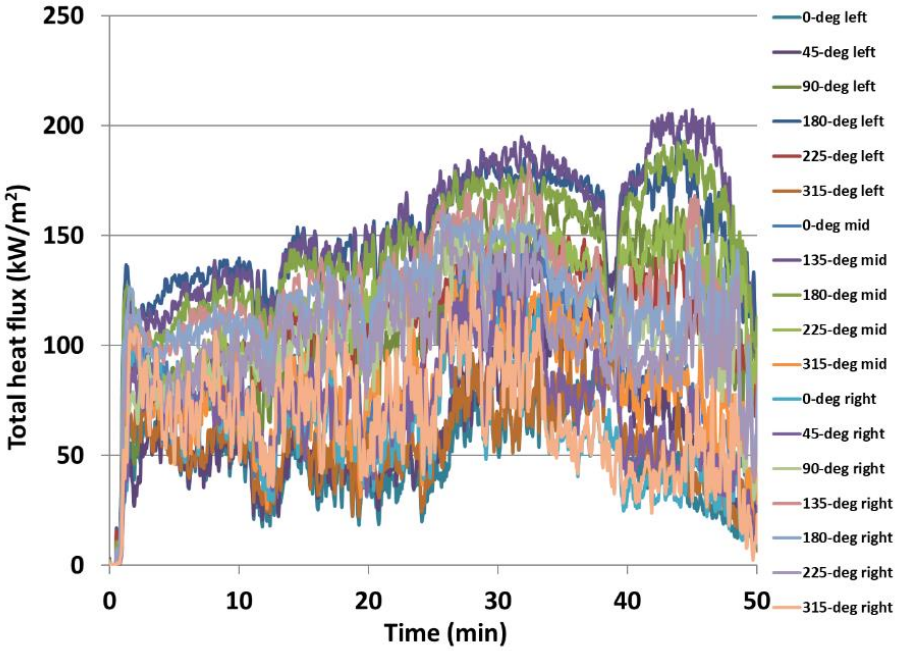

Figure 6-195: Total heat flux to calorimeter (Test 3.5).

6.3.5.9. Heat release rate

Data from the combustion gas analyzer was collected for this test but provided erroneous readings. The heat release rate based on evaluating the product of the heat of combustion (43.275 MJ/kg), mass flux (0.018 kg/m^{2}s), and pan area (3.14 m^2) is 2.45 MW.

6.3.5.10. Flame Height

Figure 6-196 shows the flame height as measured from the IR camera. The average flame height is 3.6 ± 0.8 m averaged over 3 to 30 minutes. Note that when the Jet-A was introduced at approximately 30 minutes the flame height increased to an average of about 5.7 m. The field of view of the camera did not encompass above 7 m due to limitation of the radial distance of the test chamber and the camera lens. Thus, the data is clipped at that height.

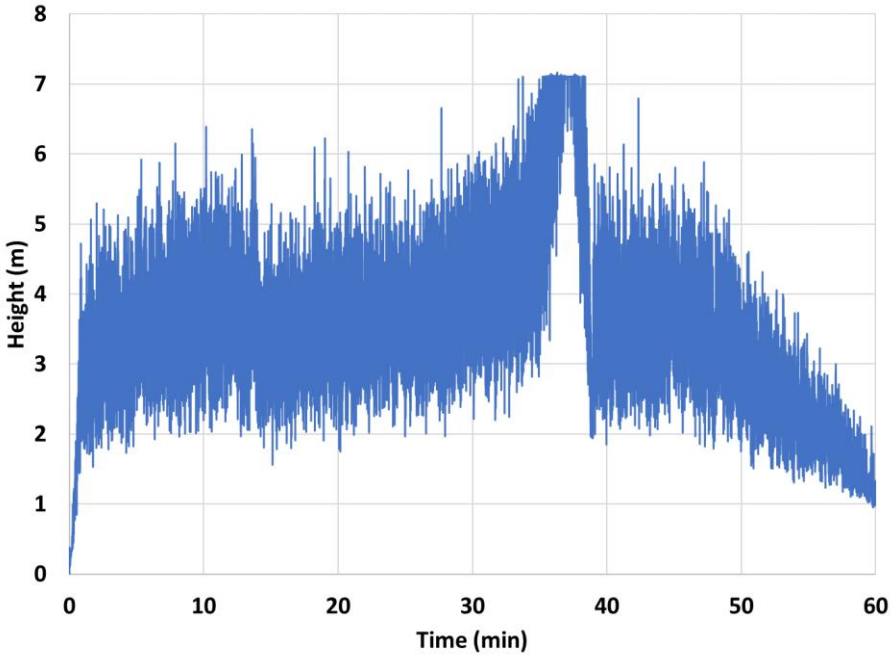

Figure 6-196: Flame height from IR camera measurements (Test 3.5).

6.3.6. Test 3.6

For this test, the calorimeter was elevated 1 m from its centerline to the bottom of the fuel pan and the Dilbit fuel was supplied at a temperature of 60 ± 5°C. The Dilbit fuel was supplied and maintained at a constant fuel level of about 30 mm (1.2 inches) for about 30 minutes. The fire was allowed to burn down without the introduction of Jet-A fuel to allow for the collection of a post-residue sample that was not contaminated with Jet-A fuel. The weight of the post-test residue in the pan was 19.6 kg (43.1 lbs). After the fire completely burned out, taking over an hour after the test was completed, one end of the calorimeter fell and landed on the pan perimeter due to the failure of one of the supports. Since this event did not occur during the tests the data was not affected.

6.3.6.1. Fuel Supply Temperature

Figure 6-197 provides the fuel supply temperature over time. The temperature averaged over 0-30 minutes is 57.3 ± 2.1°C.

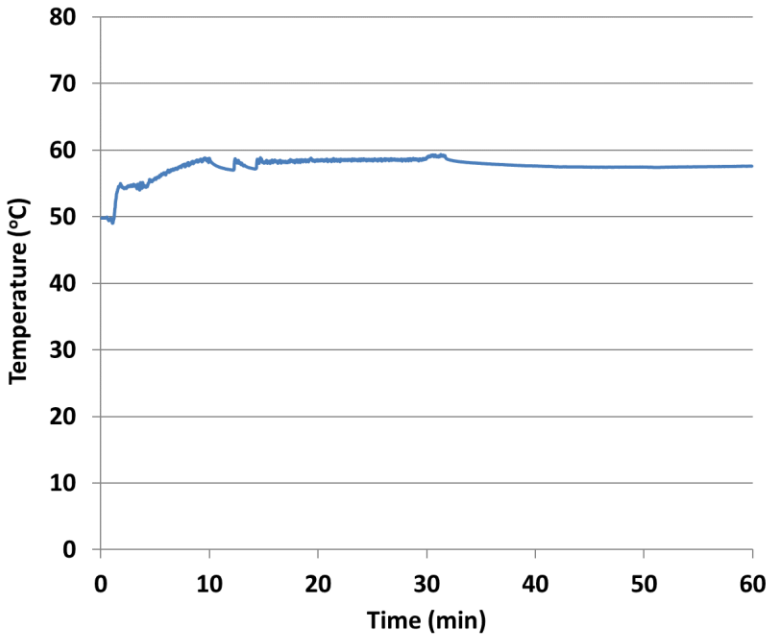

Figure 6-197: Temperature of fuel supply into pan (Test 3.6).

6.3.6.2. Fuel Rake Thermocouple Temperatures

The pan was filled to a level of approximately 30 mm (1.2”). Figure 6-198 shows temperatures from TCs within the liquid fuel. Since multiple TCs failed from the previous test, the rake was rebuilt using 20 thermocouples instead of 30 due to limited availability of in-house thermocouples. Ordering additional thermocouples would cause a significant delay in testing.

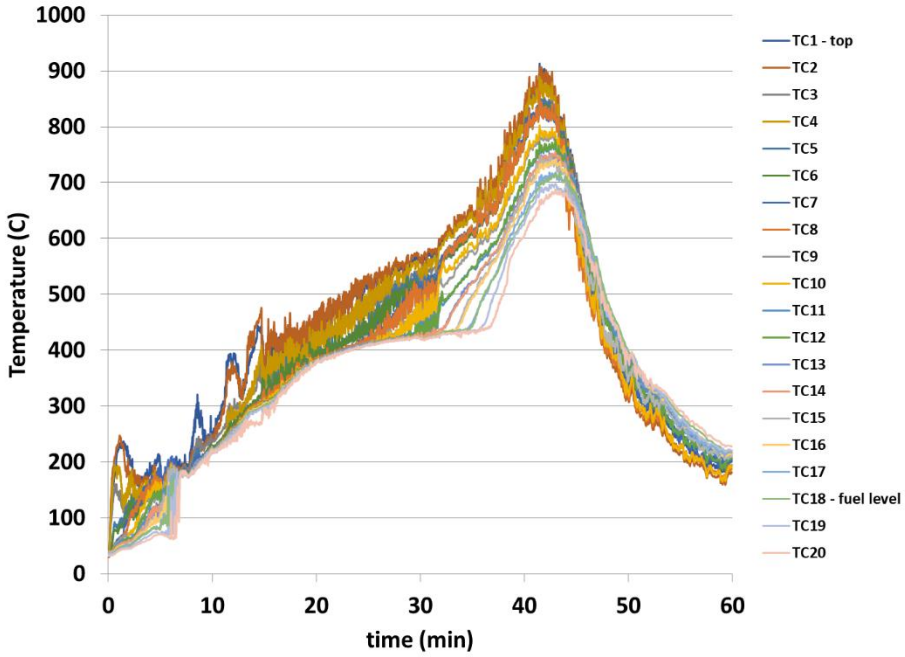

Figure 6-198: Fuel rake thermocouple temperatures (Test 3.6).

6.3.6.3. Burn Rate

The burn rate is determined by identifying a period in which the differential pressure gauge reading is nearly constant and determining the slope of the change in weight of the fuel tank during that period. As indicated in all tests, the burn rate varied over time. Two periods can be identified in which the dP gauge was constant, namely, from 6.3 to 9.6 minutes and 12.3 to 19.3 minutes. For the period from 6.2 to 9.6 minutes the slope is 3.47 kg/min (r^2 =99%) which corresponds to a mass flux of 0.018 kg/m^{2}s (Figure 6-199). Over the period of 12.3-19.3 minutes the slope varied and is indicated in Figure 6-200 which shows the burn rate (kg/min) over this duration varying from 0.95 kg/min (0.005 kg/m^{2}s) to 1.8 kg/min (0.01 kg/m^{2}s). The residue in the pan was 19.6 kg (43.1 lbs).

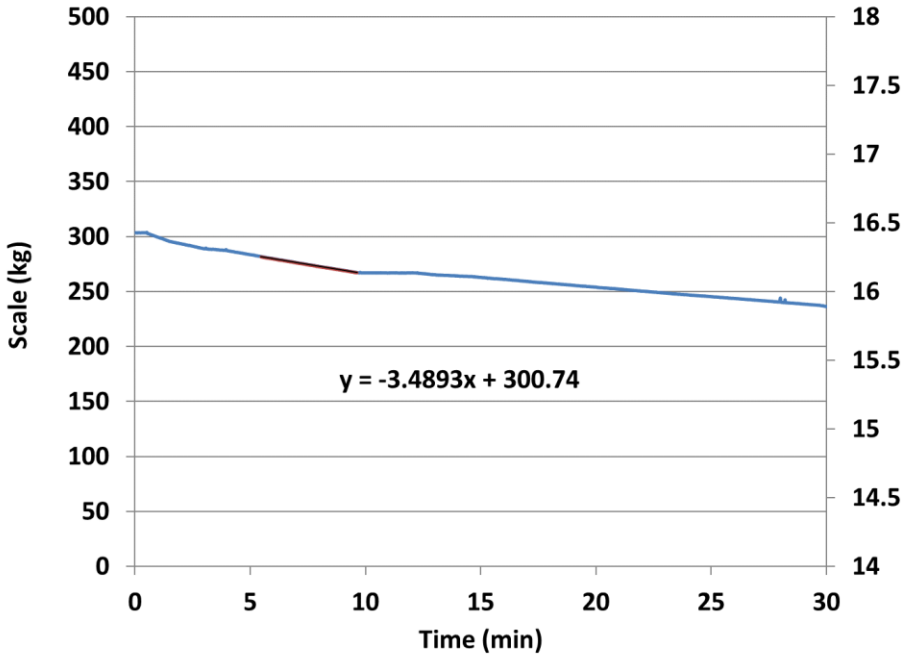

Figure 6-199: Fuel weight over time during filling the pan (Test 3.6).

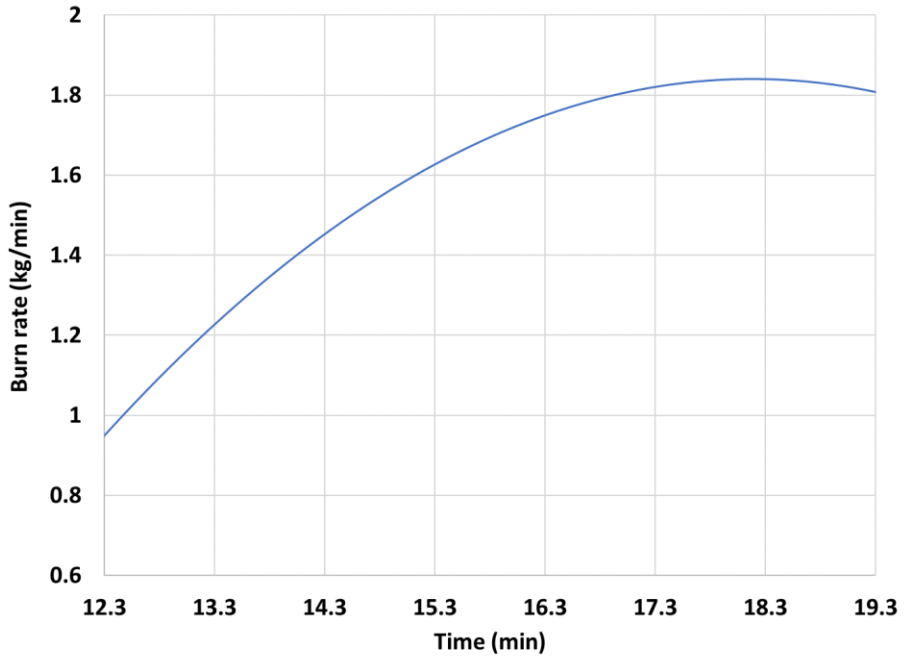

Figure 6-200: Burn rate (kg/min) over period 12.3-19.3 minutes (Test 3.6).

6.3.6.4. Radiometers

Figure 6-201 and Figure 6-202 provide the heat flux over time from six narrow-angle and five wide-angle radiometers at the various height locations.

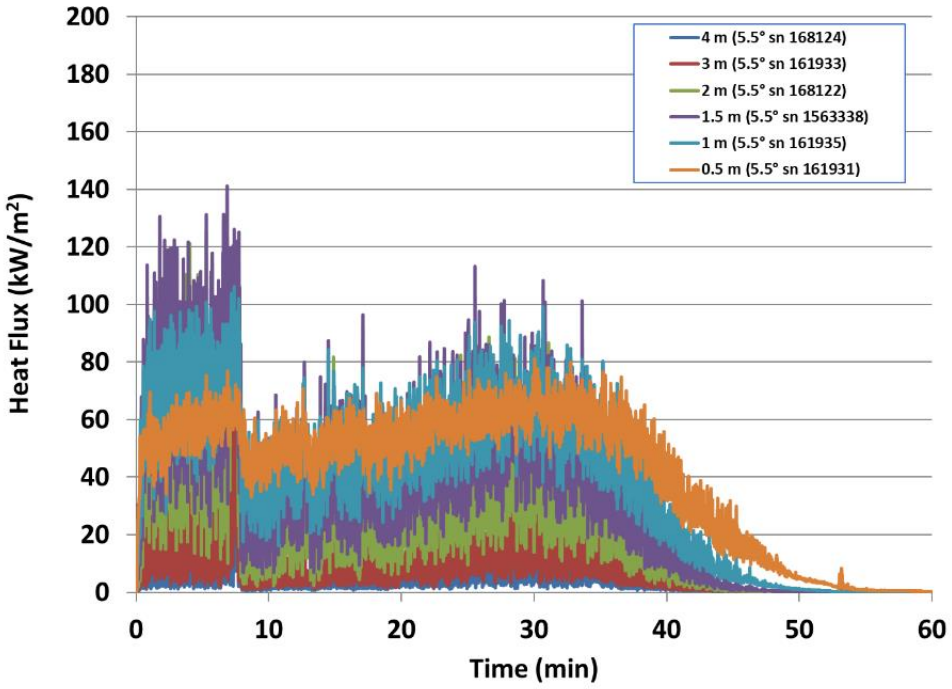

Figure 6-201: Heat flux measurement from narrow view radiometers at different heights (Test 3.6).

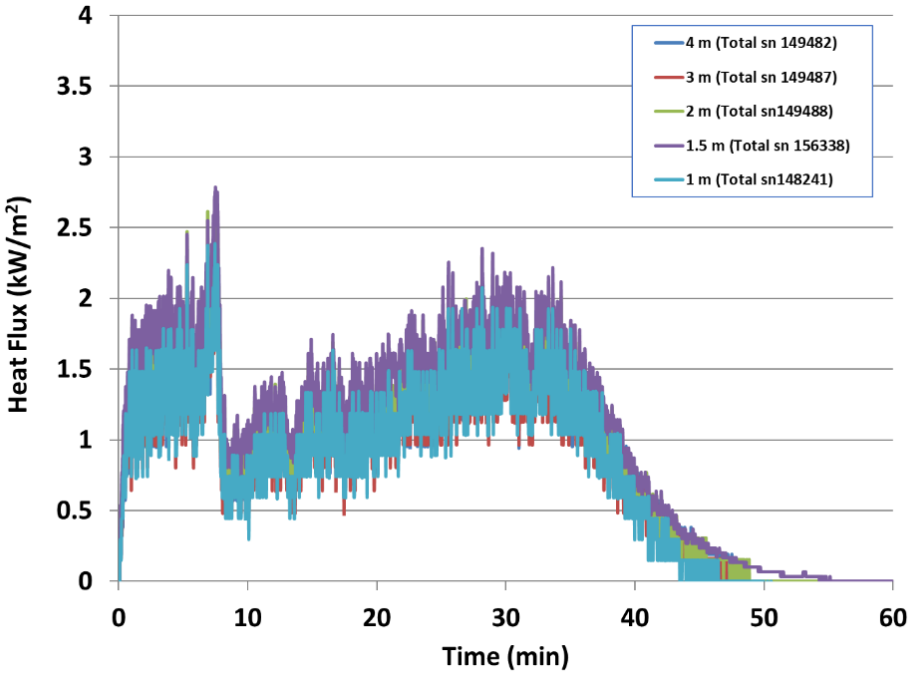

Figure 6-202: Heat flux measurement from wide view radiometers at different heights (Test 3.6).

6.3.6.5. Thermocouple Rake in Fire Plume

Figure 6-203 provides temperature measurements over time from the TCs placed within the fire plume at its vertical centerline.

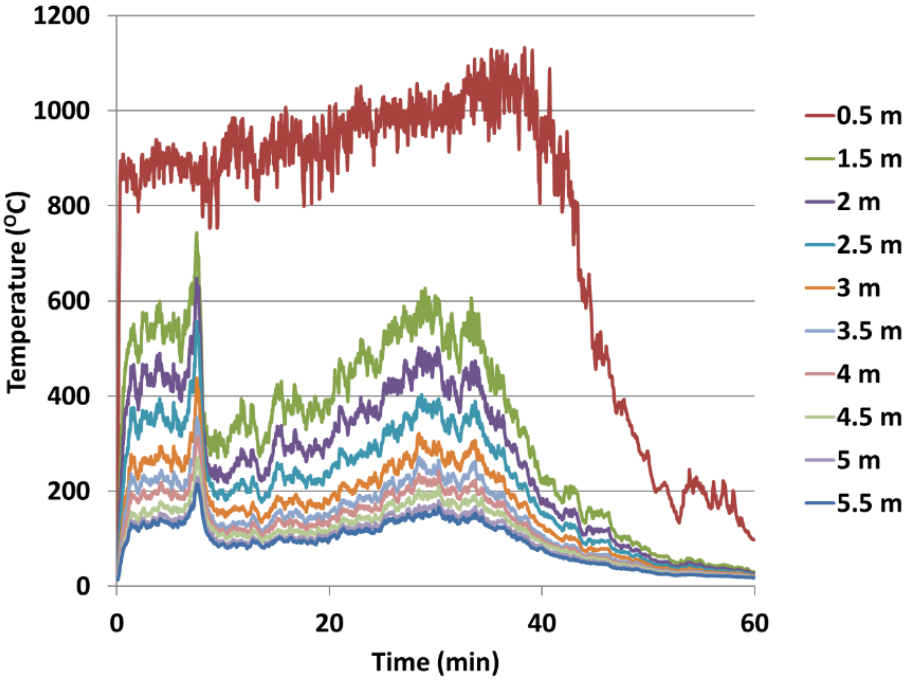

Figure 6-203: Temperature measurements from vertical thermocouple rake in centerline of fire plume (Test 3.6).

6.3.6.6. Plume Temperature and Surface Emissive Power

Figure 6-204 provides IR camera measurements of surface temperatures of the fire plume and surface emissive power averaged over the time during which the Dilbit crude oil was burning. The time and spatially averaged SEP is 72.2 ± 7.6 kW/m^2 and the time-averaged local maximum SEP is 192.7 ± 19.2 kW/m^2.

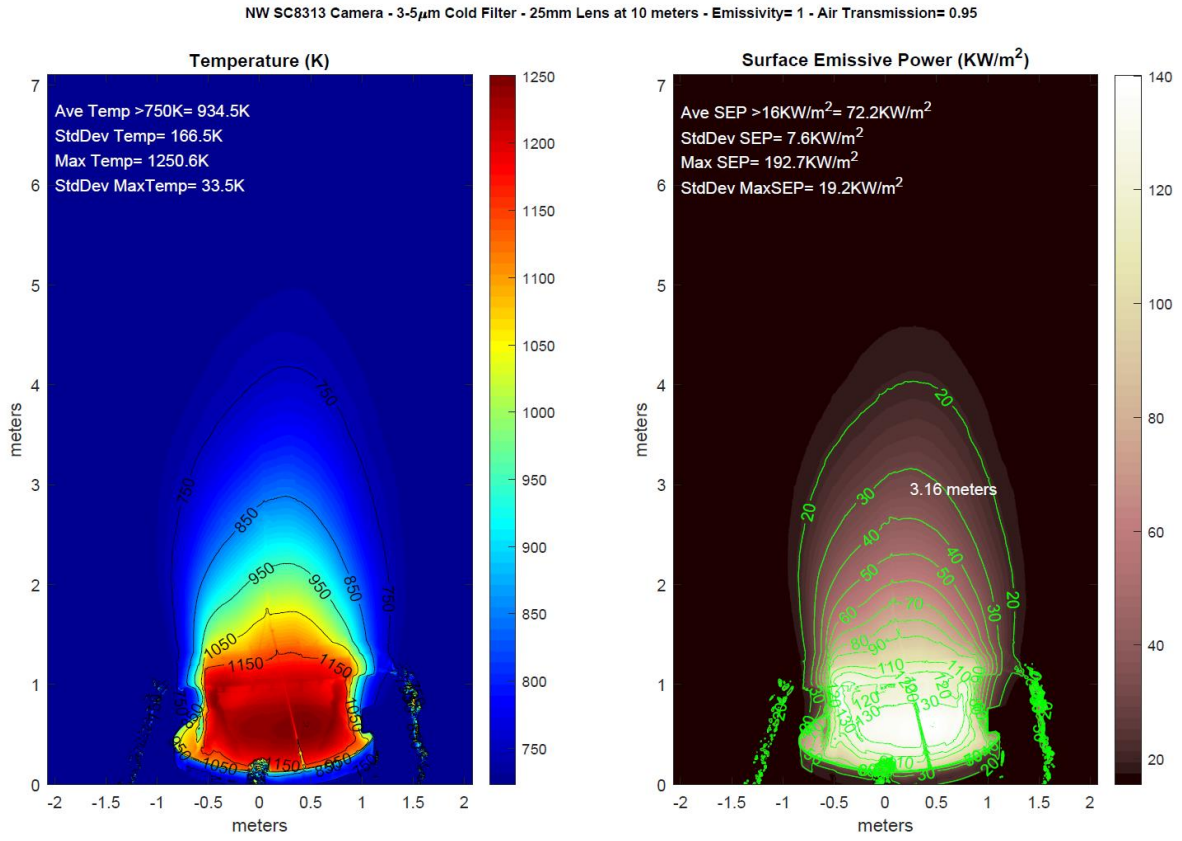

Figure 6-204: Fire plume temperatures and surface emissive power values from IR camera measurements (Test 3.6).

6.3.6.7. DFT TC Temperature and Derived Heat Flux

Figure 6-205 and Figure 6-206 provide DFT temperatures and heat flux, respectively. The term 'front' refers to the thermocouple measurement for the plate closest to the fire, while the term 'back' refers to the thermocouple measurement for the plate furthest from the fire.

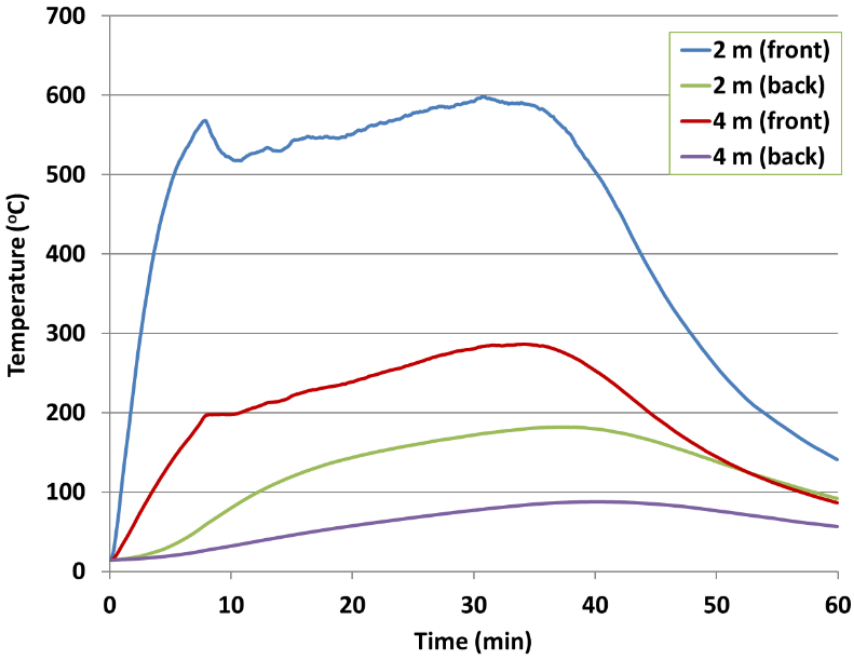

Figure 6-205: Thermocouple temperatures from DFT instruments. Distances are from center of pan (Test 3.6).

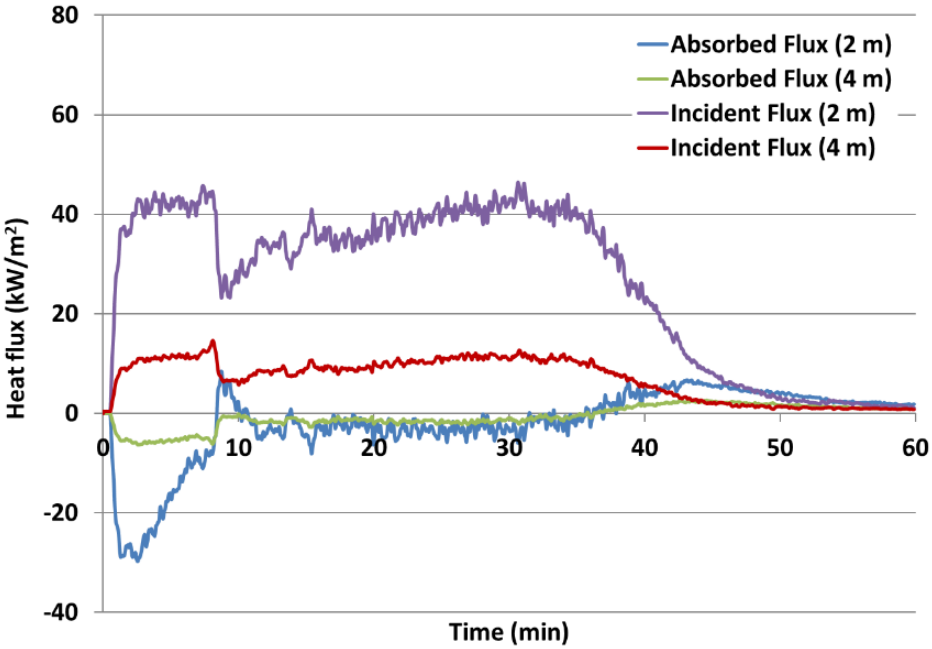

Figure 6-206: Derived heat flux values from DFT instruments. Distances are from center of pan (Test 3.6).

6.3.6.8. Calorimeter TC Temperature and Derived Heat Flux

Figure 6-207 through Figure 6-209 provide temperatures over time from TC measurements placed on the inner and outer cylinders, as well as external to the calorimeter. Figure 6-207 provides thermocouple temperatures on the outer surface of the inner cylinder. None of the inner thermocouples failed. Figure 6-208 provides thermocouple temperatures from the inner surface of the outer shell (midcase) of the calorimeter. The thermocouples at location 2L135°, 2L270°, 2C45°, 2C90°, and 2C270° failed. Figure 6-209 provides thermocouple temperatures on the exterior of the outer cylinder. None of the exterior thermocouples failed.

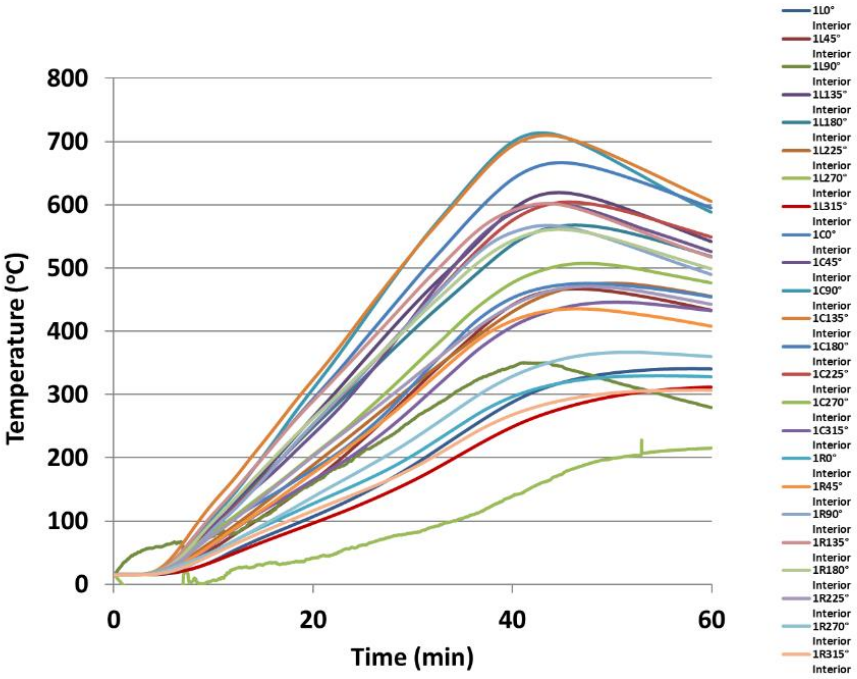

Figure 6-207: Thermocouple temperatures at inner cylinder stations (Test 3.6).

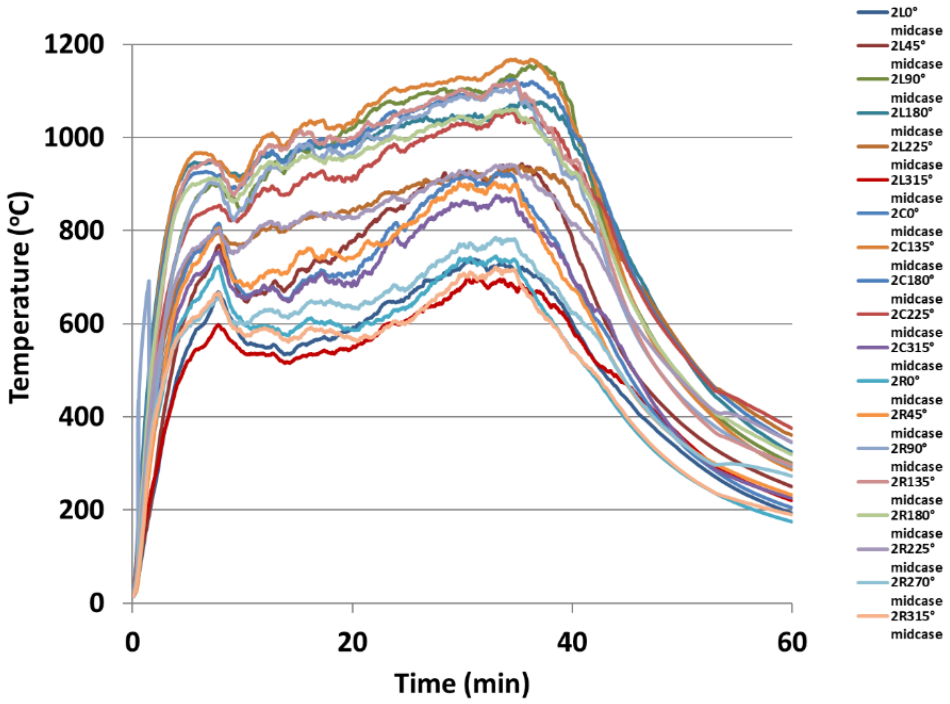

Figure 6-208: Thermocouple temperatures at outer cylinder stations (Test 3.6).

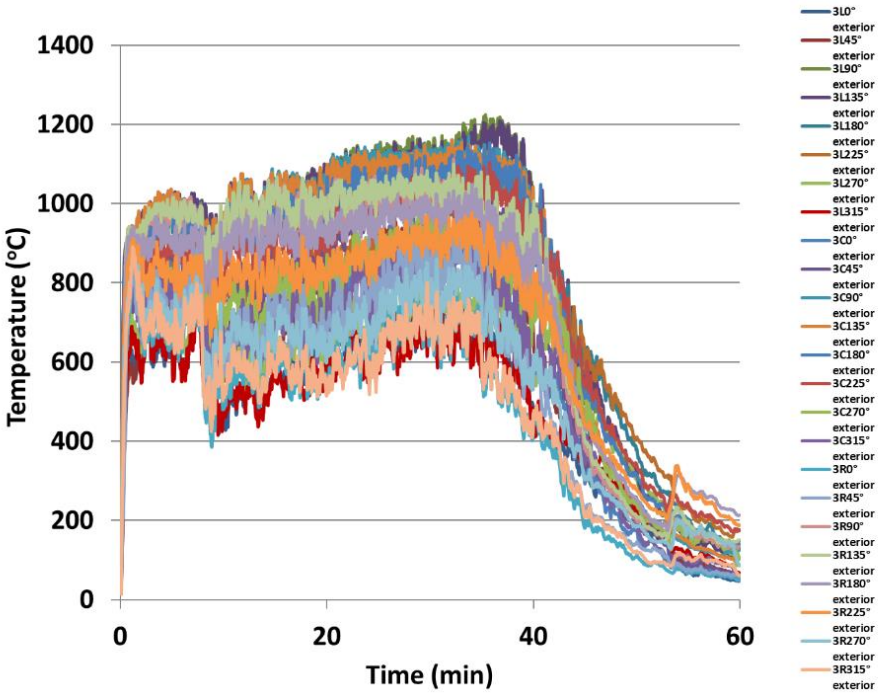

Figure 6-209: Thermocouple temperatures at exterior cylinder stations (Test 3.6).

6.3.6.8.1. Heat Flux to Calorimeter

Figure 6-210 and Figure 6-211 provide the absorbed and total heat flux to the calorimeter, respectively.

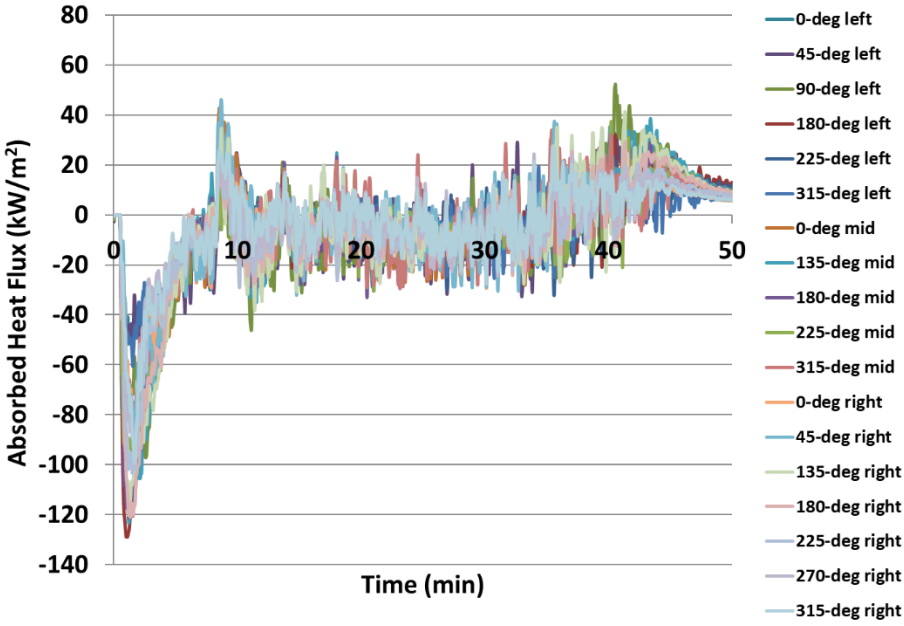

Figure 6-210: Absorbed heat flux to calorimeter (Test 3.6).

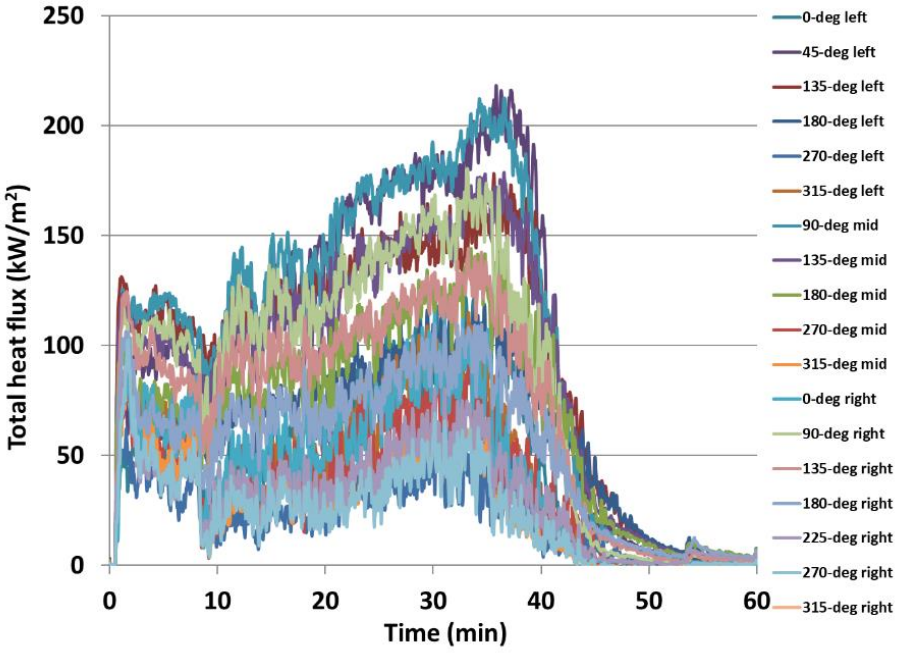

Figure 6-211: Total heat flux to calorimeter (Test 3.6).

6.3.6.9. Heat release rate

Data from the combustion gas analyzer was collected for this test but provided erroneous readings. The heat release rate based on evaluating the product of the heat of combustion (43.275 MJ/kg), mass flux (0.018 kg/m^{2}s), and pan area (3.14 m^2) is 2.45 MW.

6.3.6.10. Flame Height

Figure 6-212 shows the flame height as measured from the IR camera. The average flame height is 3.5 ± 0.8 m averaged over 3 to 30 minutes.

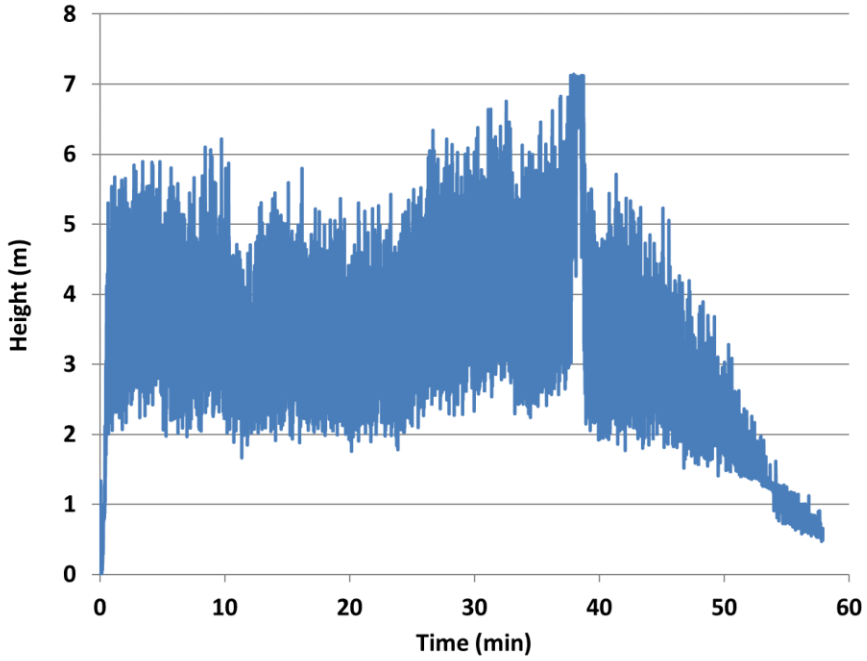

Figure 6-212: Flame height from IR camera measurements (Test 3.6).

This page left blank

7. COMPARISON OF TESTS WITHIN A SERIES

7.1. Burn rate

The following provides comparison of the burn rate among the tests within a series.

7.1.1. Heptane Pool Fire Tests

Table 7-1 and Table 7-2 provide the volume of fuel used and burn rate for each test, respectively. Figure 7-1 provides the burn rate data in graphical form. The burn rate for Test 1.1 was about 10% lower than for Tests 1.2 and 1.3. For Test 1.3, the fuel supply temperature was about a factor of 3 higher, thereby reducing the amount of energy required from the flame to bring the fuel to boiling temperature, thus allowing more energy from the flame to contribute towards fuel vaporization. If a linear trend can be assumed, then a 20% increase in burn rate compared to Test 1.1 is anticipated for a test with no calorimeter and the fuel heated to about 60°C. Individually, however, the fuel temperature and presence of the calorimeter do not have a large effect on the burn rate. This is based on a very limited number of tests. A larger dataset of around 10 to 15 repeat tests would allow assessment of this trend.

Table 7-1: Volume of heptane used for each heptane test.

Test	Volume gallons (liters)
1.1	138 (522)
1.2	145 (549)
1.3	144 (545)
Total	**427 (1616)**

Table 7-2: Burn rate for each heptane test.

Test	Calorimeter	Fuel supply temperature (°C)	burn rate		
			kg/min	mm/min	kg/m^{2}s
1.1	Yes (1 m)	22.3 ± 0.2	6.94	3.21 ± 0.04	0.037
1.2	No	24.2 ± 0.3	7.59	3.51 ± 0.04	0.040
1.3	Yes (1 m)	57.7 ± 0.4	7.54	3.49 ± 0.04	0.040

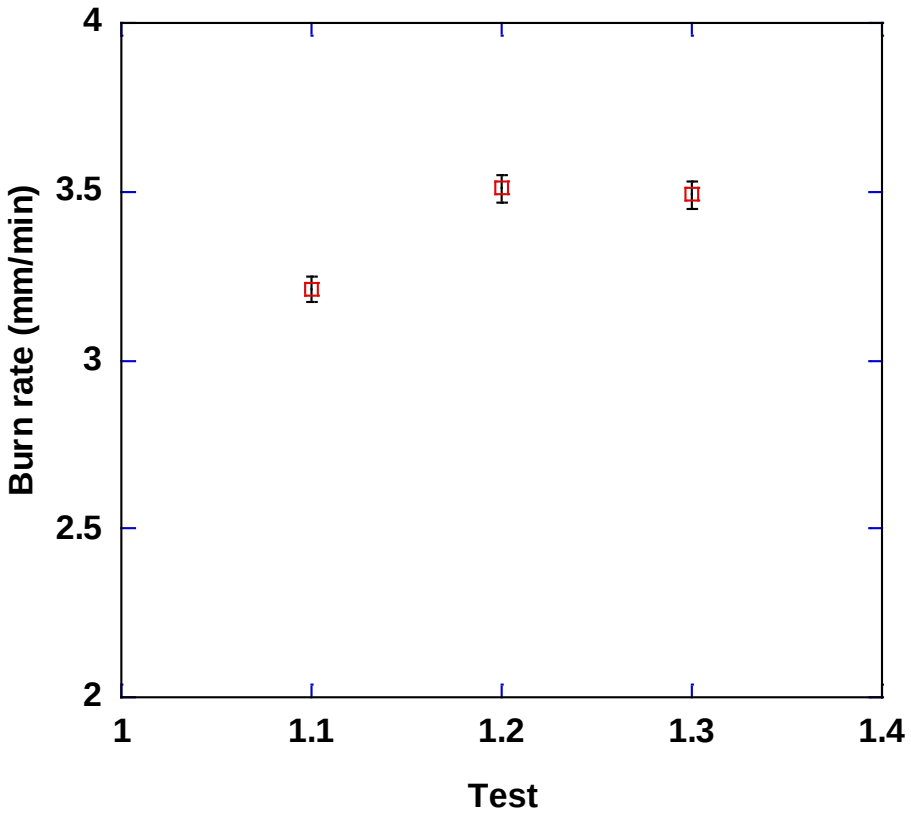

Figure 7-1: Burn rates for heptane tests.

7.1.2. Bakken Crude Pool Fire Tests

The burn rate averaged among all the tests is 2.1 mm/min. Table 7-3 and Table 7-4 provide the volume of fuel used and burn rate for each test, respectively. Figure 7-2 shows the burn rate for each test. The comparison among the tests indicates that fuel temperature and placement and presence of the calorimeter does not have a large effect on the burn rate. The burn rate values were higher without the calorimeter. Heating the fuel did not have a large effect on the burn rate. If the average of Tests 2.3 and 2.5 versus Test 2.4 are compared, the difference is about 8%. This is not a significant difference, as indicated by comparing the repeat Tests 2.3 and 2.5, which resulted in about a 5% difference in burn rate. For pool fire tests, having up to a 20% variation is not uncommon, due to the stochastic nature of pool fires.

Heating the fuel did not have a significant effect because the fuel becomes heated by the flame throughout its depth, thereby overriding the effect of incoming fuel temperature. For all the tests, the in-depth fuel temperature ranged from 200°C to 400°C which is significantly higher than the temperature of the incoming fuel. For example, Test 2.6, in which the fuel was immediately ignited upon introduction into the pan and then filled to 3 inches and allowed to burn down, all fuel rake TCs were at the same temperature of 100°C after the fuel reached target level. This temperature was reached at about the time fueling ended (~5 minutes). All TCs were submerged at this time since the height of the rake is about 2 inches and the fuel level 3 inches. The fuel burned down to reach the top of the rake after about 15 minutes from ignition. This demonstrates the relatively high in-depth fuel temperatures that are reached in a short duration, relative to the test duration. The plus and minus values for the burn rate in terms of mm per minutes is based on the resolution of the scale (0.09 kg).

Table 7-3: Volume of oil used for each Bakken crude oil test.

Test	Volume gallons (liters)
2.1	99 (375)
2.2	99 (375)
2.3	82.5 (312)
2.4	95.5 (362)
2.5	97 (367)
2.6	66 (250)
Total	**539 (2040)**

Table 7-4: Burn rate for each Bakken crude oil test.

Test	Calorimeter	Fuel supply temperature (C)	burn rate		
			kg/min	mm/min (+/-)	kg/m^{2}s
2.1	No	21.0 ±0.9	5.69	2.23 (+0.03/-0.02)	0.030
2.2	Yes (0.5-m)	21.7 ±0.5	4.81	1.89 (+0.03/-0.03)	0.026
2.3	Yes (1-m)	22.2 ±0.5	5.12	2.01 (+0.1/-0.1)	0.027
2.4	Yes (1-m)	58.2 ±1.0	5.41	2.12 (+0.03/-0.03)	0.029
2.5	Yes (1-m)	21.3 ±0.6	4.84	1.90 (+0.03/-0.03)	0.026
2.6	No	20.0 ±1.7	5.63	2.21 (+0.1/-0.09)	0.030

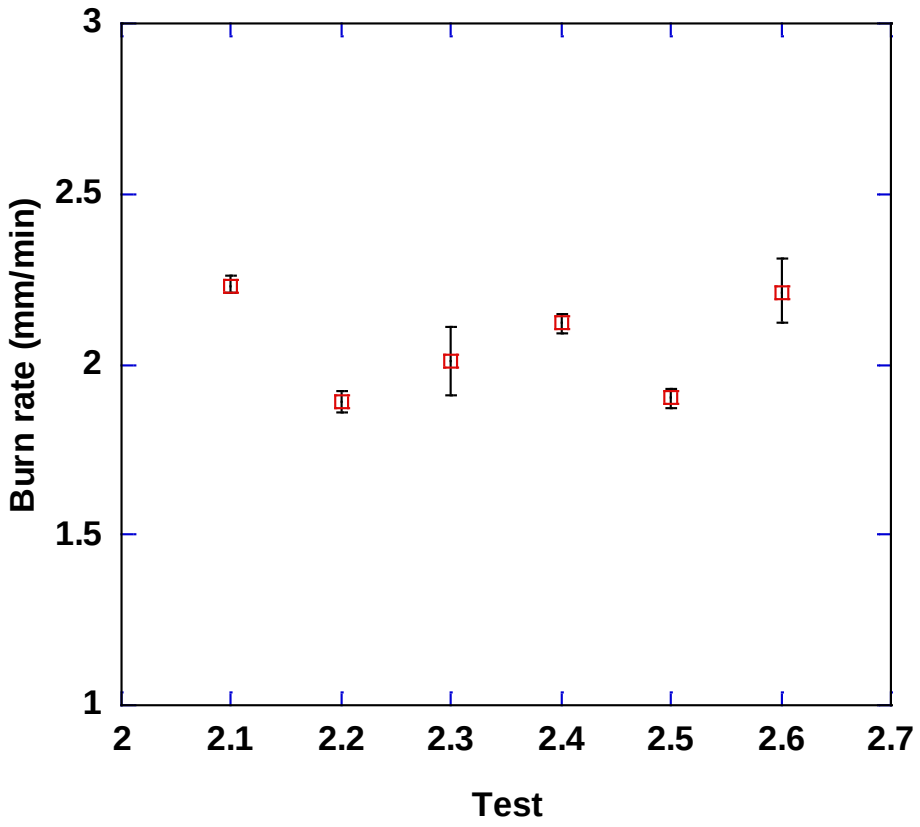

Figure 7-2: Burn rate for Bakken crude oil tests.

7.1.3. Dilbit Crude Pool Fire Tests

Table 7-5 provides the volume of crude oil used, the residue mass, and the residue percentage of the total fuel used for each test. The percentage of residue is highest for Test 3.4 since it burned for the longest duration of approximately 55 minutes versus 30 minutes. Note that the repeat tests, Test 3.1 and 3.5, resulted in the same percentage of residue.

Table 7-6 provides the burn rate for each test. A density of 924.2 kg/m^3 is used for any required conversions. This value is based on analysis of samples performed by InnoTech Alberta. The tests in which two values are provided indicate different periods in which a burn rate could be identified. The tests which indicate a range are those in which a burn rate over a continuous period could be identified. The plus and minus values for the burn rate in terms of mm per minute is based on the resolution of the scale (0.09 kg). Figure 7-3 shows a graphical comparison of the burn rate for each test. The range is the minimum and maximum values with the uncertainty added.

The burn rate averaged among all the tests is 1.7 mm/min. This average includes Test 3.1 which has a much higher burn rate than the other tests, including its repeat test, Test 3.5. As explained earlier, this most likely is due to the difficulty in achieving a constant level and thus is not as reliable a measurement as the repeat test. Also, recall that the repeat test allowed for the burn rate to be determined over the longest duration among all tests. The tests in which the calorimeter was placed 1 m above the pan, average burn rates that are in the range of 1-1.5 mm/min. For the test in which the calorimeter was placed at 0.5 m above the pan, the burn rate is initially higher than this range but then decreases to be within this range. For all the tests the burn rate displayed highly variable behavior. The test with the higher-temperature fuel feed, Test 3.6, displayed a wide range of

variability. The fuel temperature may have affected the burn rate for this crude oil, however, given the difficulty in determining the burn rate over the entire duration for all the tests it is difficult to draw a firm conclusion.

Table 7-5: Volume of oil used and residue mass for each dilbit crude oil test.

Test	Volume gallons (liters)	Residue mass, kg (lbs)	%residue of total mass of fuel
3.1	76.5 (289.8)	31.5 (69.3)	12
3.2	73.0 (276.5)	28.4 (62.5)	11
3.3	69.4 (263.0)	32.9 (72.4)	14
3.4	63.2 (239.4)	39.7 (87.3)	18
3.5	69.3 (262.6)	29.3 (64.5)	12
3.6	65.7 (248.8)	19.6 (43.1)	9
Total	**417 (1580)**	**194 (426)**	

Table 7-6: Burn rate for each dilbit crude oil test.

Test	Calorimeter	Fuel supply temperature (°C)	Burn Rate		
			kg/min	mm/min (+/-)	kg/m^{2}s
3.1	Yes (1 m)	21.7 ±± 0.5	9.3	3.21 (+0.03/-0.03)	0.049
			6.3	2.18 (+0.03/-0.03)	0.034
3.2	Yes (0.5 m)	22.1 ± 1.2	11.3	3.89 (+0.03/-0.03)	0.060
			4.3	1.47 (+0.03/-0.03)	0.023
3.3	No	17.6 ±± 0.1	3.2	1.11 (+0.03/-0.03)	0.017
			2.7	0.94 (+0.03/-0.03)	0.014
3.4	No	22.1 ± 1.5	3.4	1.16 (+0.03/-0.03)	0.018
3.5	Yes (1 m)	24.9 ± 0.4	2.9 – 3.7	1.00 – 1.27 (+0.04/-0.03)	0.015 -0.019
3.6	Yes (1 m)	57.3 ± 2.1	3.5	1.20 (+0.03/-0.04)	0.018
			0.95 - 1.8	0.32 – 0.62 (+0.03/-0.04)	0.005-0.010

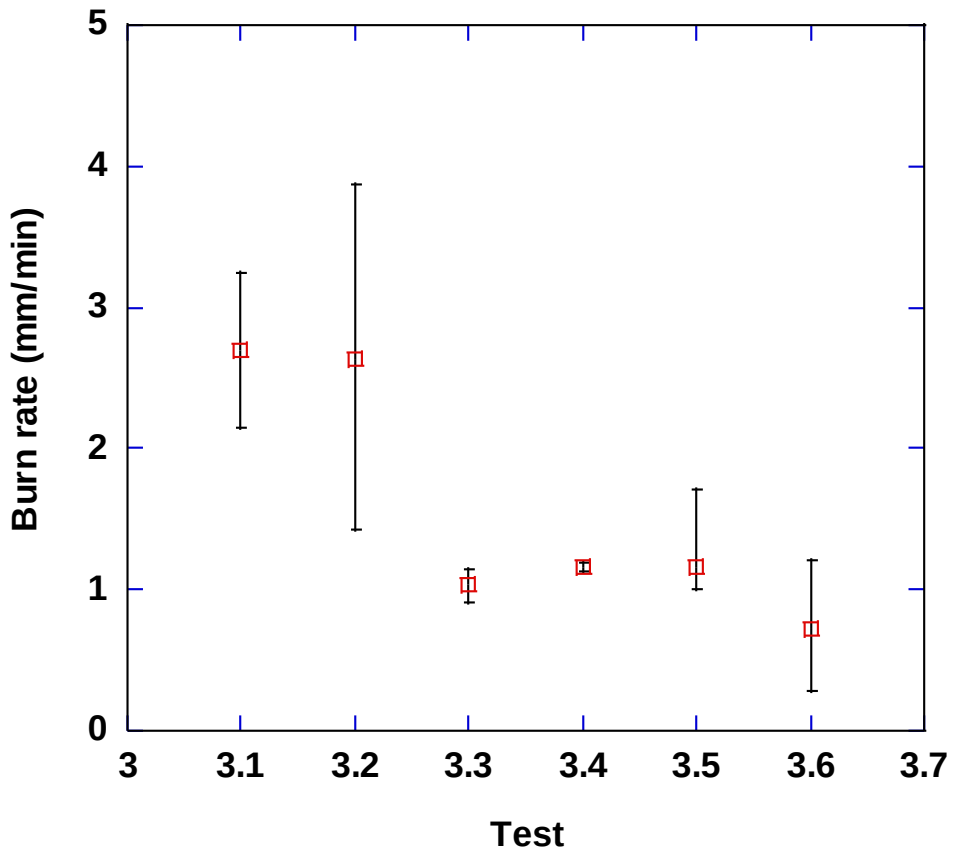

Figure 7-3: Burn rate for dilbit crude oil tests.

7.2. Radiometers

The following provides comparison of heat flux measurements from the narrow view and wide view radiometers among the tests within a series.

7.2.1. Heptane Pool Fire Tests

7.2.1.1. Narrow View

As shown in Table 7-7, measurements from the narrow view radiometers indicate that Test 1.2 had higher flux (~20 kW/m^2) readings at elevations of 3 m and 4 m, compared to Tests 1.1 and 1.3. This can be attributed to the higher flame height due to the lack of a calorimeter. Nominally, all tests had flux levels of 80-90 kW/m^2 at elevations below 3 m. When average heat flux values and their associated standard deviation for all tests are plotted (Figure 7-4), it can be seen that the ranges overlap for heights of 2 m and below, but not for the heights of 3 m and 4 m.

Table 7-7: Average heat flux measurements from narrow view radiometers for all heptane tests (measurements in kW/m^2).

	height (m)					
	0.5	**1**	**1.5**	**2**	**3**	**4**
Test 1.1*	89.1 ± 5.8	93.1 ± 7.7	91.3 ± 13.6	77.4 ± 16.5	47.6 ± 17.3	33.8 ± 17.9
Test 1.2**	94.7 ± 12.4	84.8 ± 15.3	84.4 ± 17.0	80.9 ± 17.5	70.4 ± 20.9	61.6 ± 26.5
Test 1.3***	88.9 ± 6.5	92.1 ± 7.8	96.4 ± 13.3	85.1 ± 17.7	53.9 ± 19.0	38.8 ± 20.3

*averaged over 20 – 30 minutes
** averaged over 15 – 35 minutes
***averaged over 24 – 44 minutes

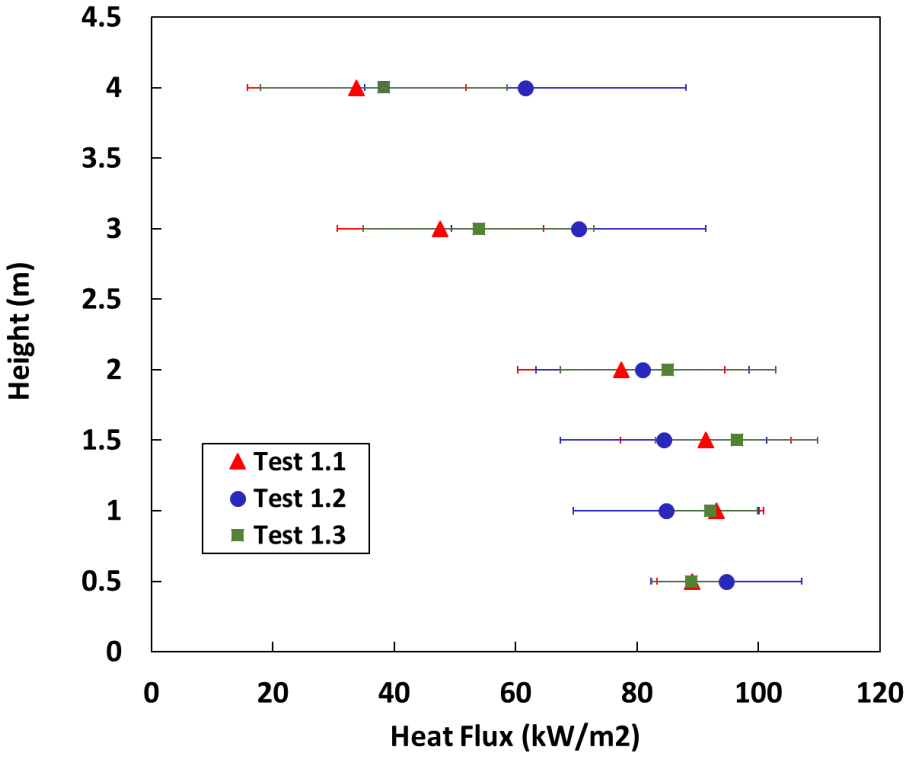

Figure 7-4: Narrow-view radiometer comparison among heptane tests.

7.2.1.2. Wide View

As shown in Table 7-8, measurements from the wide view radiometers indicate that all tests were within the range of one standard deviation of each other. Nominally, all tests had flux levels of 2.7 kW/m^2. Differences that occurred for the narrow view gauges are averaged out for the wide view radiometers, due to their greater field of view.

Table 7-8: Average heat flux measurements from wide view radiometers for heptane tests (measurements in kW/m^2).

	height (m)				
	1	**1.5**	**2**	**3**	**4**
Test 1.1*	2.3 ± 0.2	2.9 ± 0.2	2.5 ± 0.2	2.5 ± 0.2	2.3 ± 0.2
Test 1.2**	2.5 ± 0.3	3.1 ± 0.2	2.7 ± 0.3	2.7 ± 0.3	2.6 ± 0.3
Test 1.3 * **	2.4 ± 0.2	3.0 ± 0.2	2.6 ± 0.2	2.6 ± 0.2	2.4 ± 0.3

* averaged over 20 – 30 minutes
** averaged over 15 – 35 minutes
*** averaged over 24 – 44 minutes

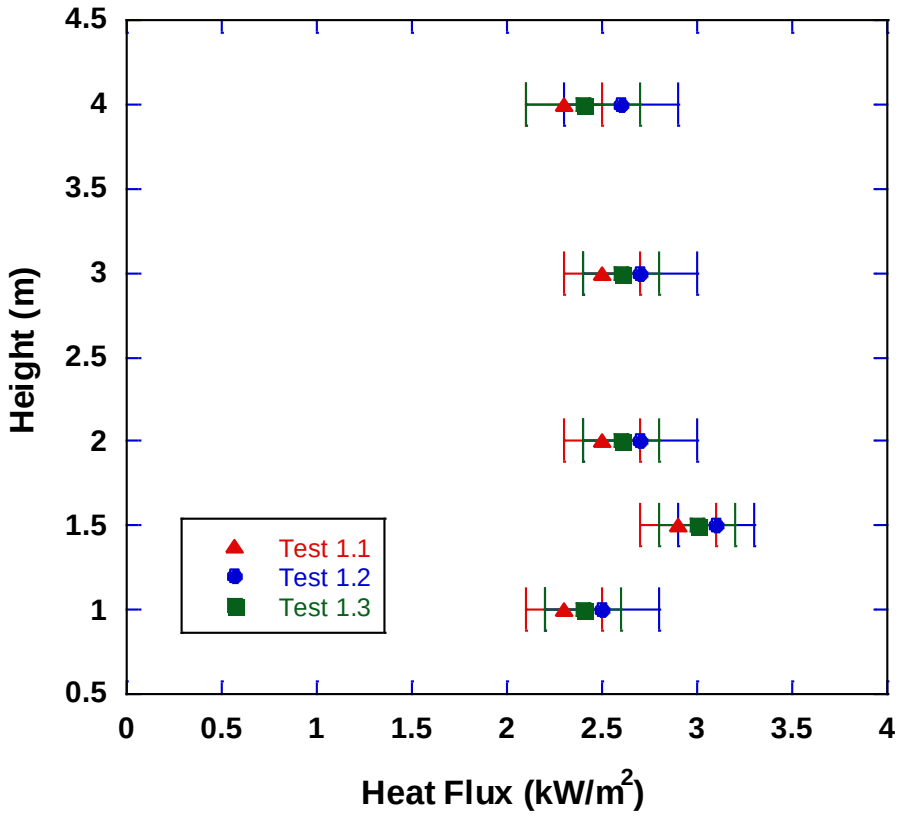

Figure 7-5: Wide-view radiometer comparison among heptane tests.

7.2.2. Bakken Crude Oil Pool Fires

7.2.2.1. Narrow View

The effect of the calorimeter is evident in comparing the narrow view radiometer measurements among tests (Table 7-9). Its presence tends to reduce the heat flux levels in its vicinity. Allowing the fuel to burn down tends to decrease the narrow view heat flux measurements, compared to maintaining a constant level. This is expected, since the height of the fire plume is decreasing in time. Tests 2.3 and 2.5 are repeat tests and indicate the stochastic nature of pool fire in the variance

of the averages; however, the standard deviation ranges do overlap. The change in fuel temperature did not seem to have a significant effect on the heat flux values. The largest variation among the tests occurs at elevations below 1 m, which is expected due to the presence of the calorimeter (Figure 7-6). Thus, the results indicate that the presence of the calorimeter has the largest effect on narrow view radiometer measurements.

Table 7-9: Average heat flux measurements from narrow view radiometers for all Bakken crude oil tests (measurements in kW/m^2).

	height (m)					
	0.5	**1**	**1.5**	**2**	**3**	**4**
Test 2.1 *	120.2 ± 10.3	102.5 ± 14.4	88.7 ± 20.2	73.9 ± 24.1	39.6 ± 23.9	22.0 ± 18.2
Test 2.2 **	99.6 ± 6.8	105.6 ± 13.6	86.5 ± 20.3	66.7 ± 23.5	31.0 ± 19.0	16.9 ± 14.4
Test 2.3 ***	58.4 ± 4.3	74.2 ± 14.3	77.0 ± 24.7	57.6 ± 25.4	24.6 ± 17.7	13.3 ± 14.3
Test 2.4 +	65.1 ± 4.2	84.1 ± 13.4	89.1 ± 23.0	68.2 ± 24.3	31.3 ± 18.0	16.4 ± 13.2
Test 2.5 ++	65.4 ± 4.0	85.1 ± 11.8	89.9 ± 20.6	68.1 ± 22.0	29.5 ± 15.9	14.8 ± 10.7
Test 2.6 +++	116.3 ± 11.2	93.6 ± 16.6	75.0 ± 22.5	60.7 ± 25.1	30.1 ± 20.8	15.5 ± 14.8

* averaged over 15 – 35 minutes
** averaged over 10 – 40 minutes
*** averaged over 10 – 30 minutes
\+ averaged over 23 – 42 minutes
\++ averaged over 20 – 35 minutes
\+++ averaged over 20 – 35 minutes

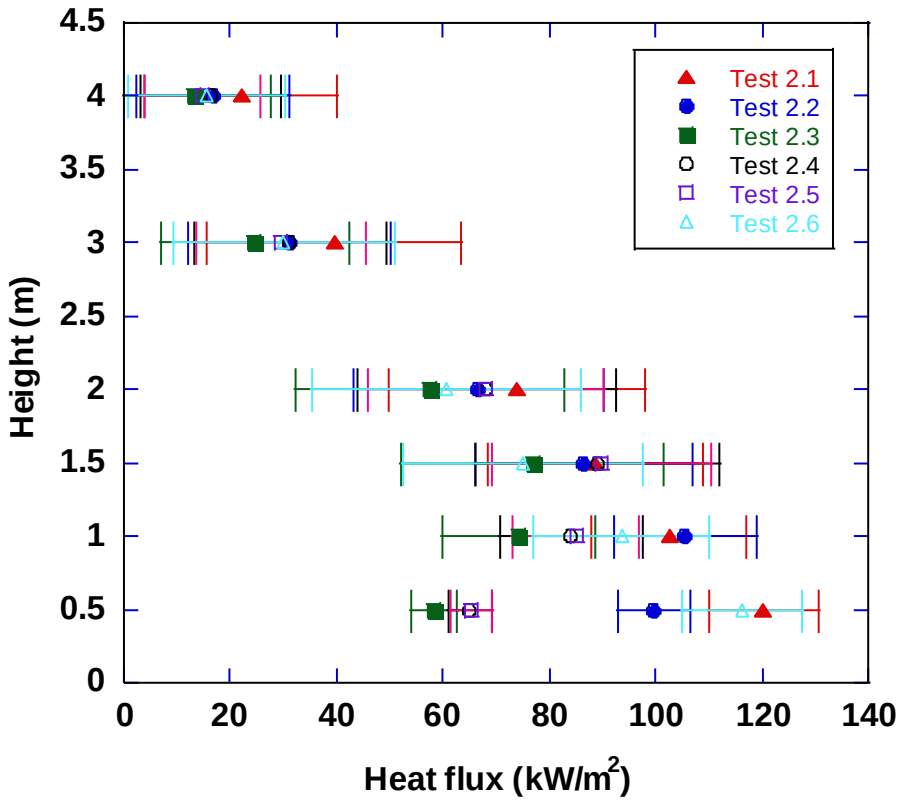

Figure 7-6: Narrow-view radiometer comparison among Bakken crude oil tests.

7.2.2.2. Wide View

As shown in Table 7-10 and Figure 7-7, the results are similar to that of the heptane tests for heat flux values measured from the wide view radiometers, in that values are fairly clustered due to the greater averaging that occurs with these instruments.

Table 7-10: Average heat flux measurements from wide view radiometers for all Bakken crude oil tests (measurements in kW/m^2).

	height (m)				
	1	**1.5**	**2**	**3**	**4**
Test 2.1*	2.3 ± 0.3	2.8 ± 0.2	2.5 ± 0.3	2.5 ± 0.3	2.2 ± 0.3
Test 2.2**	2.0 ± 0.2	2.4 ± 0.2	2.1 ± 0.2	2.1 ± 0.2	1.8 ± 0.2
Test 2.3***	1.8 ± 0.4	2.2 ± 0.4	1.9 ± 0.4	1.9 ± 0.4	1.7 ± 0.4
Test 2.4+	1.9 ± 0.3	2.4 ± 0.3	2.1 ± 0.3	2.1 ± 0.3	1.9 ± 0.3
Test 2.5++	1.9 ± 0.2	2.4 ± 0.2	2.1 ± 0.2	2.1 ± 0.2	1.9 ± 0.2
Test 2.6+++	2.1 ± 0.3	2.5 ± 0.3	2.2 ± 0.3	2.2 ± 0.3	2.0 ± 0.3

* averaged over 15 – 35 minutes
** averaged over 10 – 40 minutes
*** averaged over 10 – 30minutes
\+ averaged over 23 – 42 minutes
\++ averaged over 20 – 35 minutes
\+++ averaged over 20 – 35 minutes

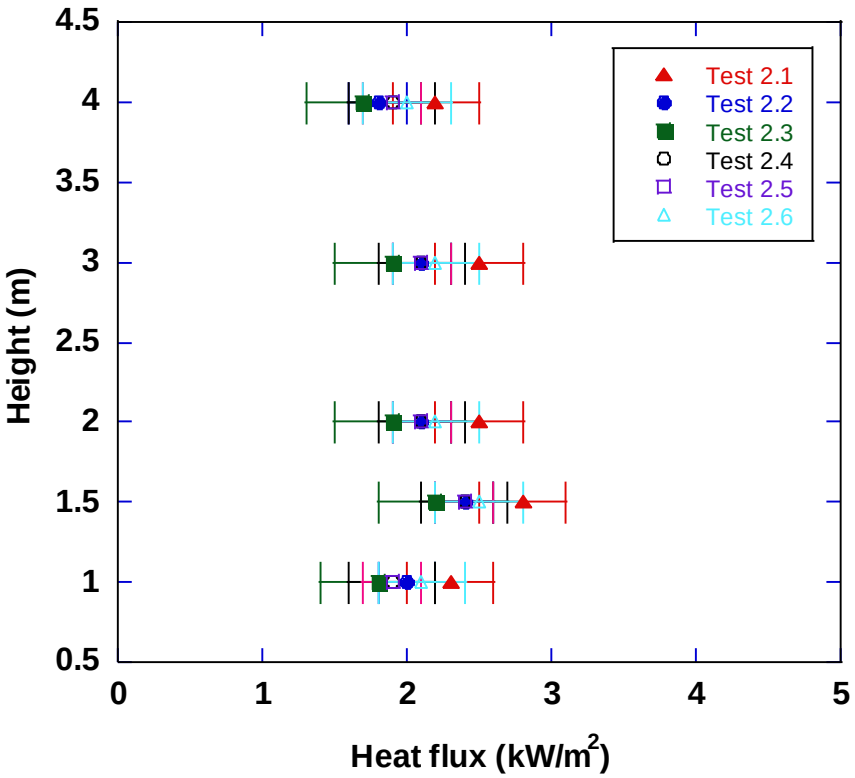

Figure 7-7: Wide-view radiometer comparison among Bakken crude oil tests.

7.2.3. Dilbit Crude Oil Pool Fires

As noted previously, none of the dilbit crude oil tests reached steady-state behavior. Thus, due to the variability in the measurements, averages are calculated by integrating the data and then dividing by the time over the period of integration. Since Test 3.1 was conducted up to 25 minutes radiometer data from all tests are integrated over the range of 0-25 minutes.

7.2.3.1. Narrow View

The integrated heat flux measurement from the narrow-view radiometers over 0-25 minutes for each test is provided in Table 7-11 and shown graphically in Figure 7-8. In comparing the tests with (Tests 3.1, 3.2, 3.5 and 3.6) and without (Tests 3.3 and 3.4) the calorimeter, the presence of the calorimeter reduces the heat flux values by about 20 – 30% at the 0.5-m and 1-m heights. Tests 3.1 and 3.5 are repeat tests and indicate the stochastic nature of pool fire in the variance of the averages; however, the standard deviation ranges do overlap. The change in fuel temperature did not seem to have a significant effect on the heat flux values. As seen with the Bakken crude oil tests, the presence of the calorimeter has the largest effect on narrow view radiometer measurements.

Table 7-11: Average heat flux measurements from narrow view radiometers for all Dilbit crude oil tests (measurements in kW/m^2).

Test	0.5	1	1.5	2	3	4
3.1	70.7 ± 12.9	56.1 ± 18.6	51.6 ± 25.0	36.9 ± 23.4	12.0 ± 12.0	5.5 ± 7.5
3.2	74.2 ± 14.8	72.5 ± 19.3	50.4 ± 20.2	36.0 ± 19.1	11.4 ± 8.3	4.9 ± 4.0
3.3	105.2 ± 21.8	73.4 ± 25.1	48.8 ± 26.6	35.1 ± 25.4	11.7 ± 12.3	4.6 ± 5.4
3.4	102.6 ± 22.6	74.3 ± 26.4	51.3 ± 27.9	37.2 ± 26.0	12.0 ± 11.8	4.9 ± 5.1
3.5	64.0 ± 14.3	59.6 ± 20.1	48.9 ± 24.4	33.0 ± 20.7	10.6 ± 8.7	4.6 ± 3.8
3.6	53.7 ± 8.2	53.0 ± 17.3	47.2 ± 24.9	33.2 ± 22.4	10.8 ± 10.3	4.8 ± 5.5

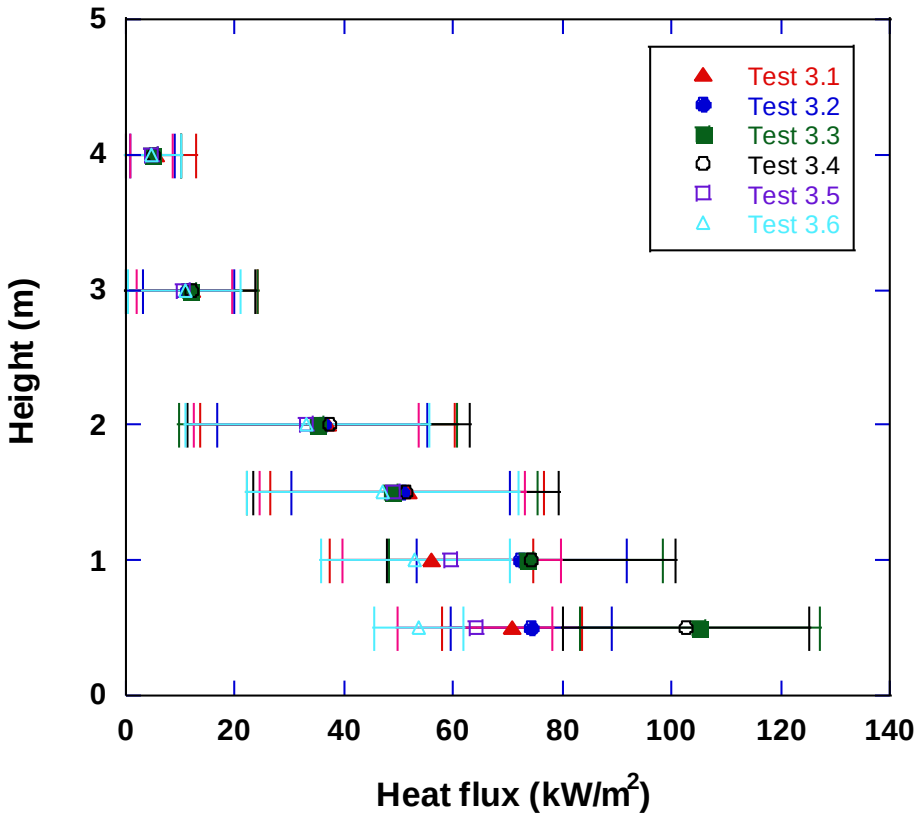

Figure 7-8: Narrow-view radiometer comparison among dilbit crude oil tests.

7.2.3.2. Wide View

The integrated heat flux measurement from the wide-view radiometers over 0-25 minutes for each test is provided in Table 7-12 and Figure 7-9. The results are similar to that for the heptane and Bakken crude oil tests, in that values are fairly clustered due to the greater averaging that occurs with these instruments.

Table 7-12: Integrated heat flux measurements from wide view radiometers for all dilbit crude oil tests (measurements in kW/m^2).

Test	1	1.5	2	3	4
3.1	1.1 ± 0.4	1.4 ± 0.4	1.2 ± 0.4	1.0 ± 0.4	1.0 ± 0.4
3.2	1.1 ± 0.3	1.4 ± 0.3	1.2 ± 0.3	1.1 ± 0.3	1.1 ± 0.3
3.3	1.4 ± 0.4	1.8 ± 0.4	1.6 ± 0.4	1.4 ± 0.4	1.4 ± 0.4
3.4	1.4 ± 0.4	1.7 ± 0.4	1.5 ± 0.4	1.3 ± 0.4	1.4 ± 0.4
3.5	1.1 ± 0.4	1.5 ± 0.4	1.3 ± 0.4	1.1 ± 0.3	1.1 ± 0.3
3.6	1.1 ± 0.3	1.4 ± 0.4	1.2 ± 0.4	1.1 ± 0.3	1.1 ± 0.3

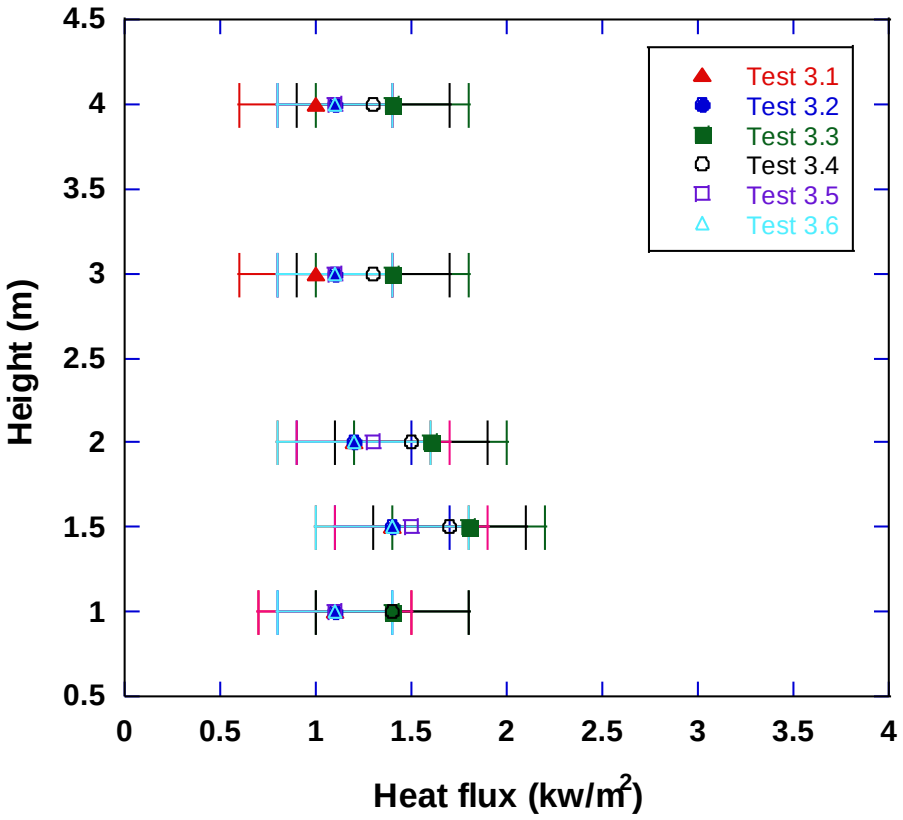

Figure 7-9: Wide-view radiometer comparison among dilbit crude oil tests.

7.3. Thermocouple Rake in Fire Plume

The following provides comparison of temperature measurements from the TC rake in the fire plume among the tests within a series.

7.3.1. Heptane Pool Fire Tests

The TC temperatures among the tests indicate that the heptane tests (1.1 and 1.3) with the calorimeter are fairly similar, thus indicating that fuel temperature did not have a significant effect (Table 7-13 and Figure 7-10). The presence of the calorimeter did significantly affect the measured

plume temperature, due to heat transfer from the flame to the calorimeter, as is evident from the much higher temperatures for Test 1.2 with no calorimeter.

Table 7-13: Average thermocouple rake temperatures in fire plume for heptane tests.

Test	1.1*	1.2**	1.3***
Height (m)	Temperature (°C)		
0.5	719.1 ± 50.1	na	660.0 ± 19.9
1.5	878.3 ± 20.7	848.2 ± 12.5	877.4 ± 18.1
2	798.6 ± 30.3	885.7 ± 15.5	835.4 ± 27.7
2.5	739.2 ± 32.8	897.4 ± 15.5	771.5 ± 31.4
3	652.1 ± 31.4	881.3 ± 21.0	698.0 ± 29.9
3.5	590.8 ± 29.2	854.5 ± 27.8	625.6 ± 33.8
4	557.5 ± 26.7	824.9 ± 32.2	591.1 ± 33.2
4.5	492.8 ± 23.7	756.7 ± 34.0	530.7 ± 29.0
5	428.4 ± 20.2	679.3 ± 31.7	460.0 ± 24.2
5.5	403.6 ± 23.2	620.3 ± 37.1	428.7 ± 28.0

* average over 20-35 minutes
** average over 20-37 minutes
*** average over 20-44 minutes

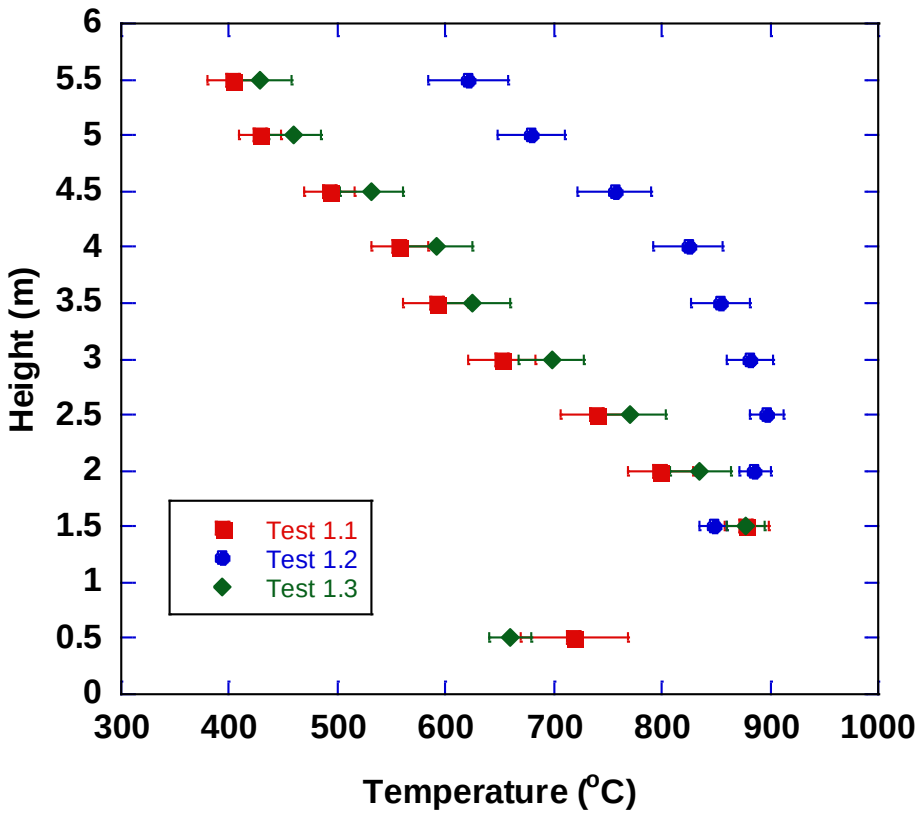

Figure 7-10: Thermocouple temperatures from fire plume rake for heptane tests.

7.3.2. Bakken Crude Oil Pool Fire Tests

For the Bakken crude oil tests, the TC temperatures did not differ significantly among the tests (Table 7-14 and Figure 7-11). Test 2.3 indicates a trend of lower temperatures, but its standard deviation does overlap with that of other tests.

Unlike the heptane tests, the presence of the calorimeter did not significantly affect the TC measurements. A possible explanation is the difference in soot production between the two fuels. Since the Bakken crude oil has heavier components, it is anticipated that it will produce more soot than heptane and consequently, there will be a higher propensity to produce smoke. The portions of the flame enveloped by the smoke have a reduction in heat transfer to the surroundings, since the smoke will absorb some of the emitted thermal radiation. This has the net effect of increasing internal flame temperatures. Thus, even though it takes energy to heat the calorimeter, it is effectively being transferred back into the flame since the loss to the surroundings is lower.

Table 7-14: Average thermocouple rake temperatures in fire plume for Bakken crude oil tests.

Test	2.1*	2.2**	2.3***	2.4+	2.5++	2.6+++
Height (m)	Temperature (°C)					
0.18	na	672.7 ± 40.4	na	na	na	na
0.5	na	na	967.8 ± 79.3	971.5 ± 51.5	973.5 ± 19.5	na
1.5	938.4 ± 30.2	935.9 ± 33.0	847.8 ± 56.5	925.7 ± 45.2	932.8 ± 33.3	949.9 ± 46.8
2	890.3 ± 34.3	904.3 ± 33.2	757.5 ± 68.2	854.3 ± 60.2	858.1 ± 35.6	882.6 ± 52.2
2.5	799.9 ± 43.2	814.5 ± 41.1	621.3 ± 83.4	727.4 ± 74.9	726.0 ± 38.1	770.3 ± 63.4
3	688.3 ± 43.5	714.3 ± 43.7	521.7 ± 85.6	616.2 ± 78.0	615.5 ± 28.2	660.1 ± 59.6
3.5	573.8 ± 48.0	610.6 ± 47.9	420.2 ± 95.0	504.7 ± 81.1	507.4 ± 23.2	537.4 ± 63.1
4	485.3 ± 41.6	529.3 ± 48.4	360.8 ± 87.5	431.3 ± 74.1	423.8 ± 17.2	447.5 ± 57.3
4.5	391.8 ± 30.1	439.0 ± 40.9	302.7 ± 74.8	349.4 ± 59.0	343.0 ± 12.0	366.9 ± 38.6
5	318.1 ± 22.9	355.8 ± 32.9	250.1 ± 60.6	282.4 ± 43.9	275.9 ± 9.6	302.7 ± 25.2
5.5	269.0 ± 20.2	301.3 ± 27.6	220.2 ± 58.1	243.6 ± 37.2	238.0 ± 10.0	253.8 ± 21.6

* averaged over 15 – 35 minutes
** averaged over 10 – 40 minutes
*** averaged over 10 – 30minutes
+ averaged over 23 – 42 minutes
++ averaged over 20 – 35 minutes
+++ averaged over 22.5 – 32.5 minutes

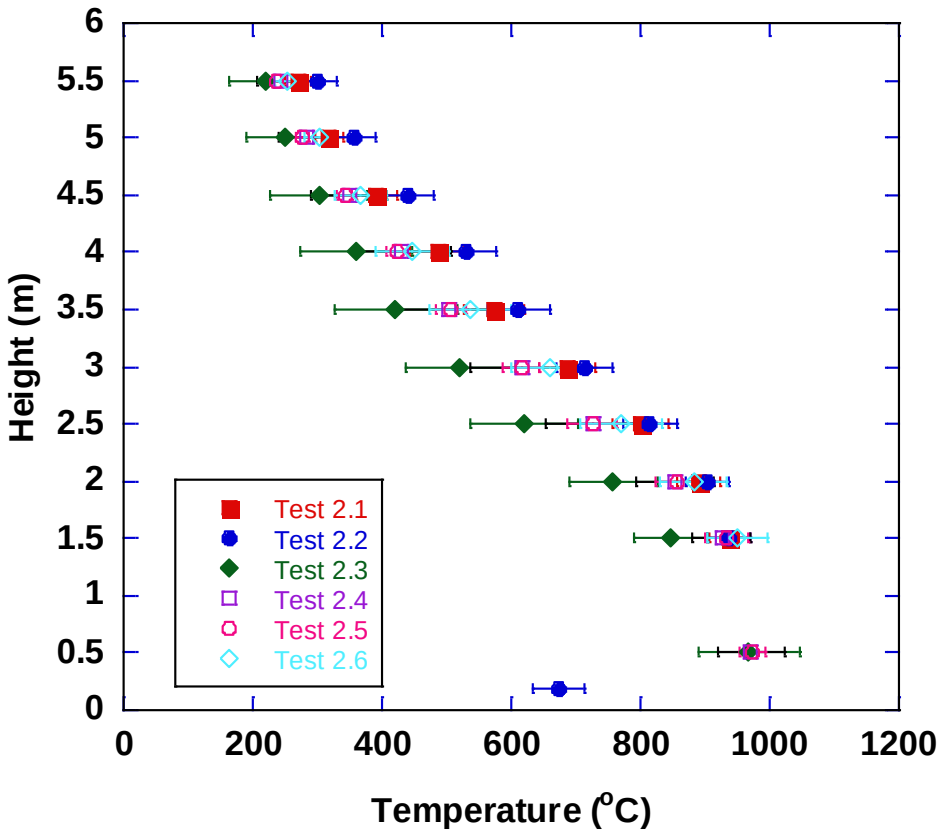

Figure 7-11: Thermocouple temperatures from fire plume rake for Bakken crude oil tests.

7.3.3. Dilbit Crude Oil Pool Fire Tests

Similar to the radiometer data, the temperature measurements from the centerline thermocouple rake are averaged by integrating the data from 0-25 minutes and dividing by this period. Temperature measurements from the plume thermocouple rake, averaged based on integrating over 0-25 minutes, are provided in Table 7-15 and Figure 7-12. The results indicate that average temperatures are similar among all the tests and that the highest average temperatures occur at the height of 0.5 m above the pan.

Table 7-15: Average thermocouple rake temperatures in fire plume for Dilbit crude oil tests.

Test	3.1	3.2	3.3	3.4	3.5	3.6
Height (m)	Temperature (°C)					
0.18	na	874.6 ±127.2	na	na	na	na
0.5	901.9 ± 122.6	na	na	na	964 ± 186.3	903.6 ± 86.3
1.5	396.9 ± 107.2	421.9 ±81.0	430.8 ± 100.8	419.2 ± 107.8	454.2 ± 110.6	424.7 ± 104.1
2	307.9 ± 88.3	335.1 ±65.5	332.7 ± 84.6	328.6 ± 87.6	361.8 ± 90.6	338.1 ± 90.7
2.5	238.4 ± 70.1	262.5 ±52.8	248 ± 68.0	249.6 ± 66.7	290 ± 72.8	269 ± 75.7
3	191.0 ± 56.8	201.0 ±39.2	183.7 ± 51.4	185.7 ± 47.8	226.3 ± 55.6	205.4 ± 56.8
3.5	163.8 ± 49.3	172.5 ±33.1	148.2 ± 40.9	153 ± 37.6	192.6 ± 46.5	172.5 ± 47.6
4	145.4 ± 43.0	153.1 ±28.6	127.2 ± 33	134.7 ± 31.6	169.8 ± 39.6	153.3 ± 41.5
4.5	128.4 ± 36.1	134.6 ±25.1	108.5 ± 26.4	116.2 ± 25.8	147.8 ± 33	132 ± 33
5	114.7 ± 31.1	119.6 ±21.8	94.8 ± 22.5	102.5 ± 22	131.7 ± 28.7	116.6 ± 28.4
5.5	107.3 ± 28.8	111.4 ±20.0	86.5 ± 20.1	96.3 ± 20.5	122.9 ± 26.1	109 ± 26.7

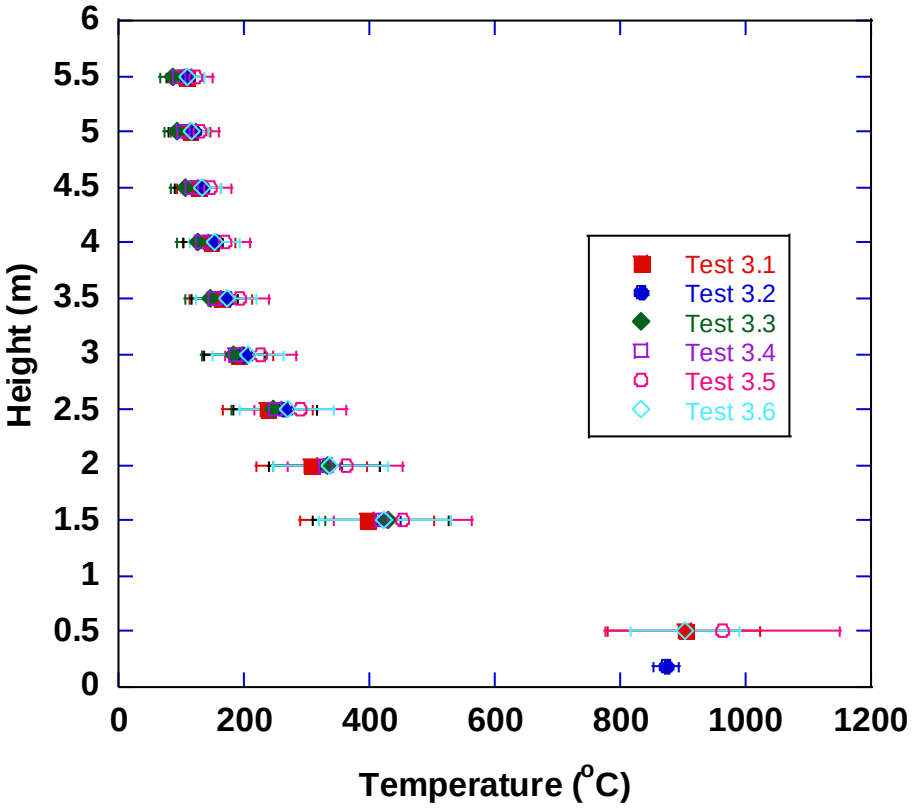

Figure 7-12: Thermocouple temperatures from fire plume rake for Dilbit crude oil tests.

7.4. Plume Temperatures and Surface Emissive Power

The following provides comparison of IR measurements of plume temperatures and surface emissive power among the tests within a series.

7.4.1. Heptane Pool Fire Tests

Table 7-16 provides the mean fire plume temperature and surface emissive power determined by the IR camera for Test 1.1. The other two tests did not include IR measurements. The period of averaging is taken over 2-53 minutes and the range is one standard deviation.

Table 7-16: Mean plume temperatures and surface emissive power for heptane test 1.1 from IR camera.

Test	Temperature (K)		Surface Emissive Power (kW/m^2)	
	Mean	Max.	Mean	Max.
1.1	917.6 ± 136.7	1219.1 ± 26.4	65.5 ± 6.3	180.6 ± 14.5

Note: Assumed optical transmission for the calculation of 0.95. Assumed emissivity of 0.97.

7.4.2. Bakken Crude Oil Pool Fire Tests

Average fire plume temperatures and surface emissive power values are provided in Table 7-17. Figure 7-13 and Figure 7-15 provide graphical comparison among the tests for average temperature

and average surface emissive power, respectively. The results indicate that the average temperature and surface emissive power are similar among the tests with no significant effect of the presence of the calorimeter, fuel supply temperature, or maintaining a constant fuel level. In comparison to the heptane test results, the average surface emissive power is slightly higher but within the range of standard deviations. As mentioned previously, the Bakken crude oil is expected to produce more soot, and therefore may be closer to the soot saturated limit than heptane, thereby resulting in a higher surface emissive power. Figure 7-13 and Figure 7-14 indicate that the IR measurements and TC rake in the fire plume are in agreement with regards to the range of measured temperatures. The ranges in Figure 7-14 are averages of the standard deviation values in Table 7-14.

Table 7-17: Average plume temperatures and surface emissive power for Bakken crude oil tests from IR camera. Optical transmission of 0.95 and emissivity of 1.0.

Test	Temperature (K)		Surface Emissive Power (kW/m^2)	
	Mean	Max.	Mean	Max.
2.1*	904.3 ± 151.3	1265.5 ± 27.7	75.2 ± 11.7	200.8 ± 16.4
2.2**	922.9 ± 158.0	1261.9 ± 31.6	74.9 ± 10.4	200.3 ± 18.4
2.3***	929.8 ± 165.6	1272.2 ± 28.8	76.5 ± 10.3	203.0 ± 17.1
2.4+	944.2 ± 172.6	1279.5 ± 25.1	78.7 ± 10.4	207.2 ± 15.1
2.5++	942.6 ± 171.6	1279.7 ± 28.1	77.3 ± 10.3	206.1 ± 16.8
2.6+++	901.3 ± 147.4	1258.0 ± 29.3	73.6 ± 11.3	195.9 ± 17.0

*averaged over 2-45 minutes
**averaged over 2-52 minutes
***averaged over 2-35 minutes
+averaged over 2-44 minutes
++averaged over 2-48 minutes
+++averaged over 2-28 minutes

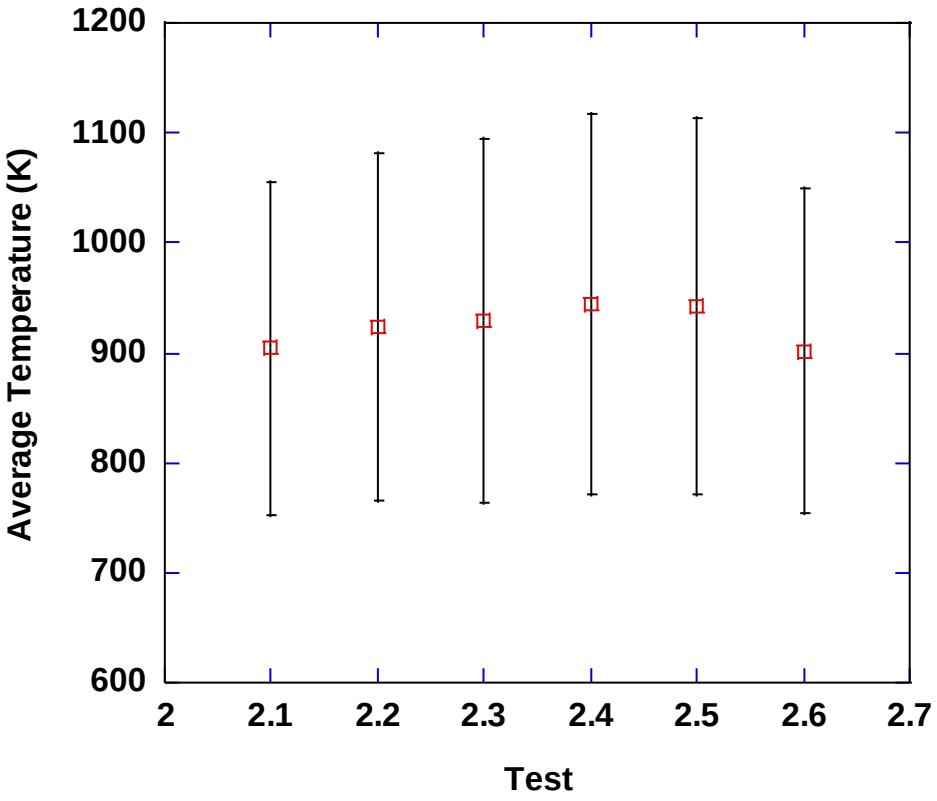

Figure 7-13: Average fire plume temperatures for the Bakken crude oil tests from IR camera.

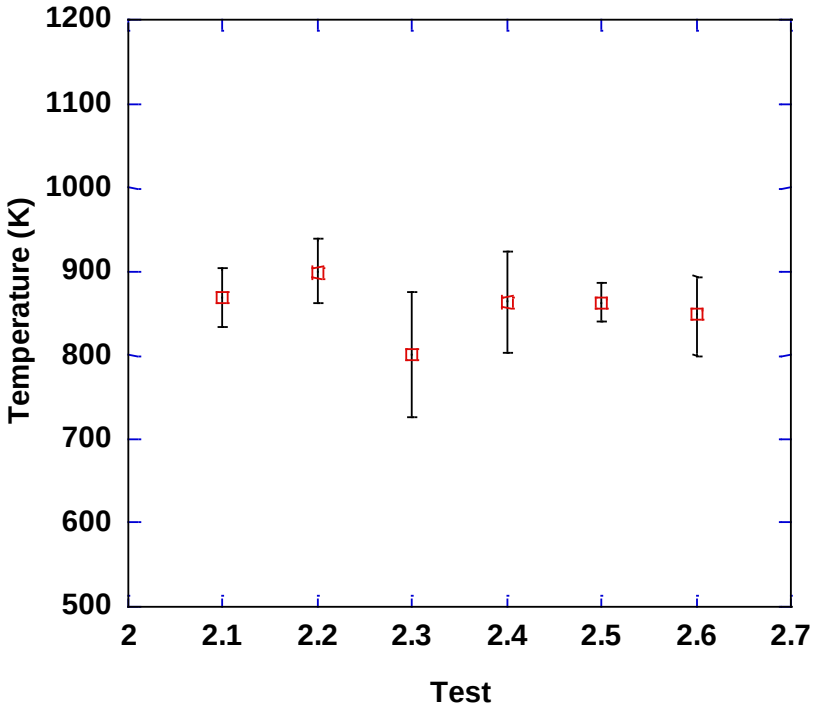

Figure 7-14: Average of all TC rake locations in fire plume for Bakken crude oil tests

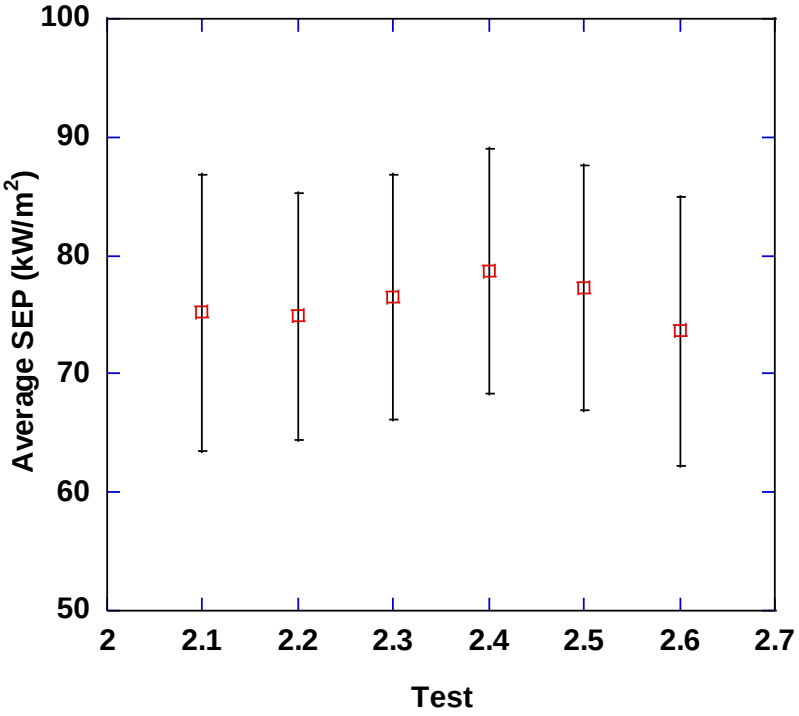

Figure 7-15: Average surface emissive power values for the Bakken crude oil tests from IR camera.

7.4.3. Dilbit Crude Oil Pool Fire Tests

Average plume temperatures and surface emissive power values from the IR camera are provided in Table 7-18. The range is standard deviation. Figure 7-16 and Figure 7-18 provide graphical comparison among the tests for average temperature and average surface emissive power, respectively. The results indicate that the average temperature and surface emissive power are similar among the tests with no significant effect of the presence of the calorimeter, fuel supply temperature, or maintaining a constant fuel level. Note that for Test 3.1 the factory calibration for the camera was used, whereas the other tests used an in-house calibration which has a lower range of temperature (450°C to 1200°C) that can be processed. The lower range for the factory calibration is about 550°C, thus the average is higher for Test 3.1 compared to the other tests. The in-house calibration was used for the previous test series; however, the factory calibration was inadvertently used for Test 3.1.

Comparison to time-averaged temperature values from the plume thermocouple rake averaged over all locations is also provided in Figure 7-17. The ranges are averages of the standard deviations in Table 7-15. Locations only up to 4-m were included in the average since the flame did not engulf thermocouples above this height. Average temperatures from the rake are lower than those measured from the IR camera which may be due to differences in the amount of data collected. Recall that the IR camera collects measurements over the entire outer surface of the flame whereas the TC rake has relatively few sampling locations internal to the flame.

Table 7-18: Average plume temperatures and surface emissive power for dilbit crude oil tests from IR camera.

Test	Temperature (K)		Surface Emissive Power (kW/m^2)	
	Mean	Max.	Mean	Max.
3.1*	1075.0 ± 157.3	1265.9 ± 103.3	77.7 ± 7.4	194.3 ± 20.3
3.2**	930.1 ± 155.8	1233.8 ± 26.2	69.8 ± 8.2	173.3 ± 13.7
3.3**	912.7 ± 158.5	1252.0 ± 30.2	71.1 ± 9.6	188.5 ± 17.1
3.4$^+$	914.1 ± 157.5	1246.3 ± 33.9	69.8 ± 8.9	188.2 ± 19.3
3.5^{++}	938.4 ± 170.6	1259.5 ± 28.6	72.6 ± 7.4	191.5 ± 16.5
3.6^{+++}	934.5 ± 166.5	1250.6 ± 33.5	72.2 ± 7.6	192.7 ± 19.2

*averaged over 2-21 minutes
**averaged over 2-24 minutes
***averaged over 2-36 minutes
$^+$averaged over 2-34 minutes
$^{++}$averaged over 2-34 minutes
$^{+++}$averaged over 2-34 minutes

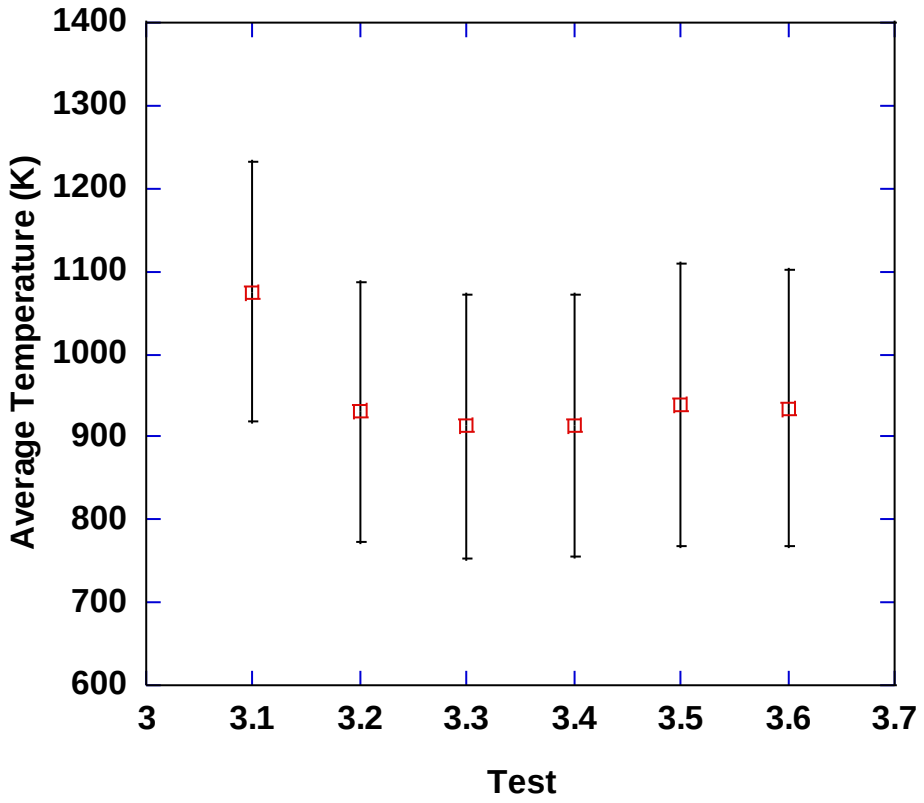

Figure 7-16: Average fire plume temperatures for the Dilbit crude oil tests from IR camera.

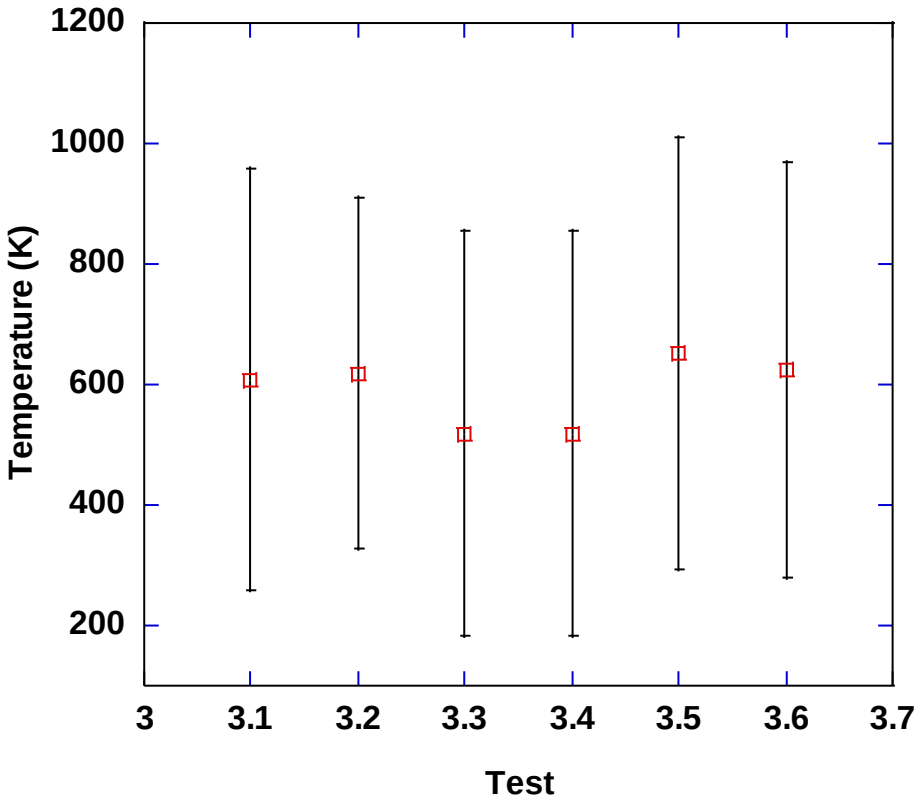

Figure 7-17: Average of all TC rake locations up to 4 m in fire plume for Dilbit crude oil tests.

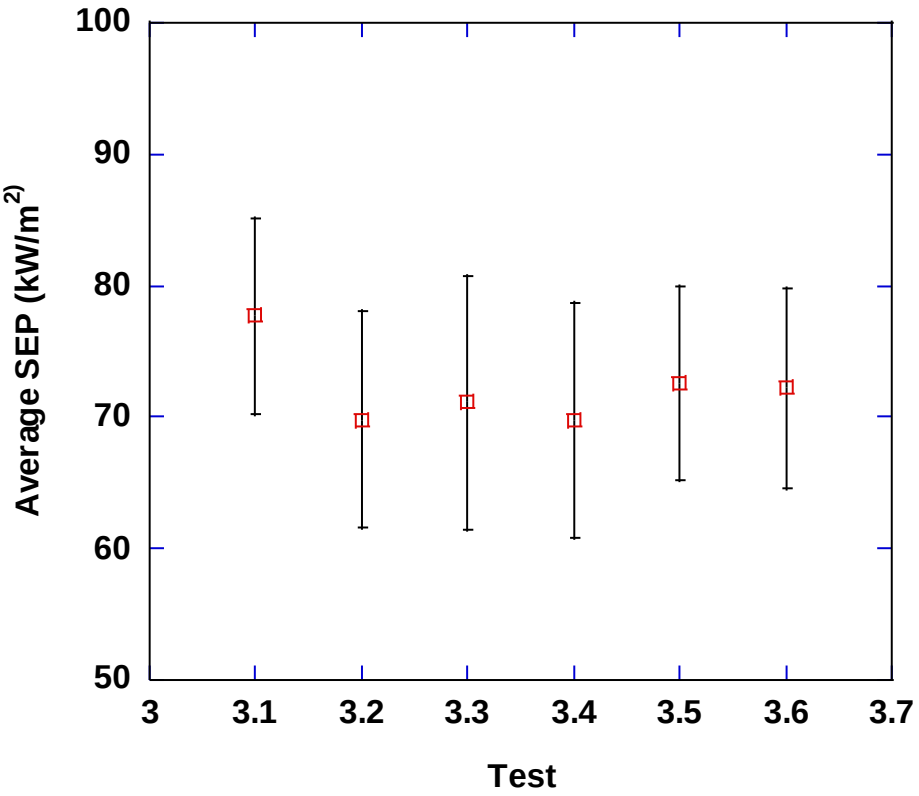

Figure 7-18: Average surface emissive power values for the Dilbit crude oil tests from IR camera.

7.5. DFT TC Temperatures and Derived Heat Flux

The following provides comparison of the DFT temperatures and derived heat flux among the tests within a series.

The heat flux from the flame to the DFT was derived from DFT TC measurements using a one-dimensional inverse heat conduction code, IHCP1D, developed by James Beck [3]. Descriptions of the energy balance, emissivity values, and thermal properties are provided in Appendix A.1.

7.5.1. Heptane Pool Fire Tests

Table 7-19 provides the average temperature and heat flux values from the DFT instruments for each test. The range is one standard deviation. Figure 7-19 and Figure 7-20 provide graphical comparison of absorbed and incident heat flux, respectively. The results indicate that Test 1.3 had a higher incident heat flux level than the other tests. The lowest incident flux level occurred for Test 1.2 without the calorimeter. The calorimeter potentially contributed to the flux due to reradiation from the calorimeter back to the DFT. Reradiation refers to the calorimeter emitting radiative heat after absorbing heat from the flame. The results indicate that the absorbed flux is similar among the tests.

Table 7-19: Average DFT temperature and heat flux values for the heptane tests.

Test	Distance from pool center (m)	Temperature (°C)		Heat flux (kW/m^2)	
		Front plate	Back plate	Absorbed	Incident
1.1*	2	494.3 ± 1.7	178.4 ± 3.8	-1.5 ± 1.0	39.4 ± 1.2
	4	304.5 ± 1.5	103.2 ± 5.4	-0.9 ± 0.4	18.2 ± 0.5
1.2**	2	466.0 ± 1.2	156.4 ± 3.4	-1.5 ± 0.8	35.5 ± 1.0
	4	264.5 ± 2.1	88 ± 4.6	-0.8 ± 0.3	15.1 ± 0.4
1.3***	2	525.0 ± 1.1	188.9 ± 2.2	-1.8 ± 0.9	44.2 ± 1.1
	4	299.6 ± 2.1	101.9 ± 3.6	-0.9 ± 0.4	17.8 ± 0.5

*averaged over 20-35 minutes
**averaged over 20-37 minutes
***averaged over 24-44 minutes

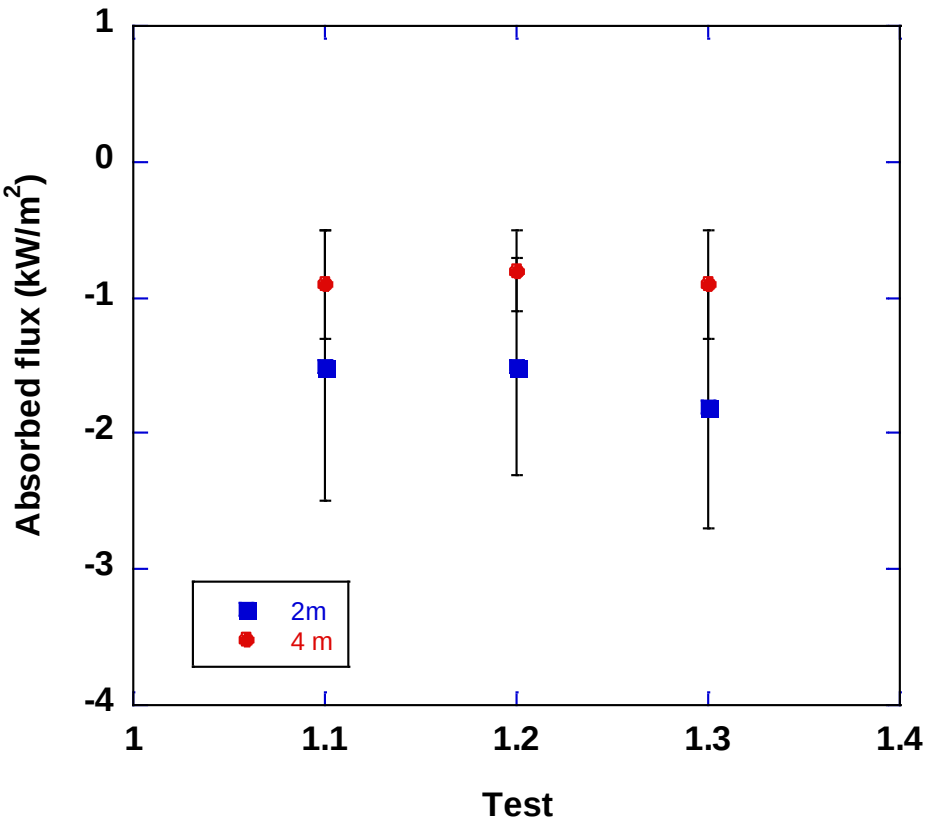

Figure 7-19: Average DFT absorbed heat flux for heptane tests.

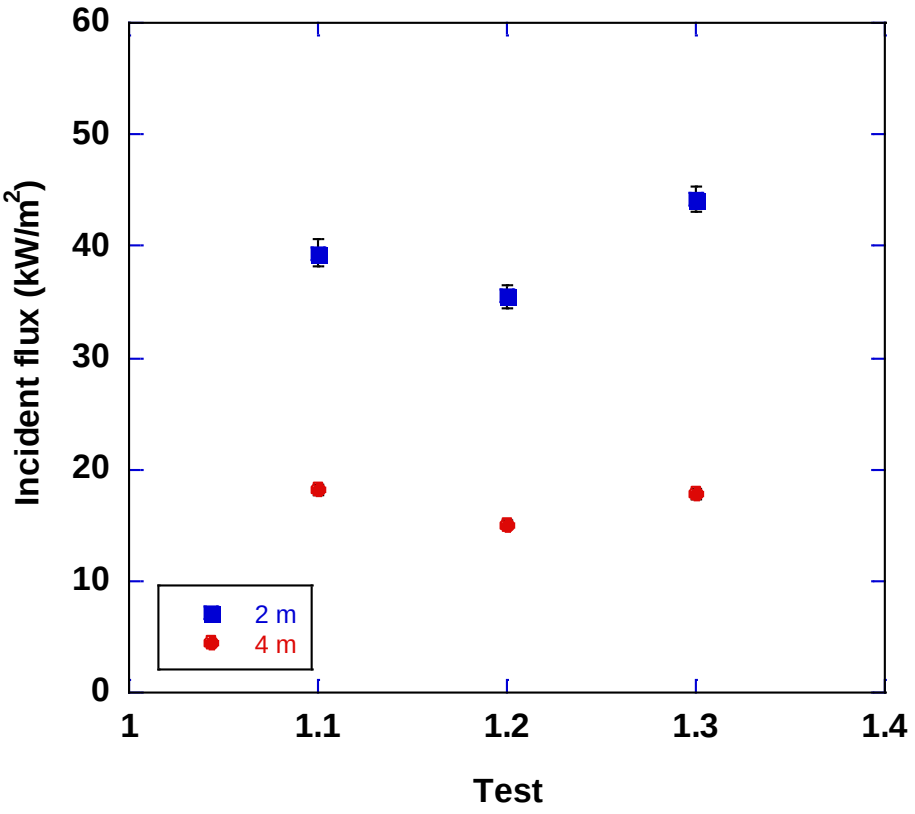

Figure 7-20: Average DFT incident heat flux for heptane tests.

7.5.2. Bakken Crude Oil Pool Fire Tests

Table 7-20 provides average DFT temperature and heat flux values for all Bakken crude oil tests. As seen in Figure 7-21, the absorbed flux are fairly similar among the tests, while Figure 7-22 indicates that the incident heat flux for Tests 2.2 and 2.6 are lower than other tests. Test 2.2 had the calorimeter at the lowest elevation and Test 2.6 did not maintain a constant fuel level. The range is one standard deviation.

Note that the repeat tests, Tests 2.3 and 2.5 differ by about 8 kW/m^2, which is indicative of the inherent stochastic nature of fire.

Table 7-20: Average DFT temperature and heat flux values for the Bakken crude oil tests.

Test	Distance from pool center (m)	Temperature (°C)		Heat flux (kW/m^2)	
		Front plate	Back plate	Absorbed	Incident
2.1*	2	558.0 ± 2.0	191.8 ± 4.4	-2.1 ± 1.3	49.8 ± 1.6
	4	292.3 ± 2.1	97.5 ± 5.8	-0.7 ± 0.6	17.0 ± 0.7
2.2**	2	466.0 ± 1.2	156.4 ± 3.4	-1.5 ± 0.8	33.6 ± 1.2
	4	264.5 ± 2.1	88 ± 4.6	-0.8 ± 0.3	15.1 ± 0.4
2.3***	2	574.3 ± 3.7	199.0 ± 5.7	-2.0 ± 1.5	52.5 ± 2.0
	4	302.9 ± 4.9	92.0 ± 6.4	-1.1 ± 1.4	18.3 ± 1.7
2.4+	2	581.2 ± 4.0	203.0 ± 4.8	-2.1 ± 1.4	53.8 ± 1.9
	4	310.4 ± 5.1	99.4 ± 7.5	-0.9 ± 0.9	18.8 ± 1.1
2.5++	2	525.0 ± 1.1	188.9 ± 2.2	-2.1 ± 1.1	32.1 ± 1.4
	4	299.6 ± 2.1	101.9 ± 3.6	-1.1 ± 0.4	7.8 ± 0.4
2.6+++	2	539.4 ± 2.6	181.1 ± 9.9	-1.5 ± 1.1	32.4 ± 1.4
	4	279.2 ± 4.5	90.7 ± 9.2	-0.7 ± 0.4	8.3 ± 0.3

*averaged over 20-37 minutes
**averaged over 20-40 minutes
***averaged over 20-33 minutes
+averaged over 20-40 minutes
++averaged over 20-33 minutes
+++averaged over 15-36 minutes

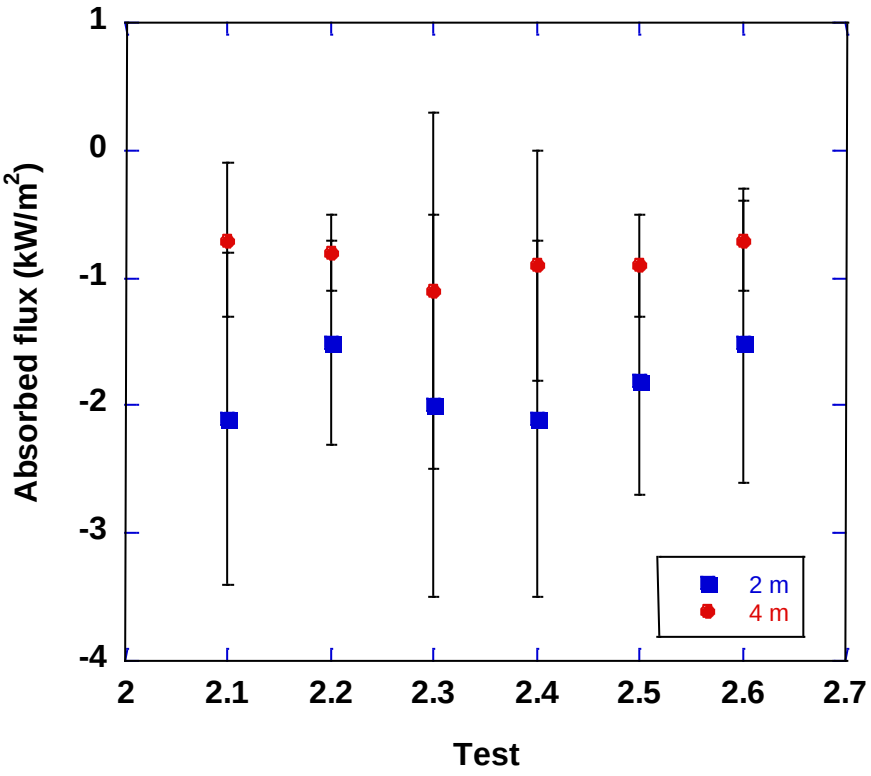

Figure 7-21: Average DFT absorbed heat flux for Bakken crude oil tests.

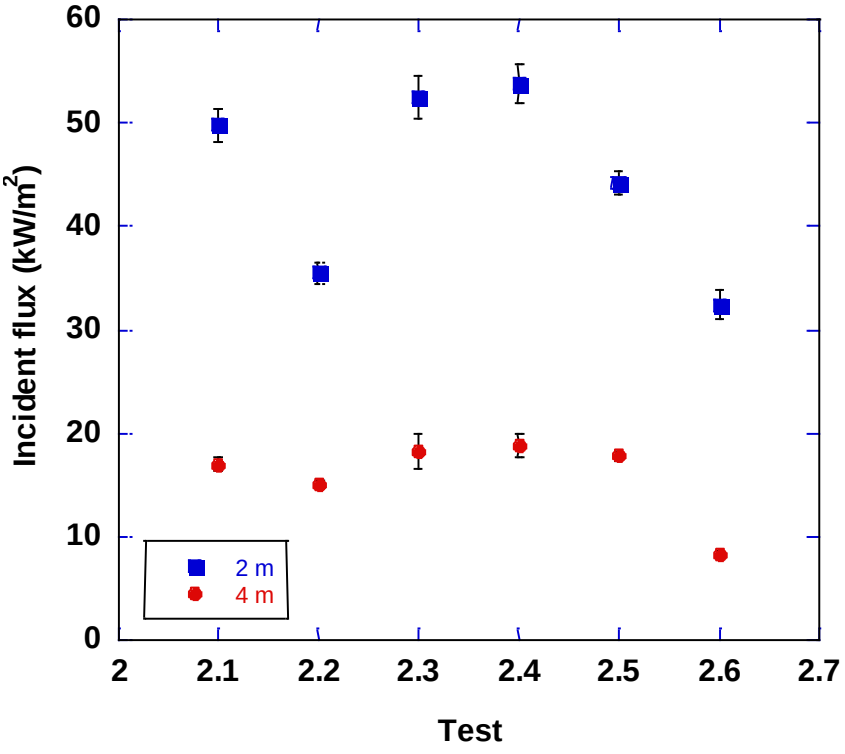

Figure 7-22: Average DFT incident heat flux for Bakken crude oil tests.

7.5.3. Dilbit Crude Oil Pool Fire Tests

Similar to the radiometer and centerline TC rake data, the temperature measurements from the DFT instruments are averaged by integrating the data from 0-25 minutes and dividing by this period. The range is one standard deviation. Table 7-21 provide average temperatures, absorbed, and incident heat flux values for the DFTs placed 2-m and 4-m from the center of the pool. Figure 7-23 and Figure 7-24 provide average absorbed and incident heat flux values, respectively, in graphical form. The comparison indicates that average values did not vary significantly among the tests.

Table 7-21: Average DFT temperature and heat flux values for the Dilbit crude oil tests.

Test	Distance from pool center (m)	Temperature (°C)		Heat flux (kW/m^2)	
		Front plate	Back plate	Absorbed	Incident
3.1	2	479.2 ± 147.1	90.0 ± 54.5	-6.6 ± 8.6	35.2 ± 7.0
	4	190.2 ± 73.9	35.9 ± 19.3	-2.5 ± 2.2	9.5 ± 2.2
3.2	2	465.8 ± 149.9	83.7 ± 50.8	-6.9 ± 6.7	34.2 ± 5.7
	4	169.4 ± 70.9	34.7 ± 16.7	-2.4 ± 1.3	8.5 ± 1.5
3.3	2	477.5 ± 137.8	83.8 ± 50.5	-7.0 ± 9.0	36.0 ± 4.3
	4	185.6 ± 68.7	32.1 ± 18.6	-2.6 ± 2.0	9.8 ± 1.3
3.4	2	486.8 ± 129.4	93.8 ± 51.3	-6.6 ± 9.3	35.2 ± 6.5
	4	192.0 ± 66.8	40.2 ± 19.2	-2.4 ± 2.2	9.3 ± 2.0
3.5	2	462.6 ± 148.4	88 ± 49.9	-6.6 ± 8.2	33.2 ± 7.1
	4	179.5 ± 69.5	39.4 ± 17.4	-2.4 ± 1.8	8.8 ± 1.9
3.6	2	489.5 ± 129.2	92.2 ± 49.6	-7.2 ± 8.8	36.3 ± 5.8
	4	188.5 ± 65.5	39 ± 17.1	-2.6 ± 1.9	9.5 ± 1.8

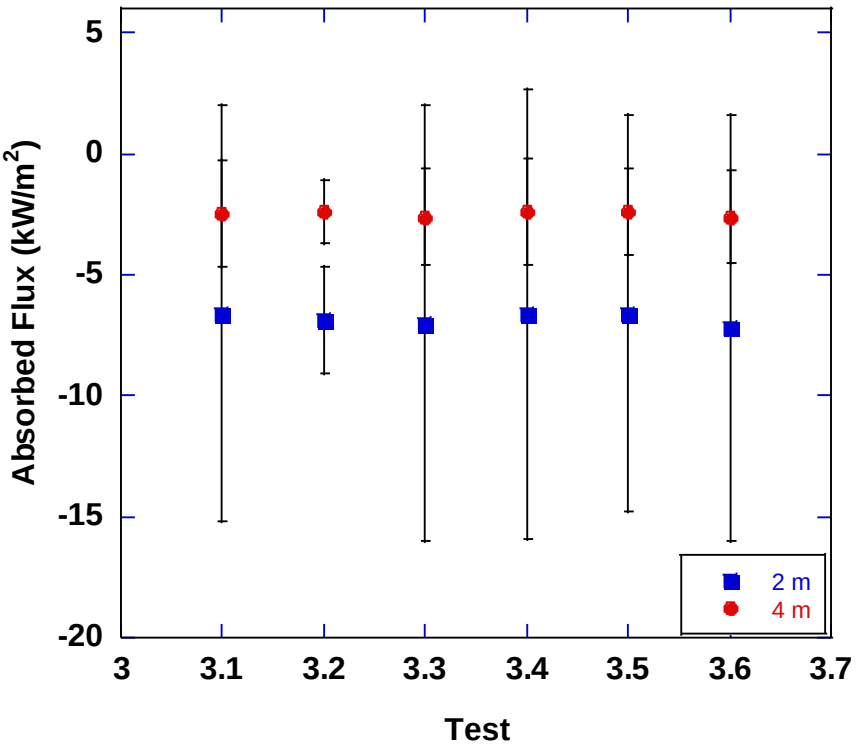

Figure 7-23: Average DFT absorbed heat flux for dilbit crude oil tests.

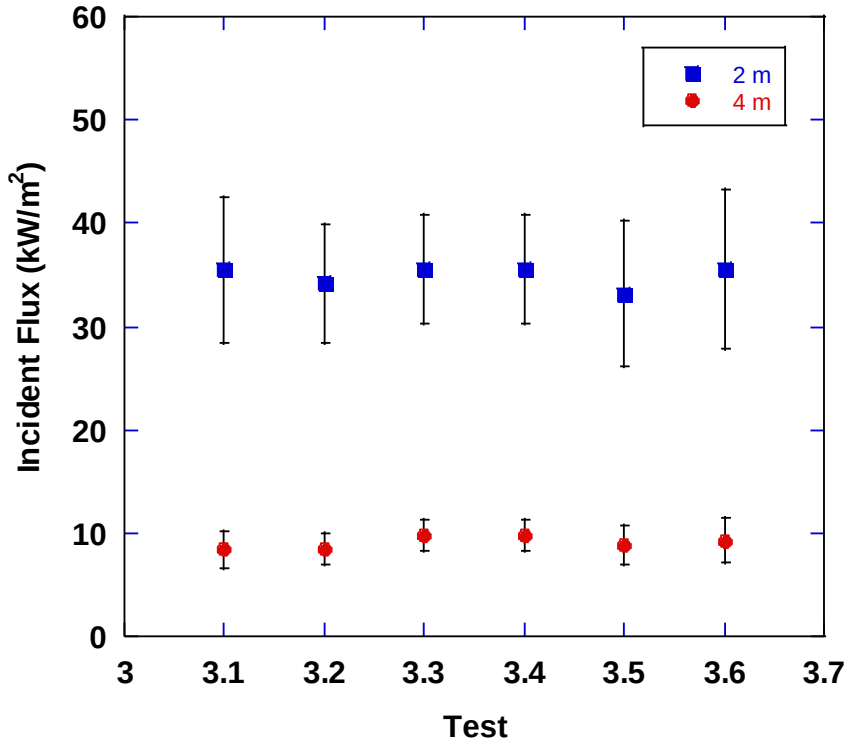

Figure 7-24: Average DFT incident heat flux for dilbit crude oil tests.

7.6. Calorimeter TC Temperature and Derived Heat Flux

The following provides comparison of the TC temperature and derived heat flux to the calorimeter among the tests within a series.

The heat flux from the flame to the calorimeter was derived from calorimeter TC measurements using a one-dimensional inverse heat conduction code, IHCP1D, developed by James Beck [3]. Description of the energy balance, emissivity values, and thermal properties are provided in Appendix A.1. The heptane tests used the same calorimeter, whereas the Bakken crude oil tests used the second of two calorimeters that were provided to SNL by NRCC for Tests 2.3, 2.4, and 2.5, but not for Test 2.2 which used the first calorimeter. This is due to the opening of the side seams of the second calorimeter observed after Test 2.5 (Figure 7-25).

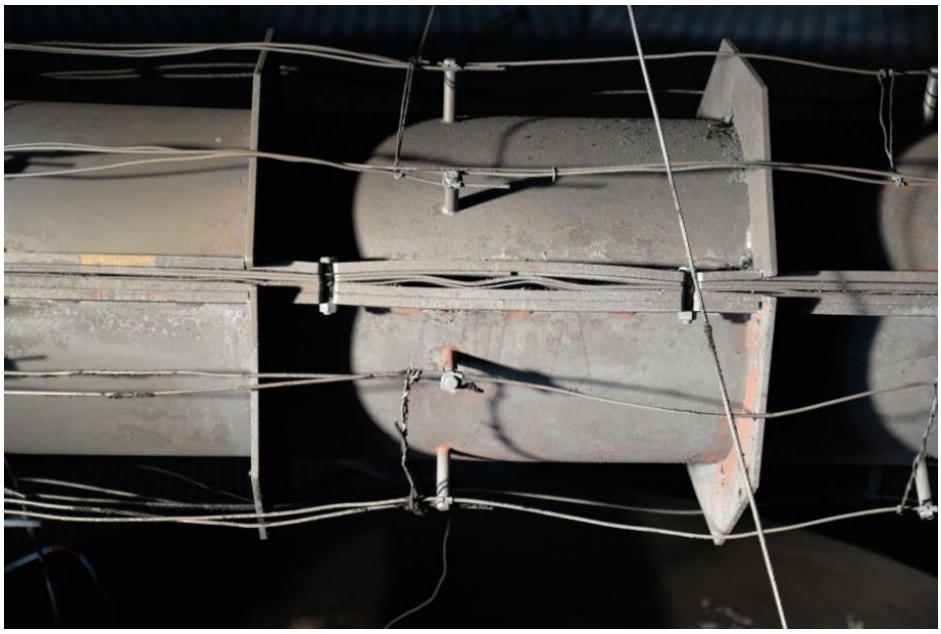

Figure 7-25: Side seam of second calorimeter after Test 2.5.

7.6.1. Heptane Pool Fire Tests

Two of the three heptane tests included a calorimeter, namely Test 1.1 and 1.3. Table 7-22 provides average temperatures and heat flux values for these two tests. The average temperature of the inner cylinder is not provided, since it was steadily climbing throughout the test, thus an average is not representative of steady state. As indicated in

Figure 7-26, Test 1.1 is slightly higher than Test 1.3 in which the fuel was heated. Figure 7-27 indicates that the absorbed and total heat flux to the calorimeter are similar between the two tests.

Table 7-22: Average temperature and heat flux values among all calorimeter TC locations for the heptane tests.

Test	Temperature (°C)		Heat flux (kW/m^2)	
	Outer cylinder	Exterior cylinder	Absorbed	Total
1.1*	796.7 ± 3.9	863.7 ± 13.3	-2.4 ± 2.4	57.5 ± 2.6
1.3**	771.4 ± 5.5	815.8 ± 15.7	-2.4 ± 3.5	58.9 ± 3.8

*averaged over 20-35 minutes
**averaged over 24-44 minutes

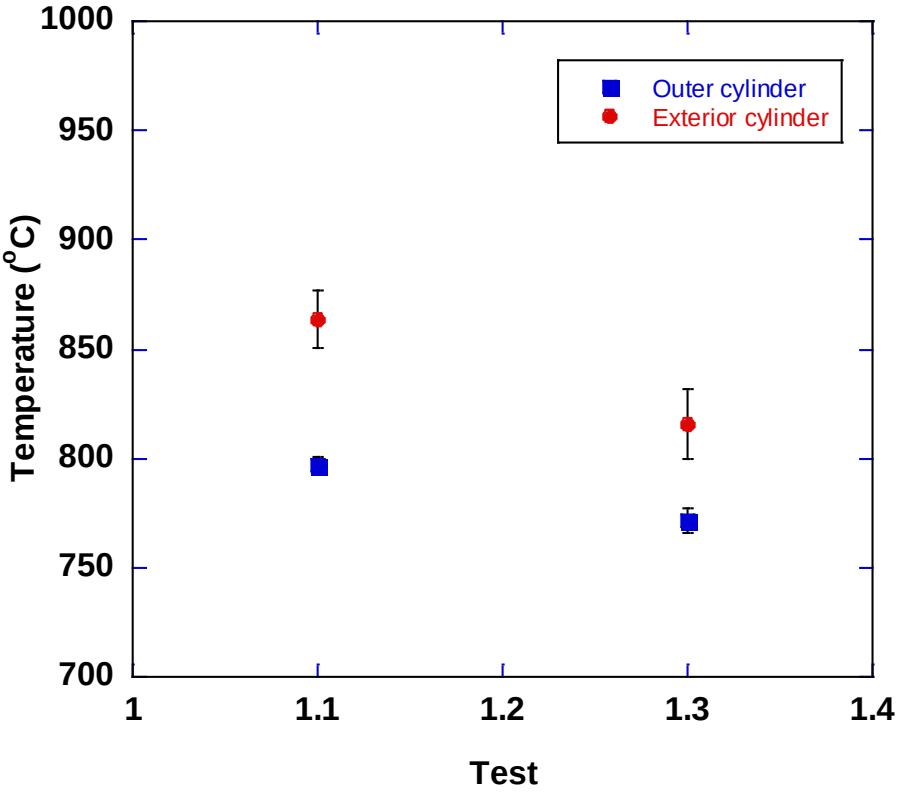

Figure 7-26: Calorimeter average temperatures for heptane tests.

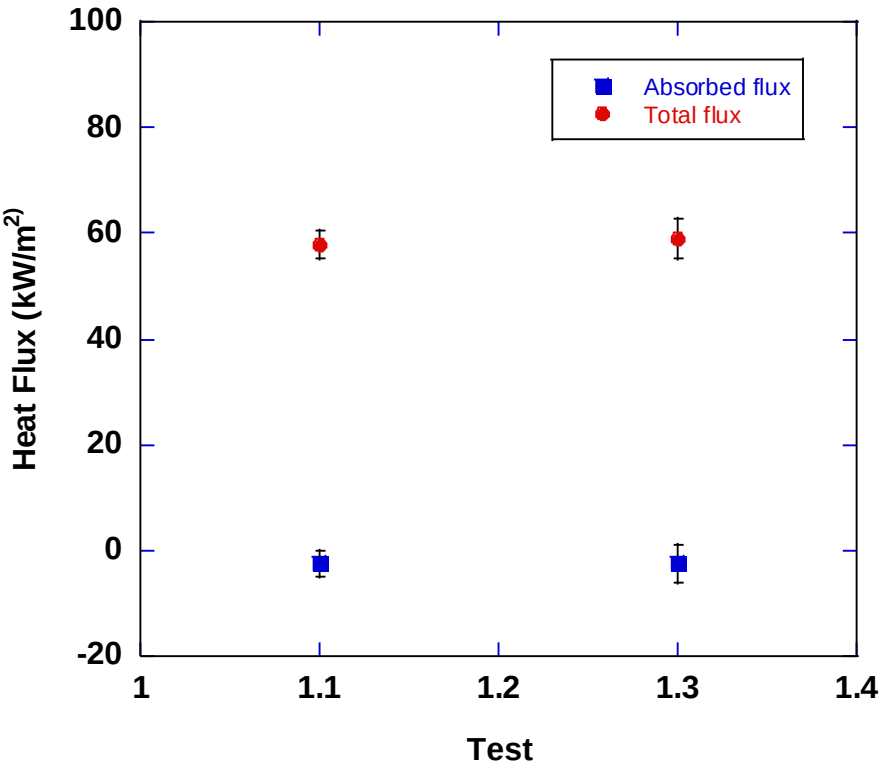

Figure 7-27: Calorimeter average heat flux values for heptane tests.

7.6.2. Bakken Crude Oil Pool Fire Tests

Table 7-23 provides average temperature and total heat flux values for all four Bakken crude oil tests that included a calorimeter. As indicated in Figure 7-28 and Figure 7-29, the average temperature and heat flux levels are similar for Tests 2.3, 2.4, and 2.5, while Test 2.2 (in which the calorimeter was closer to the pan) is lower. This is expected since it is in the fuel rich core of the flame, which tends to have lower temperatures.

Table 7-23: Average temperature and heat flux values among all calorimeter TC locations for the Bakken crude oil tests.

Test	Temperature (°C)		Heat flux (kW/m^2)	
	Outer cylinder	Exterior cylinder	Absorbed	Total
2.2*	846.4 ±7.0	880.9 ±16.7	-3.7 ±4.3	77.0 ±4.8
2.3*	908.8 ±17.1	975.4 ±37.5	-4.2 ±9.7	94.1 ±11.0
2.4$^+$	952.2 ±7.5	993.3 ±19.7	-4.9 ±5.2	109.5 ±5.8
2.5^{++}	945.5 ±7.9	990.8 ±15.5	-5.2 ±4.8	104.9 ±5.3

*averaged over 20-40 minutes
**averaged over 20-33 minute
+averaged over 20-33 minutes
++averaged over 20-33 minutes

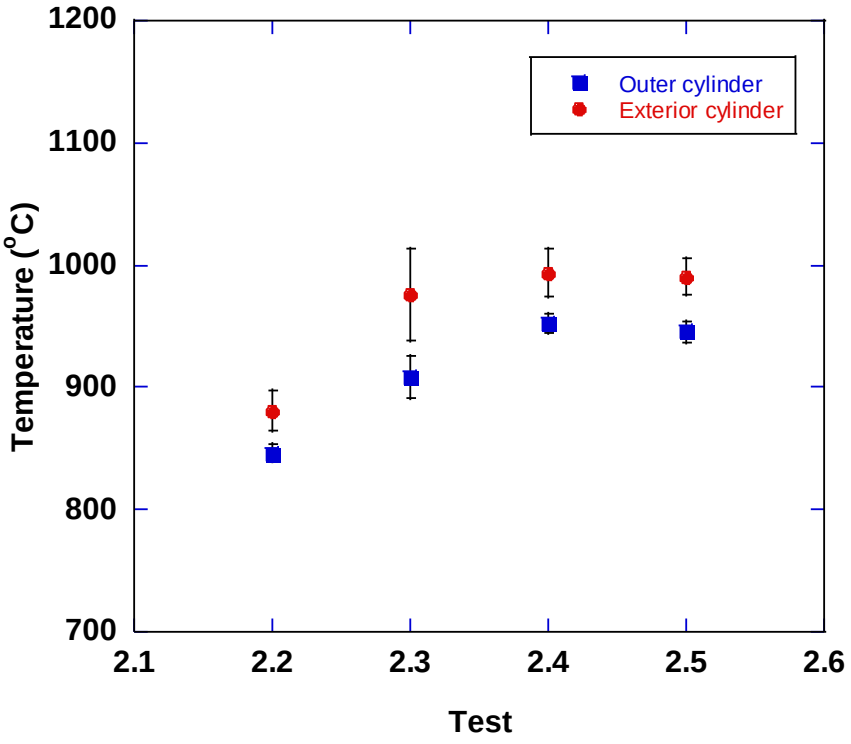

Figure 7-28: Calorimeter average temperatures for Bakken crude oil tests.

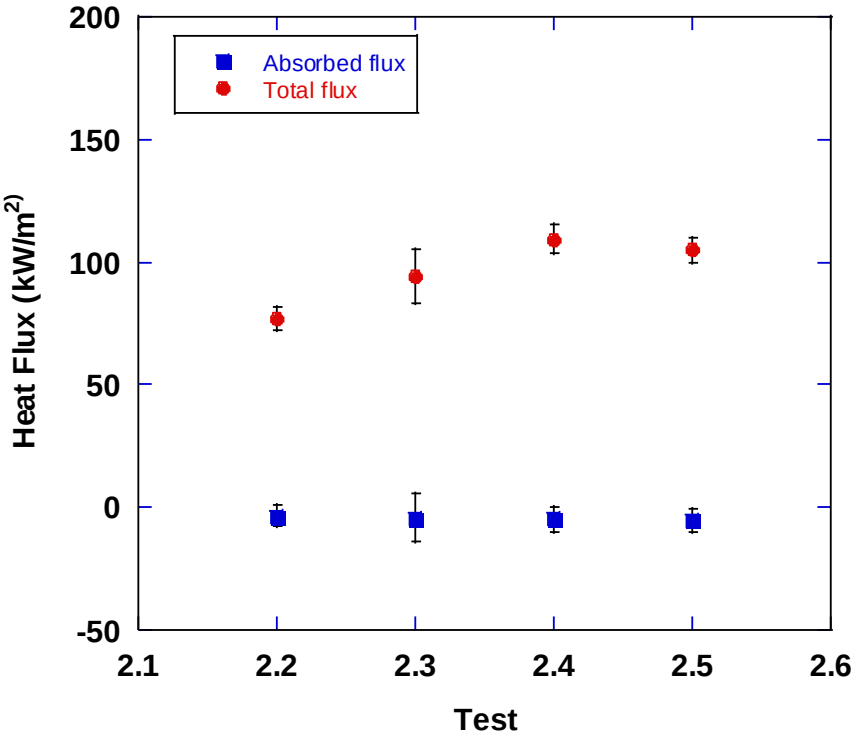

Figure 7-29: Calorimeter average heat flux values for Bakken crude oil tests.

7.6.3. Dilbit Crude Oil Pool Fire Tests

Table 7-24 and Figure 7-25 provide total and absorbed heat flux values, respectively, integrated over 0-25 minutes for the calorimeter at indicated locations. The approach to providing a fair comparison of averages is to include measurements from similar positions. The cells that are shaded are those in which either the calculated heat flux resulted in not a number or those in which the calculated heat flux is not physical. The shaded cells are uniformly applied for all tests to not skew the comparison of the average for heat flux values. Thus, the average heat flux values provided in Figure 7-26 do not include the shaded cells. The integrated temperature values provided in

Table 7-26 are averaged over all locations and do not exclude any locations.

Figure 7-30 and Figure 7-31 provide a graphical comparison of the averages provided in

Table 7-26.. The results indicate that the average temperatures are similar among the tests with this comparison. The average total heat flux values for tests 3.5 (repeat test) and 3.6 (higher-temperature test) tend to be higher than tests 3.1 and 3.2. Note however that the standard deviation ranges overlap and are much greater than the Bakken crude oil and the heptane tests. This is due to the variable behavior of the Dilbit crude oil where a steady state was not achieved.

Table 7-24: Calorimeter integrated total heat flux values for dilbit pool fire tests (kW/m^2)

Test 3.1								
	0-deg	**45-deg**	**90-deg**	**135-deg**	**180-deg**	**225-deg**	**270-deg**	**315-deg**
left	24.0	40.0	88.8	na	92.7	55.8	26.5	21.2
center	47.6	62.9	97.5	101.9	20.2	67.7	15.2	41.9
right	39.4	61.4	94.0	101.0	89.1	63.8	14.0	12.3
Test 3.2								
	0-deg	**45-deg**	**90-deg**	**135-deg**	**180-deg**	**225-deg**	**270-deg**	**315-deg**
left	34.8	52.6	90.2	20.3	90.6	81.1	13.1	9.4
center	70.4	96.3	95.5	87.0	18.0	20.6	19.0	62.4
right	67.8	87.6	82.2	77.5	71.1	78.1	20.2	1.1
Test 3.5								
	0-deg	**45-deg**	**90-deg**	**135-deg**	**180-deg**	**225-deg**	**270-deg**	**315-deg**
left	42.3	46.1	86.0	na	130.4	94.8	na	49.4
center	70.9	na	184.8	126.5	120.7	100.6	100.1	70.0
right	62.5	67.5	92.4	110.6	110.3	96.8	21.4	69.1
Test 3.6								
	0-deg	**45-deg**	**90-deg**	**135-deg**	**180-deg**	**225-deg**	**270-deg**	**315-deg**
left	31.2	54.1	112.1	na	115.2	70.5	na	27.4
center	50.6	315.4	0.0	125.0	106.0	80.5	258.0	44.1
right	35.6	54.7	100.7	107.3	91.0	66.6	38.6	32.7

Table 7-25: Calorimeter integrated absorbed heat flux values for dilbit pool fire tests (kW/m^2)

Test 3.1								
	0-deg	**45-deg**	**90-deg**	**135-deg**	**180-deg**	**225-deg**	**270-deg**	**315-deg**
left	-7.6	-10.2	-15.5	na	-15.8	-12.6	-8.4	-7.0
center	-11.0	-13.0	-16.6	-17.5	-7.7	-14.6	-6.6	-10.9
right	-10.0	-13.1	-16.9	-18.1	-17.0	-14.2	-5.8	-5.1
Test 3.2								
	0-deg	**45-deg**	**90-deg**	**135-deg**	**180-deg**	**225-deg**	**270-deg**	**315-deg**
left	-10.3	-13.0	-16.8	-7.5	-16.6	-16.1	-6.0	-4.8
center	-14.8	-17.4	-17.2	-16.6	-7.5	-8.5	-7.7	-14.4
right	-13.8	-16.5	-16.6	-16.4	-16.2	-16.5	-7.4	-0.6
Test 3.5								
	0-deg	**45-deg**	**90-deg**	**135-deg**	**180-deg**	**225-deg**	**270-deg**	**315-deg**
left	-10.9	-12.0	-16.6	na	-19.6	-17.0	na	-11.9
center	-14.6	na	-0.9	-19.9	-19.9	-18.7	-22.7	-15.2
right	-13.3	-14.3	-17.7	-19.4	-19.7	-17.8	-7.3	-14.1
Test 3.6								
	0-deg	**45-deg**	**90-deg**	**135-deg**	**180-deg**	**225-deg**	**270-deg**	**315-deg**
left	-10.3	-14.1	-19.4	na	-18.8	-15.2	0.2	-9.5
center	-13.4	-9.3	na	-20.3	-19.1	-17.2	-8.9	-12.7
right	-10.2	-13.5	-18.6	-19.3	-18.0	-14.9	-11.0	-9.7

Table 7-26: Integrated temperature and heat flux values averaged among all calorimeter TC locations for the dilbit crude oil tests.

Test	**Temperature (°C)**		**Heat flux (kW/m^2)**	
	Outer cylinder	**Exterior cylinder**	**Absorbed**	**Total**
3.1	640.7 ± 176.2	774.6 ± 133.4	-13.2 ± 23.6	63.9 ± 15.7
3.2	615.4 ± 182.6	824.8 ± 147.2	-14.4 ± 18.2	67.1 ± 13.9
3.5	707.6 ± 241.8	869.9 ± 175.6	-15.9 ± 24.3	83.1 ± 21.3
3.6	696.3 ± 219.8	773.3 ± 181.8	-15.6 ± 27.7	75.5 ± 21.5

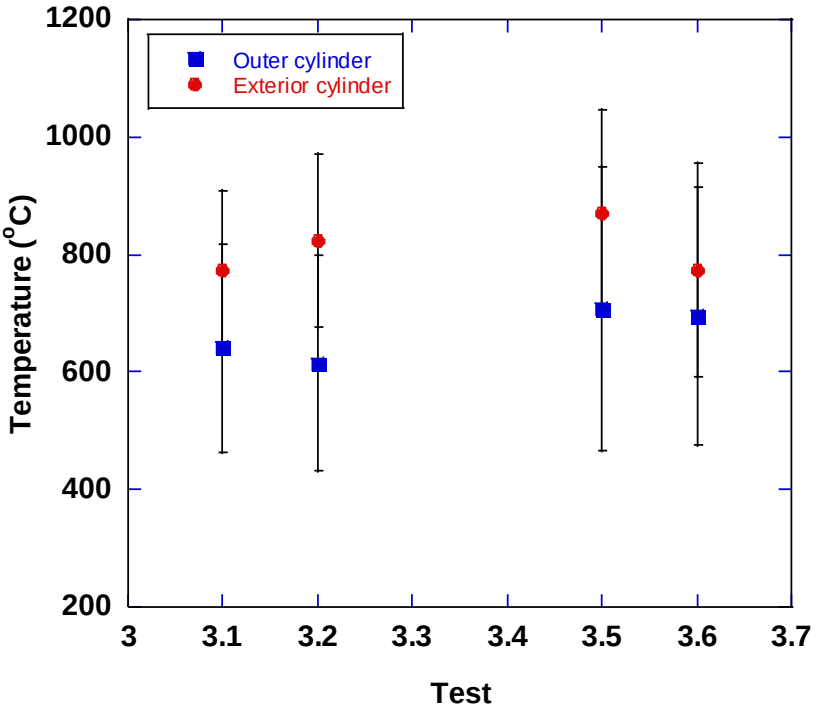

Figure 7-30: Integrated temperatures among all calorimeter TC locations for the Dilbit crude oil tests.

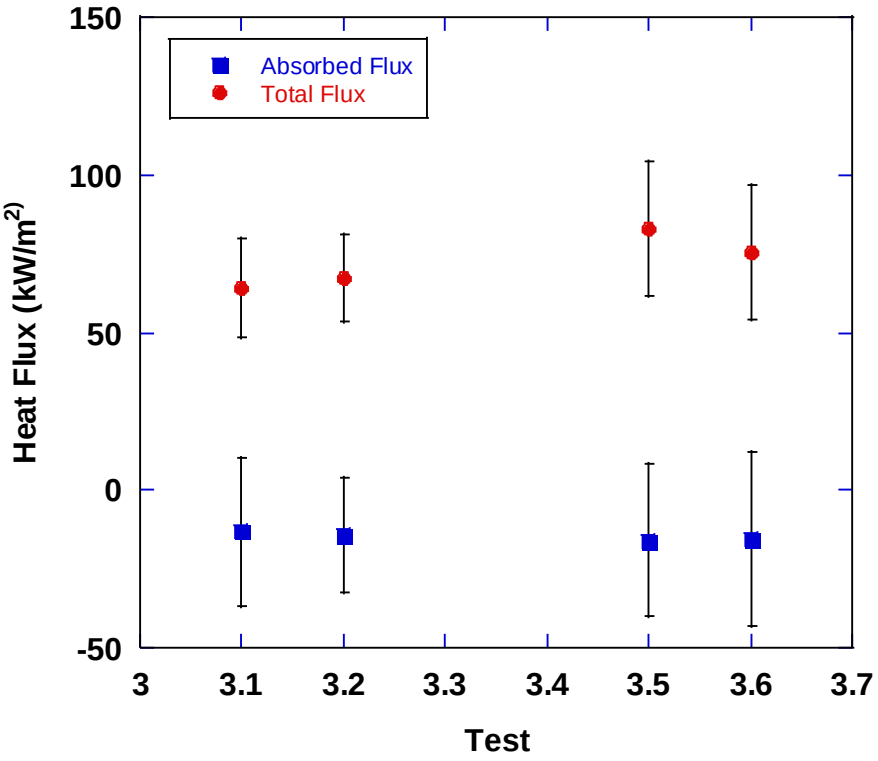

Figure 7-31: Integrated heat flux values averaged among all calorimeter TC locations for the Dilbit crude oil tests.

7.7. Heat Release Rate

The measurements from the combustion gas analyzer (CGA) were reduced using the method provided in [4]. The equations and assumptions used can be found in Appendix A. The average heat release rate (HRR) based on the CGA measurement is lower than values calculated using the theoretical approach (which is based on the measured burn rate and heat of combustion). This is because the theoretical approach assumes complete combustion, which doesn't occur in practice as evident from the production of CO and soot that are not oxidized. Thus, higher values will be calculated compared to values calculated from CGA measurements. Table 7-27 provides the heat of combustion for the fuels tested.

Table 7-27: Heat of combustion for fuels tested

Fuel	Heat of combustion (kJ/kg)
Heptane	44,560
Bakken crude oil	48,358
Dilbit crude oil	43,275

7.7.1. Heptane pool fire tests

Table 7-28 and Figure 7-32 provide a comparison of the average heat release rate in tabular and graphical form. The heat release rate from CGA measurements is lower than that based on heat of combustion.

Table 7-28: Average heat release rates for heptane tests

	Heat release rate (MW)	
Test	Based on CGA	Based on measured heat of combustion and burn rate
1.1	4.4 ± 0.2	5.2
1.2	5.2 ± 0.2	5.6
1.3	5.4 ± 0.3	5.6

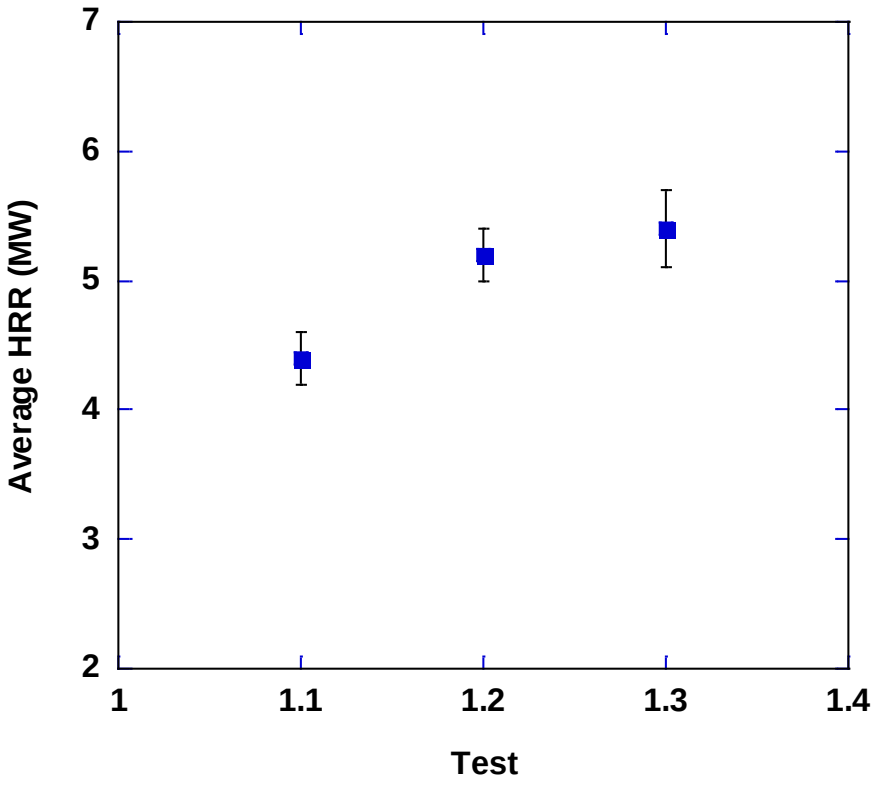

Figure 7-32: Average heat release rates from CGA measurements for heptane tests.

7.7.2. Bakken Crude Oil Pool Fire Tests

As provided in Table 7-29, all HRR values from CGA measurements are lower than the theoretical values with the exception of Test 2.1, which almost seems to be an outlier; however, its range does overlap with the range of the other tests. Figure 7-33 provides a graphical comparison of heat release rate from CGA measurements.

Table 7-29: Average heat release rates for Bakken crude oil tests (measured in MW).

Test	Based on CGA	Based on heat of combustion and burn rate
2.1	4.8 ± 0.9	4.6
2.2	3.5 ± 0.7	4.0
2.3	3.8 ± 0.9	4.1
2.4	3.2 ± 0.8	4.4
2.5	3.6 ± 0.8	4.0
2.6	3.5 ± 0.7	4.6

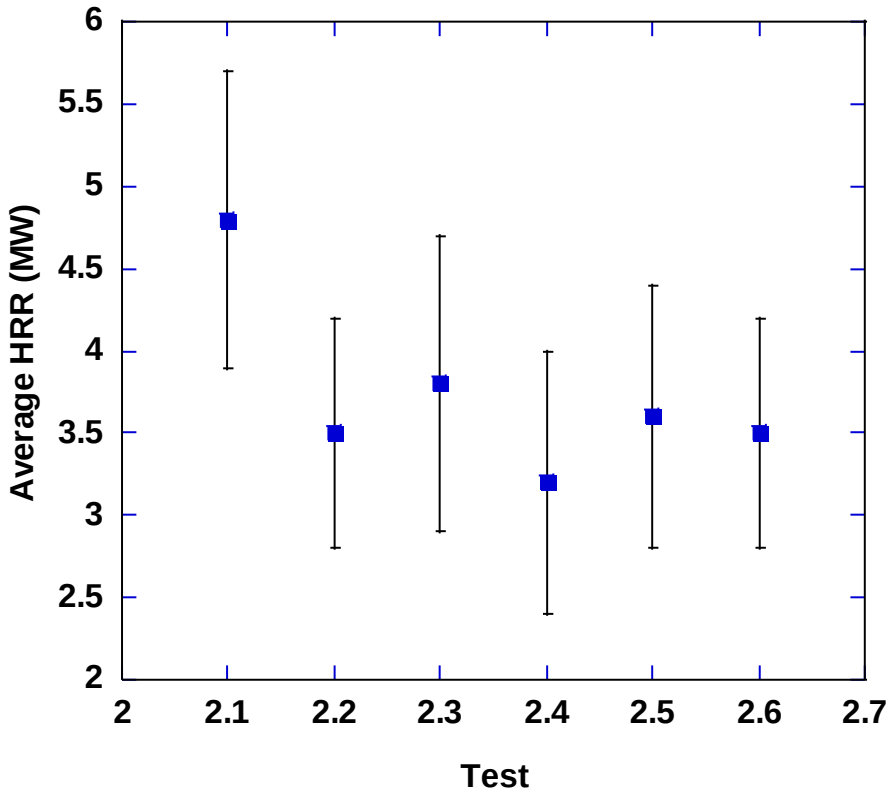

Figure 7-33: Average heat release rate from CGA measurements for Bakken crude oil tests.

7.7.3. Dilbit Crude Oil Pool Fire Tests

Test 3.4 was the only test in which CGA measurements were successfully obtained. Thus, the heat release rate for the other tests are determined by using the heat of combustion and the burn rate values provided in Table 7-30. Due to the variability in burn rate among the tests, the heat release similarly displays variable behavior. The results indicate that the heat release rate is in the range of approximately 2 – 2.5 MW for all tests except for Test 3.1 and Test 3.2 where the calorimeter was lowered to 0.5 m above the pool. Test 3.5 is a more reliable indicator of the heat release rate than Test 3.1 due to the difficulties encountered in obtaining the burn rate. With regards to Test 3.2, given the difficulty in determining the burn rate over the entire duration for all the tests it is challenging to draw firm conclusion as to whether the calorimeter placement affects the heat release rate. Figure 7-34 provides the comparison graphically where 'HC1' and 'HC2' refer to using the heat of combustion to determine the heat release rate and denotes the multiple calculated values based on the burn rate which apply to Tests 3.1, 3.2, and 3.3. The tests that allowed for a continuous range of burn rates to be identified is reflected in the heat release rate range for Tests 3.5 and Test 3.6.

Table 7-30: Average heat release rates for Dilbit crude oil tests (measured in MW).

Test	Based on CGA	Based on heat of combustion and burn rate
3.1	na	6.7, 4.6
3.2	na	8.2, 3.1
3.3	na	2.3,1.9
3.4	3.7 ±1.2	2.5
3.5	na	2.0 – 2.6
3.6	na	0.7 – 2.4

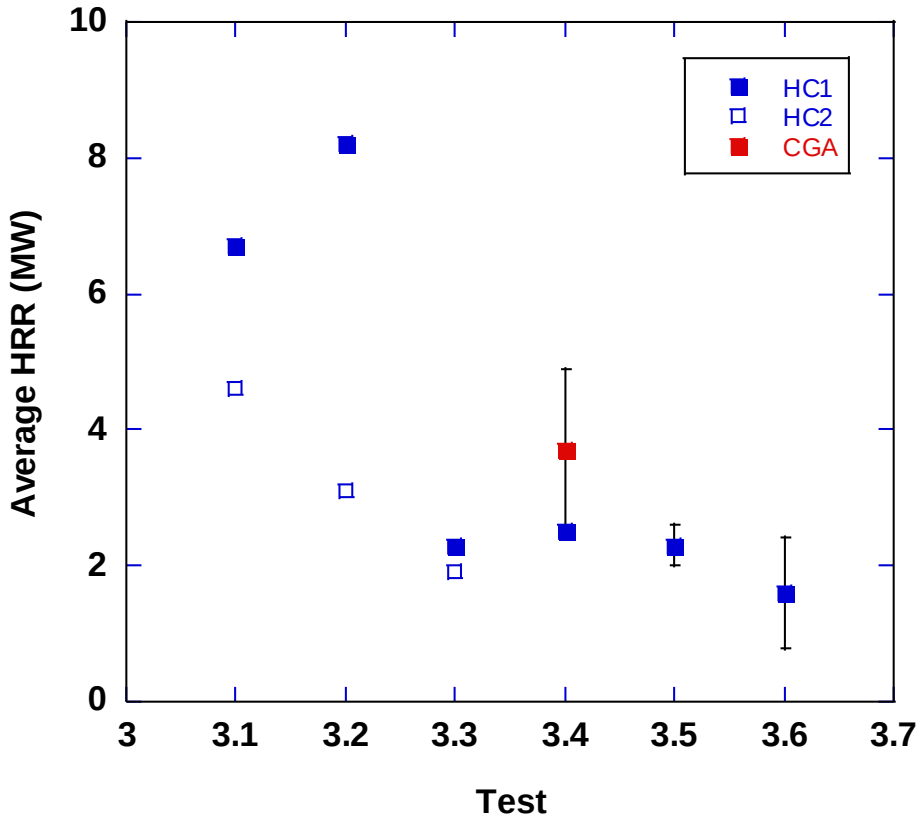

Figure 7-34: Average heat release rates for Dilbit crude oil tests.

7.8. Flame Height

The following section provides average flame heights for all test series. For two of the heptane tests, the flame height was determined using real time cameras. The flame height was assessed from images from the real time cameras that were averaged. The intensity of the average image was then evaluated at the midline and provided an indication of the flame height. For all the Bakken and Dilbit crude oil tests, flame heights were determined using the IR camera.

7.8.1. Heptane Pool Fire Tests

Table 7-31 and Figure 7-35 provide the average flame heights for the heptane tests. Test 1.1 was measured using the IR camera, whereas the other two tests used the real time camera. The results indicate that test 1.2, without the calorimeter, resulted in the highest flame height.

Table 7-31: Average flame heights of heptane tests.

Test	Average flame height (m)
1.1	5.6 ± 0.9
1.2	6.8 ± 0.9
1.3	5.8 ± 0.8

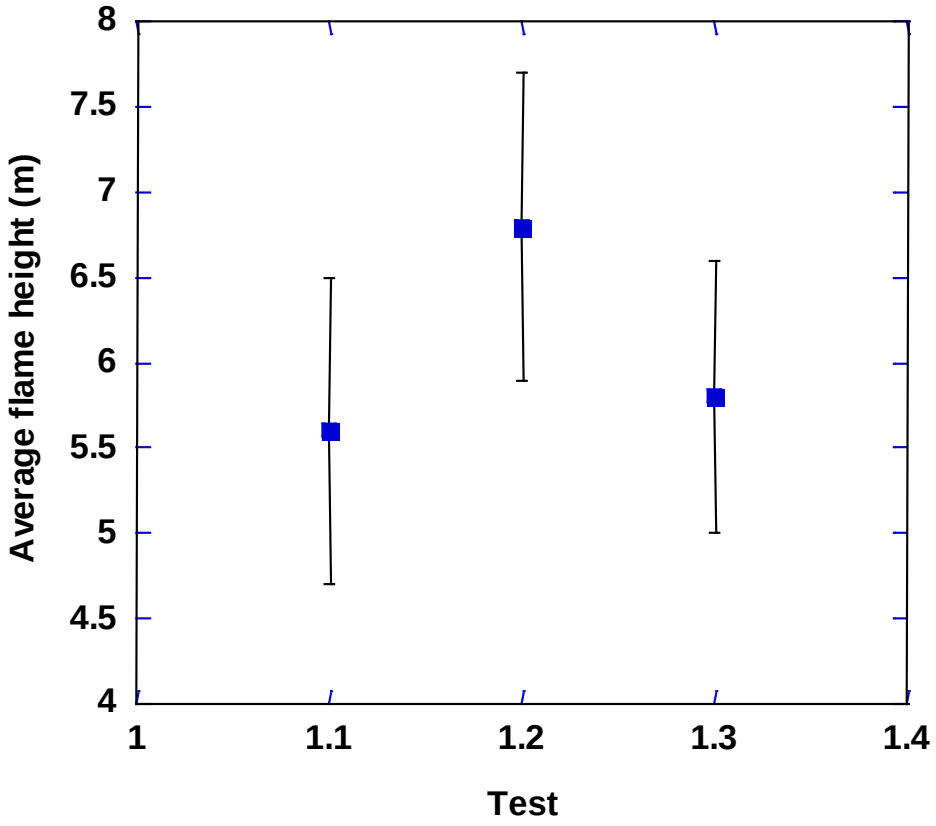

Figure 7-35: Average flame heights of heptane tests.

7.8.2. Bakken Crude Oil Pool Fire Tests

Table 7-32 and Figure 7-36 provide the average flame height for the Bakken crude oil tests. The results indicate that the flame heights are all within the range of the standard deviation of the measurements. The values were averaged over 10-20 minutes for all tests.

Table 7-32: Average flame heights for Bakken crude oil tests.

Test	Average flame height (m)
2.1	4.4 4.5 ± 1.1
2.2	4.3 ± 1.0
2.3	4.3 ± 1.1
2.4	4.5 ± 1.0
2.5	4.5 ± 0.9
2.6	4.5 ± 1.0

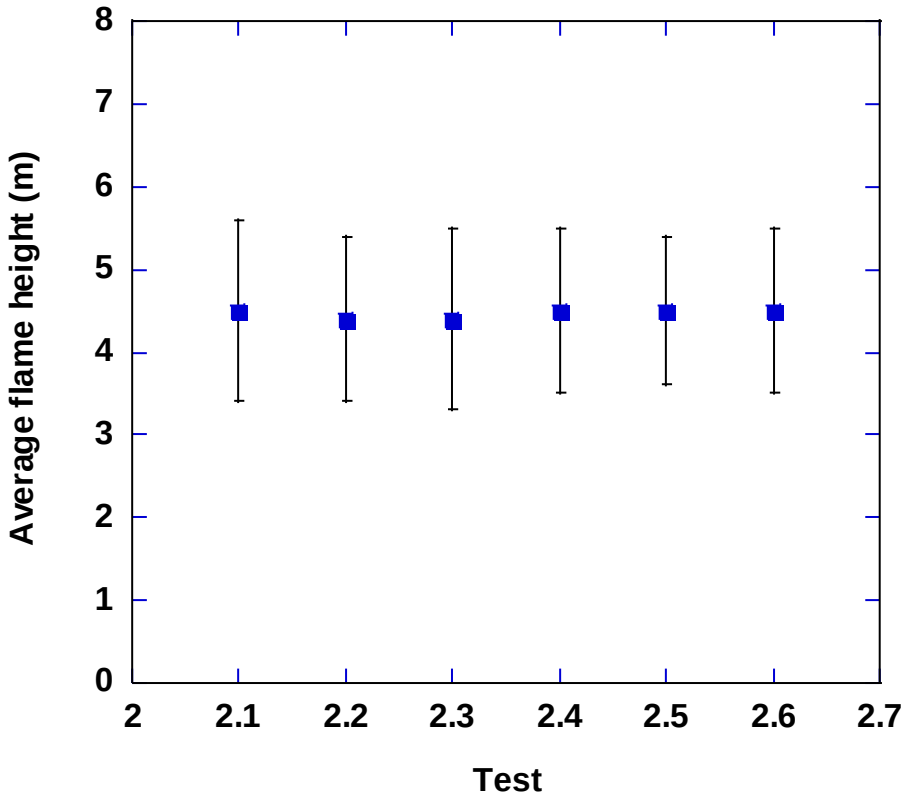

Figure 7-36: Average flame heights for Bakken crude oil tests.

7.8.3. Dilbit Crude Oil Pool Fire Tests

Table 7-33 and Figure 7-37 provide the average flame height for the Dilbit crude oil tests. The results indicate that the flame heights are all within the range of the standard deviation of the measurements.

Table 7-33: Average flame heights for Dilbit crude oil tests.

Test	Average flame height (m)
3.1*	3.4 ± 0.9
3.2**	3.6 ± 0.8
3.3***	3.4 ± 0.8
3.4+	3.5 ± 0.8
3.5++	3.6 ± 0.8
3.6+++	3.5 ± 0.8

*averaged over 5-25 minutes
**averaged over 3-30 minutes
***averaged over 3-30 minutes
+averaged over 3-25 minutes
++averaged over 3-30 minutes
+++averaged over 3-30 minutes

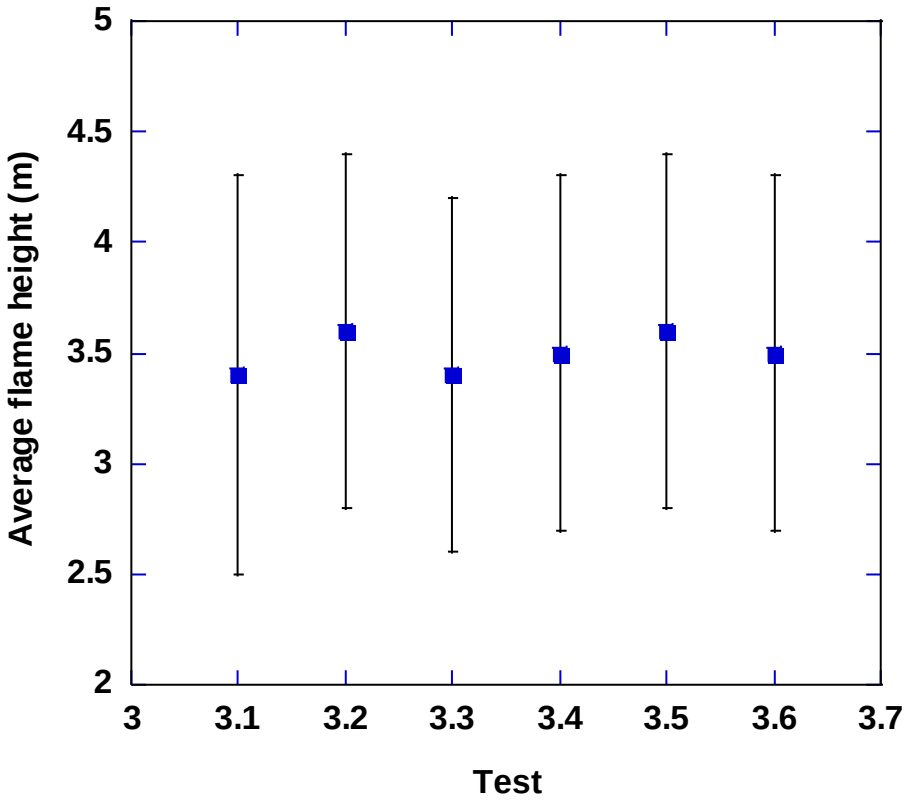

Figure 7-37: Average flame heights for Dilbit crude oil tests.

8. COMPARISON OF TEST SERIES

8.1. Burn rate

Figure 8-1 provides a comparison of burn rates for all tests conducted using heptane, Bakken crude oil, and dilbit crude oil. For the dilbit tests, the range is the minimum and maximum values with the uncertainty added. The comparison indicates that the burn rate for heptane and for Bakken crude oil are fairly consistent among the tests, however the dilbit crude oil displays significantly variable behavior. For both the heptane and Bakken test series, maintaining a constant fuel level to determine a reliable burn rate measurement posed no difficulties. This contrasts with the dilbit crude oil whose burn rate changed constantly. Thus, maintaining a constant fuel level was difficult, particularly since there was a time lag in the response of the dP gauge to changes in the fuel feed. The comparison indicates that heptane has the highest burn rate of between 3-3.5 mm/min followed by the Bakken crude oil ranging around 2 mm/min. The dilbit crude oil has the lowest burn rate ranging between 1-1.5 mm/min (not including Test 3.1). Recall that Test 3.1 was the first encounter in controlling the fuel feed to maintain a constant fuel level which was not as successful compared to subsequent tests after gaining experience, thus the burn rate for this test is considered not as accurate.

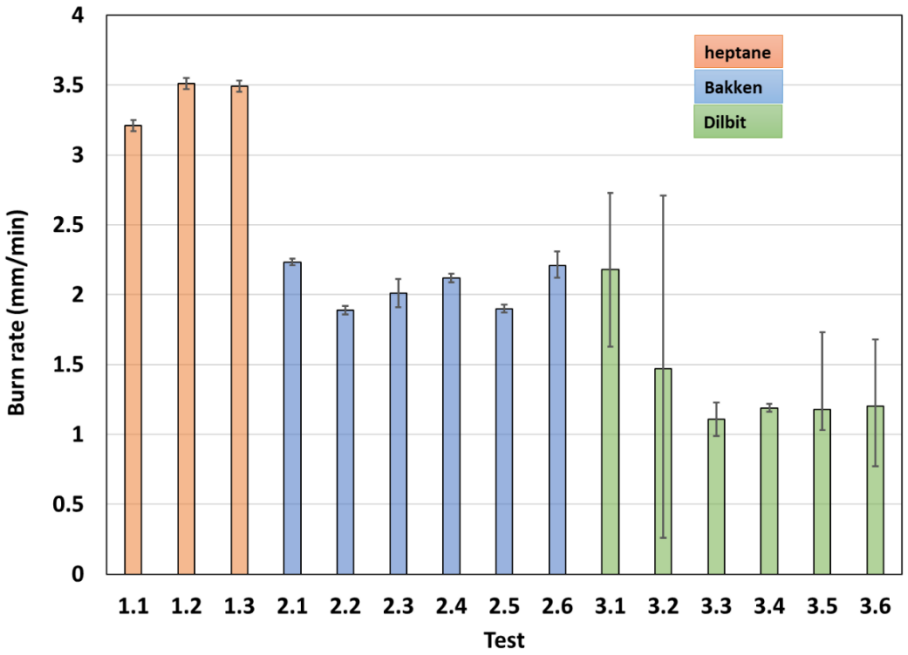

Figure 8-1: Burn rate (mm/min) for all tests.

The burn rate for the dilbit varied where high values occurred initially, then decreased followed by an increase. The burn rate affects the flame height which in turn affects measurements from the radiometers, the plume centerline thermocouple rake, DFT instruments, and heat release rate. The calorimeter thermocouples are not significantly affected because the calorimeter is stationed at positions where it is persistently engulfed. And, the average and maximum SEP values of the luminous portions of the flame are not affected since the burn rate values are not in a region to cause a significant impact (e.g. smoldering).

Indications of why the dilbit displays different burn rate behavior than the other fuels can be found from examining the boiling point distribution versus temperature curve for the tested fuels shown in Figure 8-2. The curve assumes that the fuels are not being replenished but are allowed to deplete. In this plot, composition of samples taken is represented by assigning each component a boiling point and simulating the distillation of the material with increasing temperature. Carbon numbers associated with each temperature regime are marked in the plot for reference.

The three fuels indicate very different behavior. For the n-heptane, since it is > 99 mass% pure, nearly all of it boils off at one temperature. Thus, the n-heptane curve is shown as a vertical line at 100°C with carbon number C7. The Bakken and dilbit oils contain multiple components that boil at different temperatures, resulting in more gradual distributions than the n-heptane.

Below 95°C, the Bakken and dilbit boiling point distributions are similar, reaching approximately 12 mass% boiled at 95°C. Above 95°C, the Bakken distribution has a nearly constant slope and then begins to level around 500°C. This contrasts with the dilbit which indicates a more variable slope, that is, the mass% increases with temperature up to 100°C (slope = 0.13 mass% /°C), then decreases between 100-250°C (slope = 0.06 mass% /°C), and then increases above 250°C (slope = 0.14 mass% /°C). This behavior indicates a dip in the carbon number distribution between C7 and C12 relative to the overall distribution.

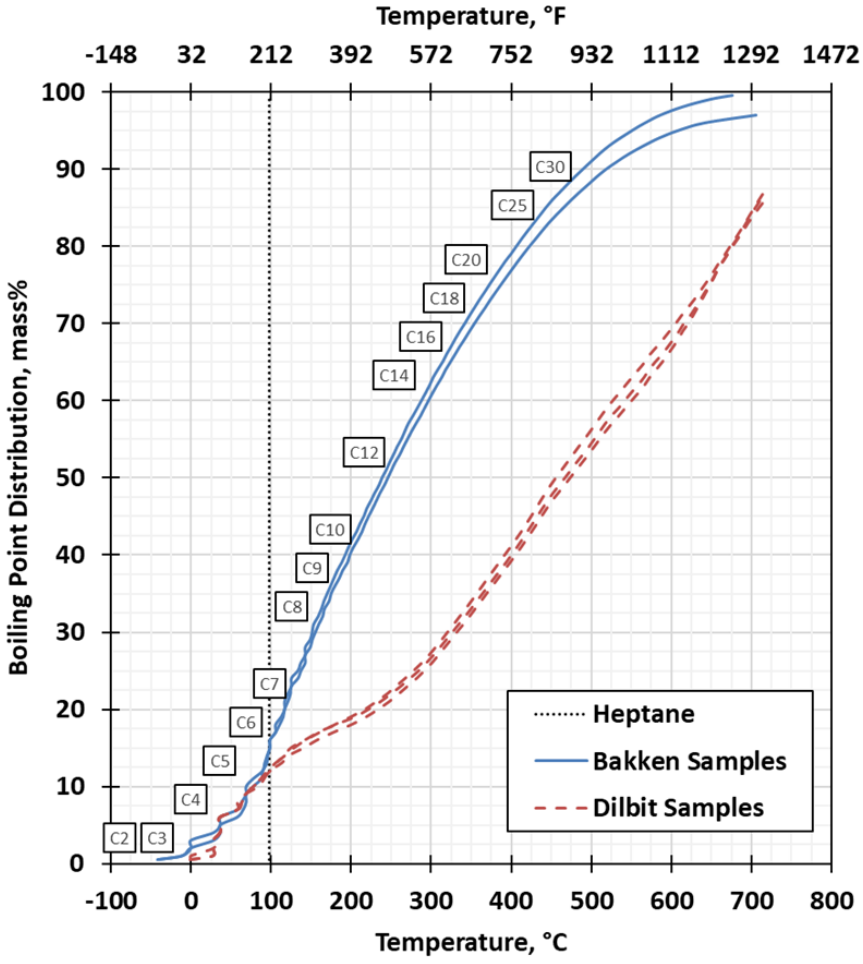

Figure 8-2: Temperature versus boiling point distribution for fuel samples

Figure 8-3 and Figure 8-4 show carbon number distributions for the average compositions of the Bakken and dilbit samples below C15 and the entire range of carbon content, respectively. For carbon numbers below C15, the Bakken distribution shows a peak at C8, while the dilbit distribution shows a spike at C5 and a local minimum at C11. This behavior was observed in all three of the dilbit samples. The fuels that were combined to create the dilbit can explain this distribution.

.

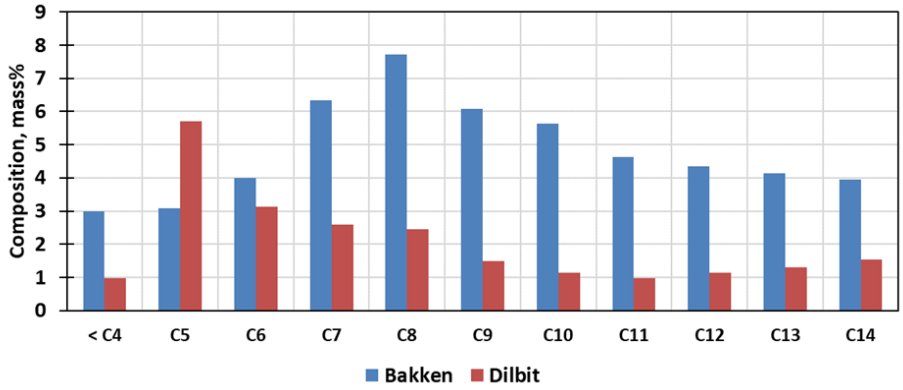

Figure 8-3: Carbon number vs. mass content averaged over the Bakken and dilbit samples (<C15).

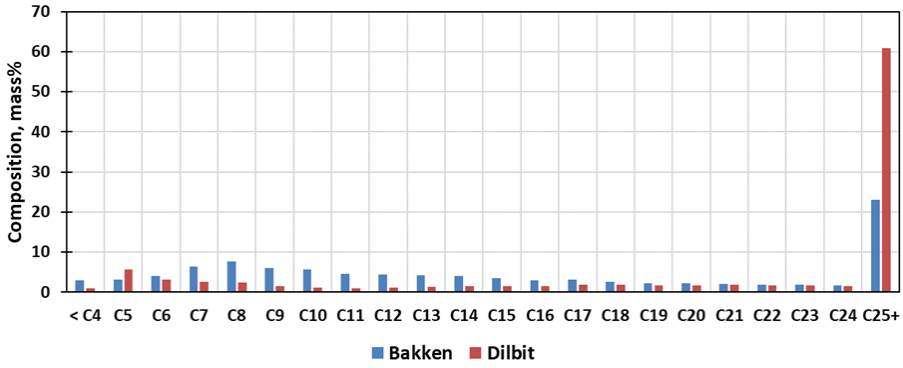

Figure 8-4: Carbon number vs. mass content averaged over the Bakken and dilbit samples.

The dilbit supplier noted that the dilbit was likely a mixture of condensate and bitumen. Figure 8-5 shows the distributions of the dilbit, condensate, and bitumen. The condensate data is from the 12/7/2018 sample converted from a vol% distribution found at the Canada Crude Quality Monitoring Program [5] and bitumen data is from the 2018 sample converted from a boiling point distribution taken as part of the Bitumen Assay Program by the government of Alberta. The condensate shows a clear peak at C5, with gradually decreasing composition as carbon number increases. The bitumen contained very little material up to C8, with gradually increasing compositions at C9 and above. Thus, the diluent in the dilbit caused the spike at C5, while the minimum at C11 can be explained by overlapping diluent and bitumen distributions.

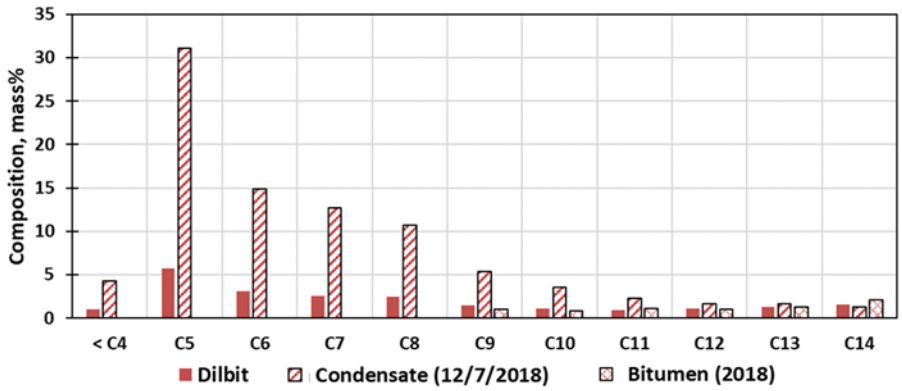

Figure 8-5: Carbon number vs. mass content for the dilbit, condensate, and bitumen.

To determine if the dilbit is a mixture of condensate and bitumen their compositional data was numerically mixed and compared to the loading dilbit sample. A mixture of 20-25 vol% condensate and 75-80 vol% bitumen matches the dilbit composition well. According to members of industry, this type of mixture can be found in the supply chain. The composition of such a mixture (22 vol% condensate, 78 vol% bitumen) is plotted in Figure 8-6 with the dilbit.

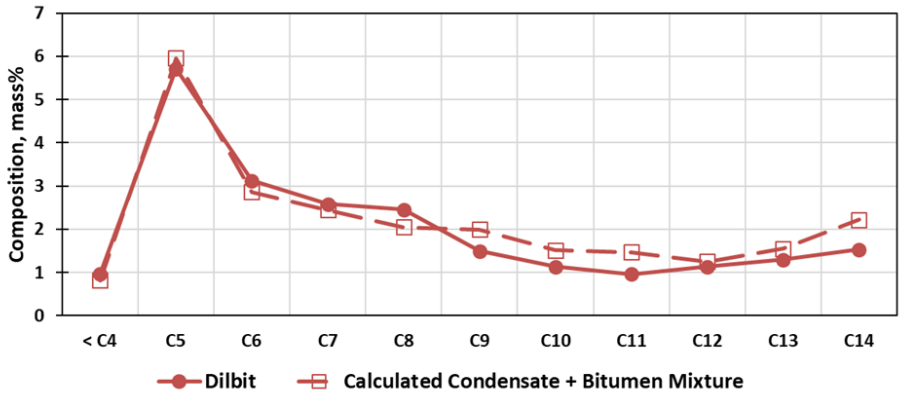

Figure 8-6: Carbon number vs mass content for the dilbit fuel and a simulated mixture of condensate and bitumen.

Figure 8-7 shows temperatures from the fuel thermocouple rake and flame height to illustrate how the temperature within the fuel in conjunction with knowledge of the boiling point distribution impacts the flame height from Test 3.4. This test is illustrated since it reflects the assumptions used to calculate the boiling point distribution curve, namely, not having a constant fuel feed. The thermocouple measurements within the fuel indicate that once all thermocouples reach above 100°C the flame height starts to decrease and then continues to decrease up until about 25 minutes. Once all thermocouple temperatures are above about 350°C the flame height starts to increase again. The boiling point distribution curve indicates that once temperatures surpasses approximately 300°C the slope begins to significantly steepen. Note that it is expected that the timing of fuel temperatures and flame height will not be perfectly synchronized since the dynamics of a fire do not instantaneously respond to changes in burn rate. What can be concluded from this comparison is that fuel temperature, boiling point distribution, and measured data are correlated. This variable behavior of the measurements was observed in all the dilbit crude oil tests.

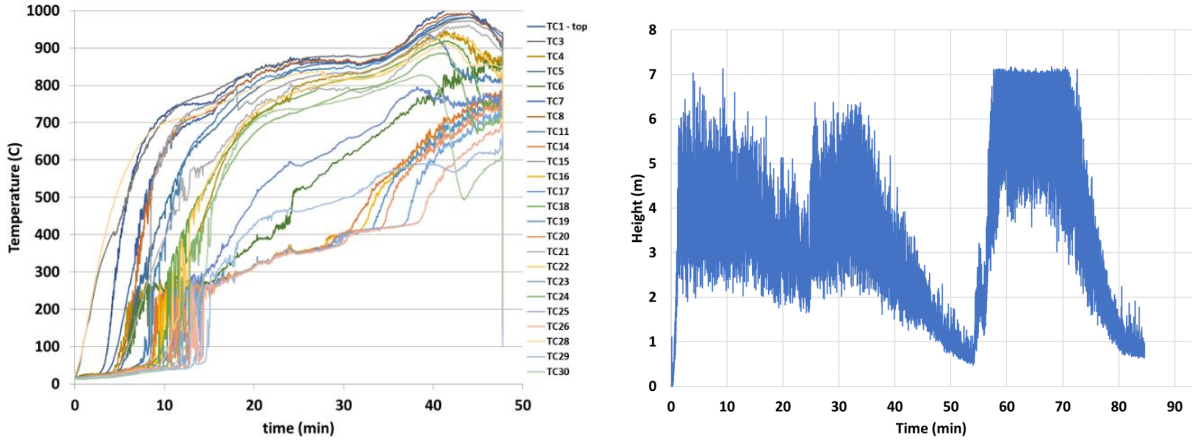

Figure 8-7: Temperatures from the fuel thermocouple rake and flame height for Tests 3.4

The same comparison as shown in Figure 8-7 cannot be provided for the Bakken crude oil because the fuel was immediately ignited once the fuel was introduced into the pan. Thus, the fuel thermocouples were directly engulfed in the flame at the beginning of the test. This approach was used to prevent significant vapors from forming before ignition. Measurements from the Bakken crude oil tests did not display distinct segments of behavior such as those found with the dilbit crude oil, rather an identifiable steady state was reached within about 5 minutes after ignition. Thus, representative averages of the measurements could be determined. This is not true of the dilbit crude oil since measurements constantly changed reflecting the unsteady burn rate.

Another difference between the Bakken and dilbit crude oil is the amount of remaining residue. The post-test residue from the Bakken crude oil was much lower compared to the dilbit crude oil as shown in Figure 8-8 for the non-continuous fuel feed tests. It is difficult to determine if and how the layer of residue affected the burn rate for the dilbit crude oil since the inception and rate of formation is uncertain. Also, the understanding of how a fuel burns through a dynamically forming porous layer is very challenging experimentally and would warrant a separate research investigation.

(a) (b)

Figure 8-8: Post-test residue remaining from the (a) Bakken crude oil and (b) dilbit crude oil for non-continuous fuel feed tests.

8.2. Radiometers

Figure 8-9 provides a comparison of heat flux from the narrow-view radiometers averaged over time and among all locations. The ranges are averages of the standard deviations. These instruments are aimed at points on the flame at various heights. Thus, the average will be affected by flame height. Since the heptane tests resulted in the highest average flame height the average heat flux over all locations is the highest among the fuels tested, followed by the Bakken and then the dilbit, which had the lowest average flame height.

The maximum average heat flux over a steady-state duration occurred with the Bakken crude oil at the lowest measurement location of 0.5 m above the pool with a value of 120 kW/m^2 (Figure 7-6). The highest values measured at this location for heptane and dilbit crude oil were about 95 kW/m^2 (Figure 7-4) and 105 kW/m^2 (Figure 7-8), respectively. The heat flux to the bottom of the calorimeter reflects this trend in which the highest total heat flux occurred with the Bakken crude oil tests followed by the dilbit, then the heptane.

Figure 8-10 provides a comparison of heat flux from the wide-view radiometers averaged over time and among locations. Their field of view is much wider, 150° vs. 5.5°, than the NV radiometers, thus they are receiving signals that encompass regions outside the flame. Due to this, their average is lower than the NV radiometers. Their trend follows that of the NV radiometers with the heptane fuel having the highest average heat flux values and dilbit crude oil the lowest.

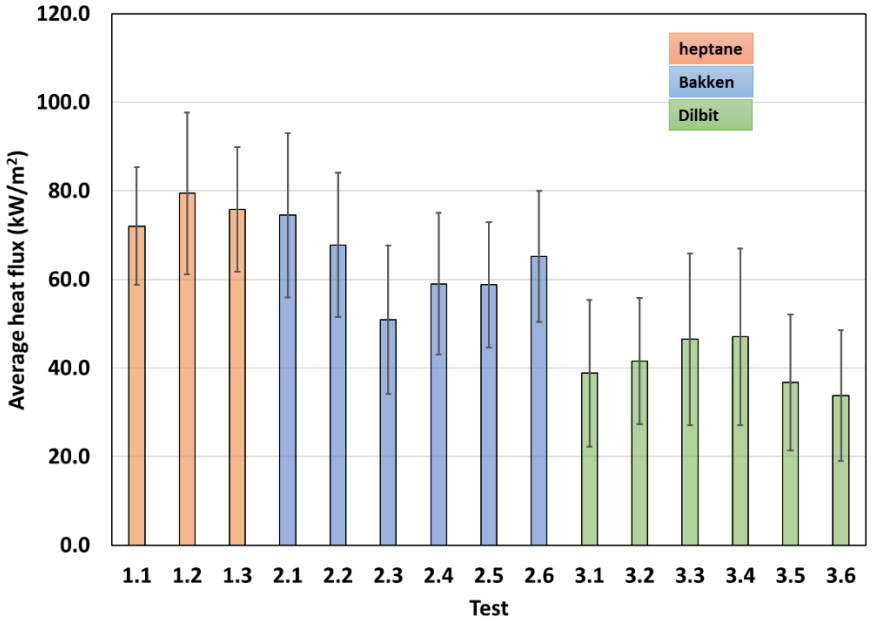

Figure 8-9: Comparison of averaged heat flux from narrow-view radiometers for all fuels tested.

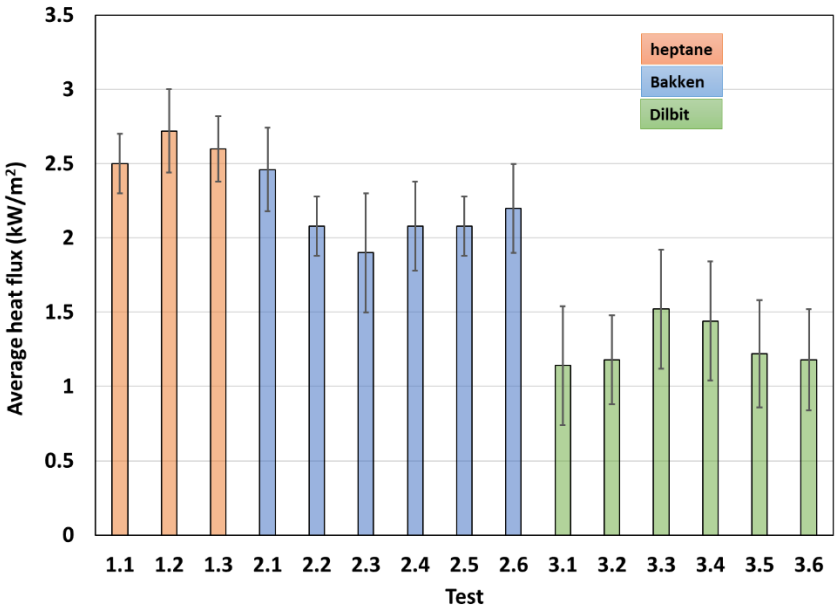

Figure 8-10: Comparison of averaged heat flux from wide-view radiometers for all fuels tested.

8.3. Thermocouple rake in fire plume

Figure 8-11 shows time-averaged temperatures averaged over locations from the centerline TC rake in the fire plume for all fuels. The ranges are average standard deviations. The comparison indicates that the heptane fuel has the highest average, followed by the Bakken crude oil. The dilbit fuel has the lowest average, but indicates large deviations compared to the other fuels. This can be attributed to the time-varying burn rate as explained in section 8.1. Also, note that since only TC locations up to 4 m were included in the averaging due to the lower flame height for the dilbit fuel.

The interesting feature of the thermocouple rake data is that in all the crude oil tests with the calorimeter placed at 1-m the temperatures at the lowest location of 0.5 m were the highest among other locations. Typically for a 2-m pool, these locations will be in a region that is fuel rich, termed the 'vapor dome', which has lower temperatures due to its fuel-rich state. The heptane data does show that the 0.5 m location had a lower temperature among locations up to 3 m and then a higher temperature for locations above 3 m (Figure 7-10), whereas the Bakken and dilbit tests did not have this trend (Figure 7-11 and Figure 7-12, respectively).

A factor that could contribute to this is the difference in burn rate among the fuels. The heptane had an average burn rate about 30% greater than the Bakken crude oil and about 60% greater than the dilbit crude oil. A higher burn rate will increase the height of the fuel-rich region above the pool, thus the height of this region may have been very low for the crude oils. The Bakken test 2.2 with the calorimeter placed at 0.5 m resulted in the lowest temperature occurring at 0.18 m above the pool which reflects the lower height for the vapor dome. The dilbit test 3.2 with the calorimeter placed at 0.5 m resulted in the highest temperature occurring at 0.18 m above the pool which indicates the height of vapor dome is lower than that for heptane and the Bakken crude oil.

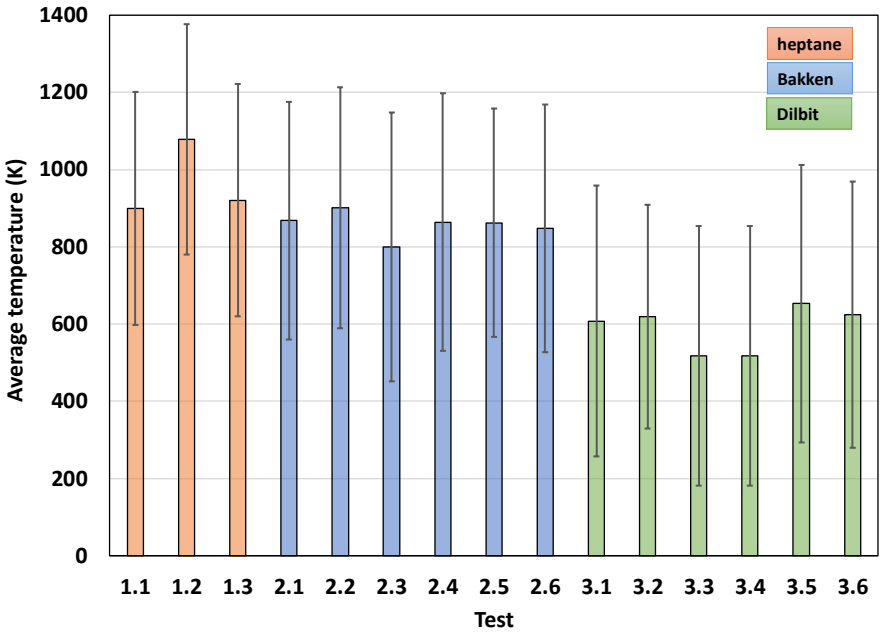

Figure 8-11: Comparison of averaged temperatures from centerline fire plume TC rake for all tests.

8.4. Plume temperatures and surface emissive power

Figure 8-12 and Figure 8-13 show average fire plume temperature and surface emissive power, respectively, for all test series. As noted in section 7.4.3, the average fire plume temperature for test 3.1 is dissimilar to the other dilbit tests due to the inadvertent use of the factory calibration for the camera instead of the in-house calibration which was used for the remaining tests. The comparison indicates that average temperature and surface emissive power do not significantly vary among the fuels. The dominant mode of heat transfer for hydrocarbon pool fires is radiative emission from soot particles. Thus, the surface emissive power will be driven by the emission from the soot particles regardless of fuel composition which can explain the similarity among the fuels. Also, note that the measurements from the narrow-view radiometers are not equivalent to the average surface emissive power measured by the IR camera since the radiometers are focused on an area of about 0.8 m in diameter, whereas the IR camera collected measurements from the entire flame. The vertical profile plots (Figure A-4 through Figure A-16) from the IR camera provided in the Appendix A.3 are higher than the NV radiometer data because the IR camera at these equivalent locations are time-averages at points and not averaged over a 0.8-m diameter area. Thus, the IR camera readings at similar heights as the radiometers will have higher time-averaged values. Also note that the IR camera had an origin 0.3 m higher than all the radiometers, so adjustment is required if compared. Additionally, the plume centerline thermocouple measurements and heat flux to the calorimeter are not equivalent to the measurements presented here because the IR camera is obtaining surface rather than interior measurements.

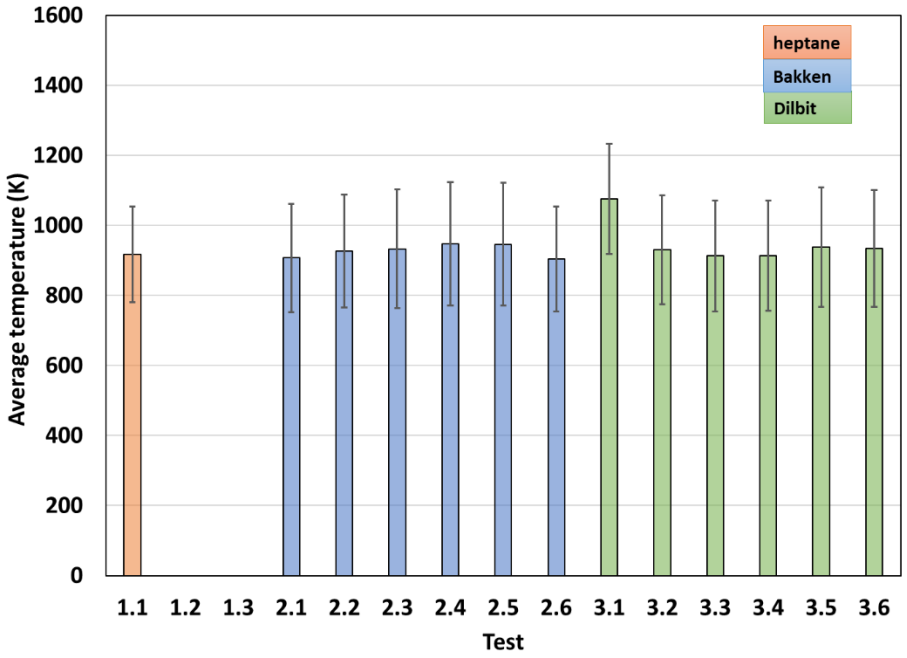

Figure 8-12: Average fire plume temperatures from IR measurements for all tests.

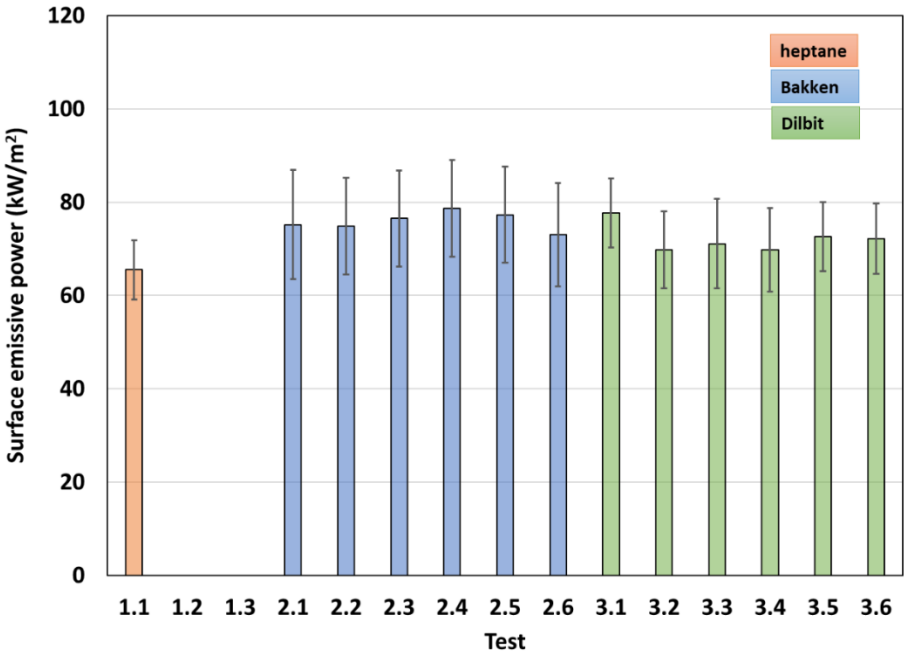

Figure 8-13: Average surface emissive power from IR measurements for all tests.

8.5. DFT heat flux

Figure 8-14 and Figure 8-15 show the average absorbed heat flux from DFT instruments placed at 2 m and 4 m from the center of the pool, respectively, for all tests. Figure 8-16 and Figure 8-17 show the average incident heat flux from DFT instruments placed at 2 m and 4 m from the center of the pool, respectively, for all tests. The comparison indicates that at both locations the highest average absorbed heat flux occurs with the dilbit tests, while the heptane and Bakken tests are similar. The

comparison also indicates that at both locations the lowest average incident heat flux occurs with the dilbit tests overall, while the highest occurs with the Bakken tests. Note that the incident heat flux from the DFT placed at the 2-m location receives a greater percentage of its field of view filled with the fire plume compared to the 4-m location and thus has higher values. The percentage will depend on the flame height and placement of the receiver. Since the dilbit displayed variable burn rates it resulted in variable flame heights which affected the DFT measurements which is indicated by the large deviation compared to the other fuels.

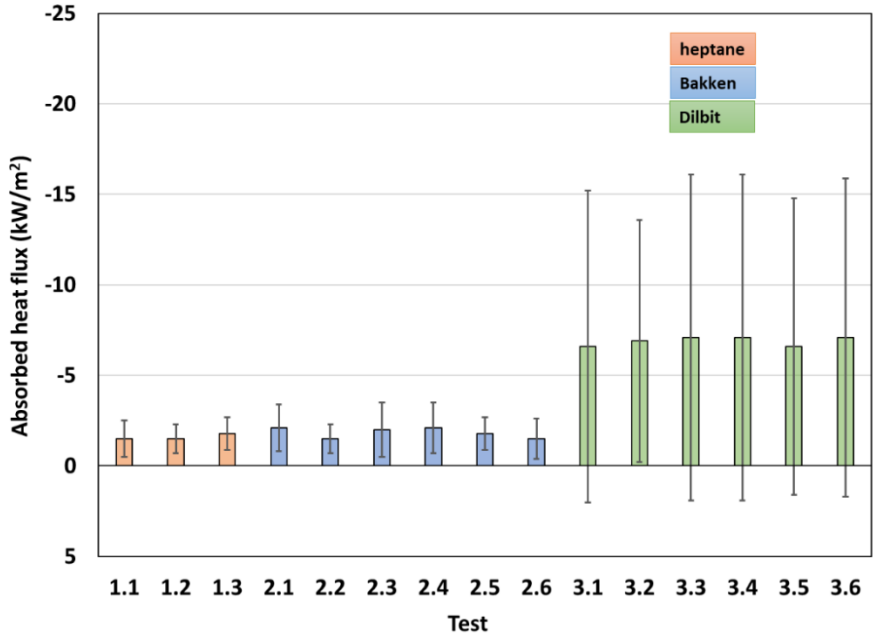

Figure 8-14: DFT average absorbed heat flux at 2 m from center of pool for all tests.

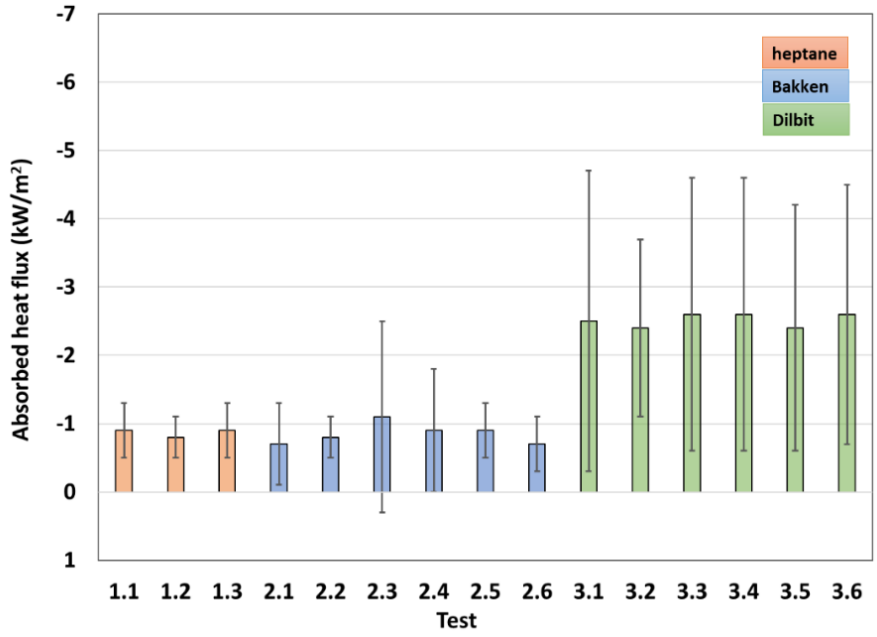

Figure 8-15: DFT average absorbed heat flux at 4 m from center of pool for all tests.

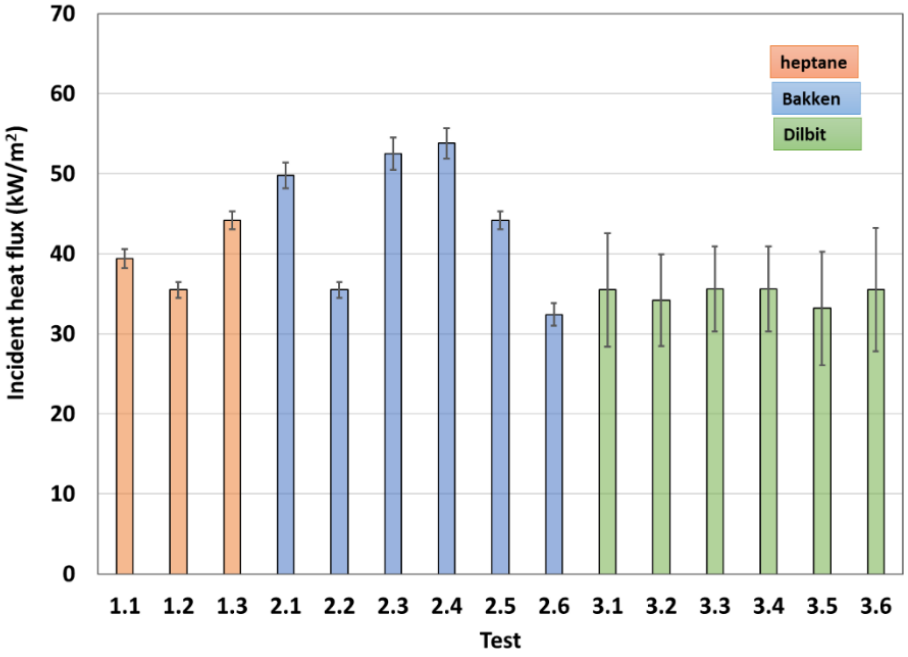

Figure 8-16: DFT average incident heat flux at 2 m from center of pool for all tests.

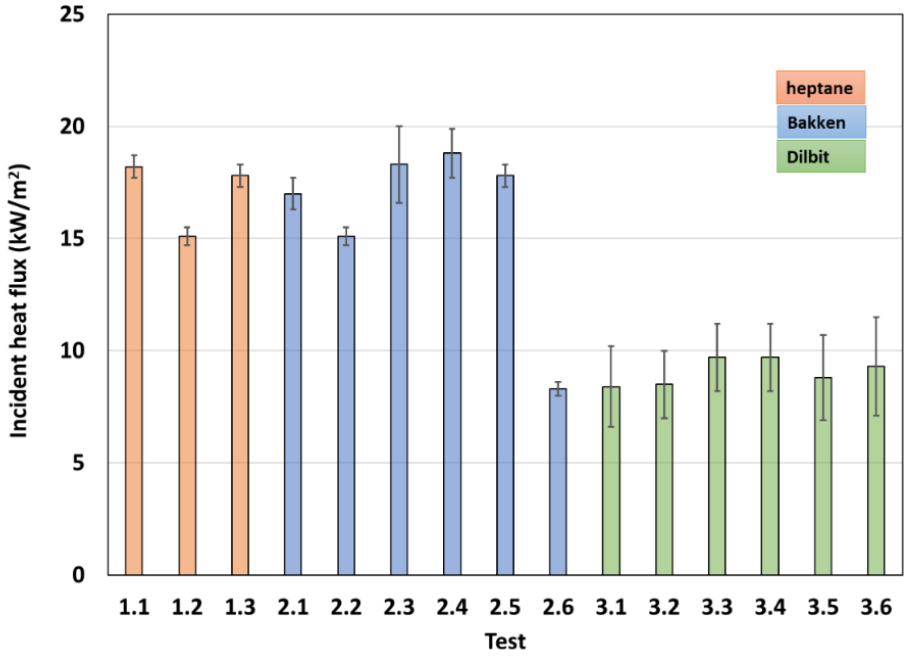

Figure 8-17: DFT average incident heat flux at 4 m from center of pool for all tests.

8.6. Calorimeter TC temperatures and heat flux

Figure 8-18 and Figure 8-19 show temperatures averaged over time and over all locations from thermocouple measurements at the inner surface of the outer cylinder of the calorimeter and for those exterior to the calorimeter for all tests, respectively. The calculated absorbed and total heat flux averaged over time and over all locations is shown in Figure 8-20 and Figure 8-21 for all tests, respectively. Also provided in Figure 8-22 through Figure 8-30 are radar plots of temperature

averaged over time at the left, center, and right planes of the calorimeter for the inner and outer cylinders, as well as those exterior to the calorimeter. Figure 8-31 through Figure 8-33 are radar plots of total heat flux averaged over time at the left, center, and right planes of the calorimeter for the inner and outer cylinders, as well as those exterior to the calorimeter. Note that in some of the temperature plots there are some measurements that seem to be outliers indicating that the thermocouples probably were not providing a reliable reading.

Comparison among the test series indicates that the Bakken tests resulted in the highest outer cylinder and exterior temperatures shown in Figure 8-18 and Figure 8-19, respectively. Similar to other measurements presented for the dilbit crude oil, the calorimeter temperatures reflect much higher variability compared to the heptane and Bakken tests.

The dilbit tests had the highest values of absorbed heat flux among the test series, indicating that the surface temperature is lower for the dilbit tests compared to the heptane and Bakken tests. The radar plots (Figure 8-25 through Figure 8-27) of temperature measurements at the inner surface of the outer cylinder reflect lower temperatures for the dilbit tests compared to the other tests. This indicates that the dilbit tests resulted in lower temperatures at the outer surface of the outer cylinder.

The Bakken tests have the highest average total heat flux by about a factor of 1.5 higher compared to the other fuels. Comparing Figure 8-25 through Figure 8-27, the temperatures at the inner surface of the outer cylinder indicate that the Bakken tests resulted in the highest average temperatures among the fuels, explaining the higher total heat flux.

Radar plots Figure 8-31 through Figure 8-33 indicate that for the heptane tests the total heat flux at the uppermost location (0°) was higher than the lowest locations (180°) which agrees with the trend discussed in section 8.3 for the plume thermocouple rake data where the lowest temperatures occurred beneath the calorimeter. For the Bakken tests the 180° location predominantly has the highest total heat flux among all locations. The exception to this is the Bakken test 2.2 where the calorimeter was placed 0.5 m above the pool instead of 1 m. The highest total heat flux at the 180° location also agrees with the trend discussed in section 8.3 for the plume thermocouple rake data where the highest temperatures occurred beneath the calorimeter except for Test 2.2. The trend of a higher total heat flux at 180° is more strongly seen by the left and right planes which is expected since the upper surface of the calorimeter at these planes was not as persistently engulfed as the center plane due to the periodic contracting behavior of the flame.

The dilbit tests indicate that the 180° location resulted in the highest total heat flux among the locations for all tests. The highest total heat flux at the 180° location also agrees with the trend discussed in section 8.3 for the plume thermocouple rake data where the highest temperatures occurred beneath the calorimeter.

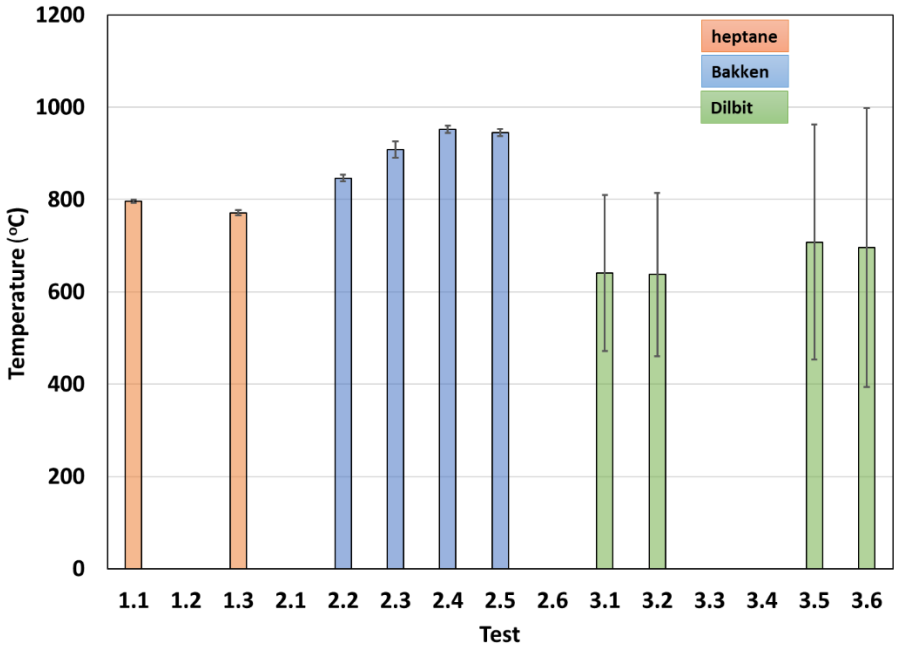

Figure 8-18: Calorimeter outer cylinder temperatures averaged over time and all locations from all tests.

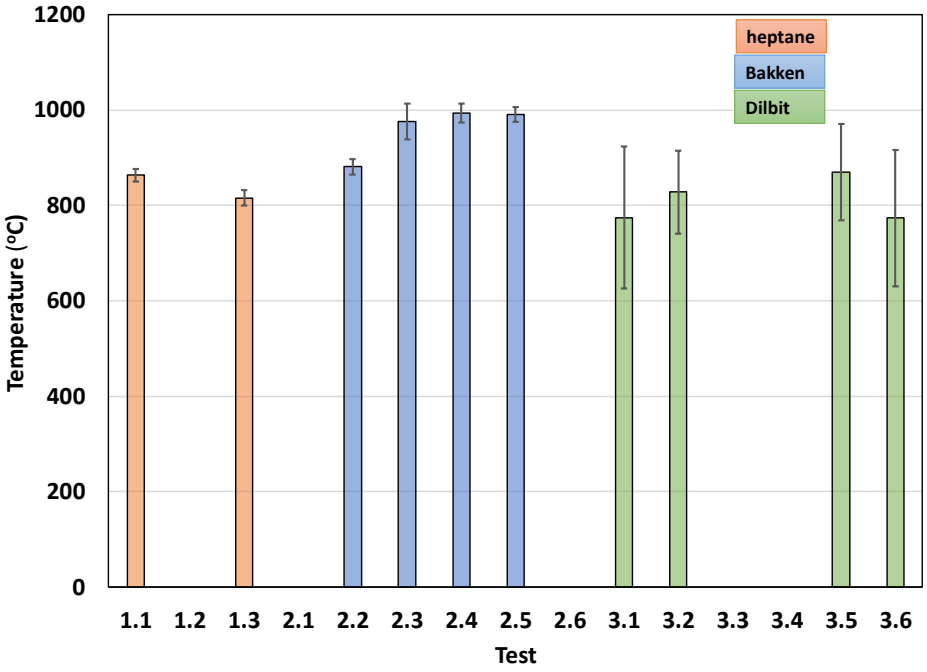

Figure 8-19: Calorimeter exterior temperatures averaged over time and all locations from all tests.

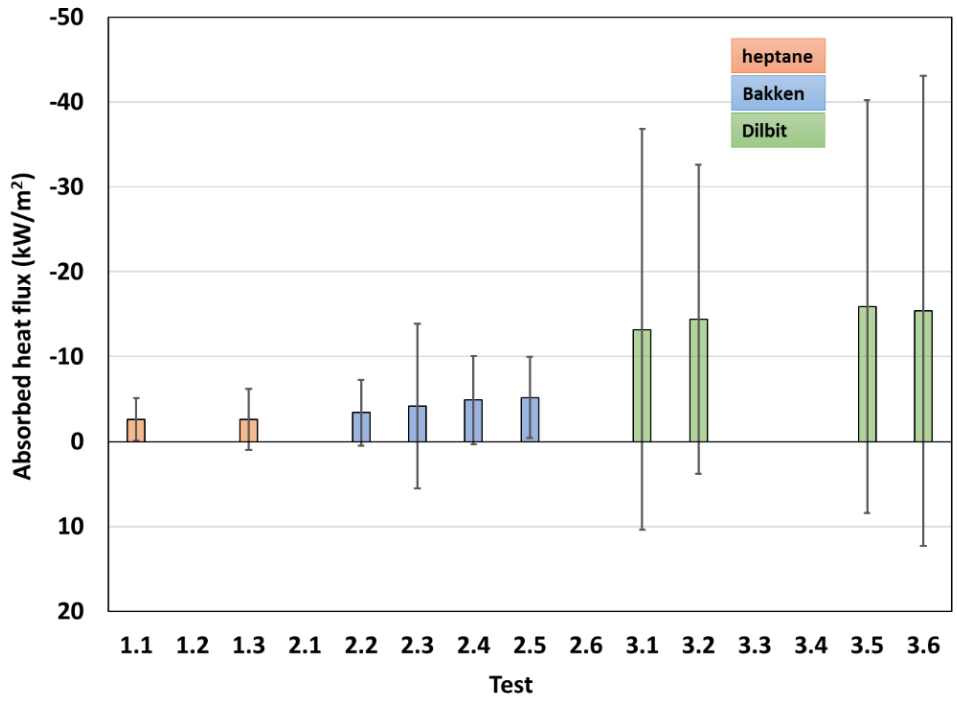

Figure 8-20: Calorimeter absorbed heat flux averaged over time and all locations for all tests.

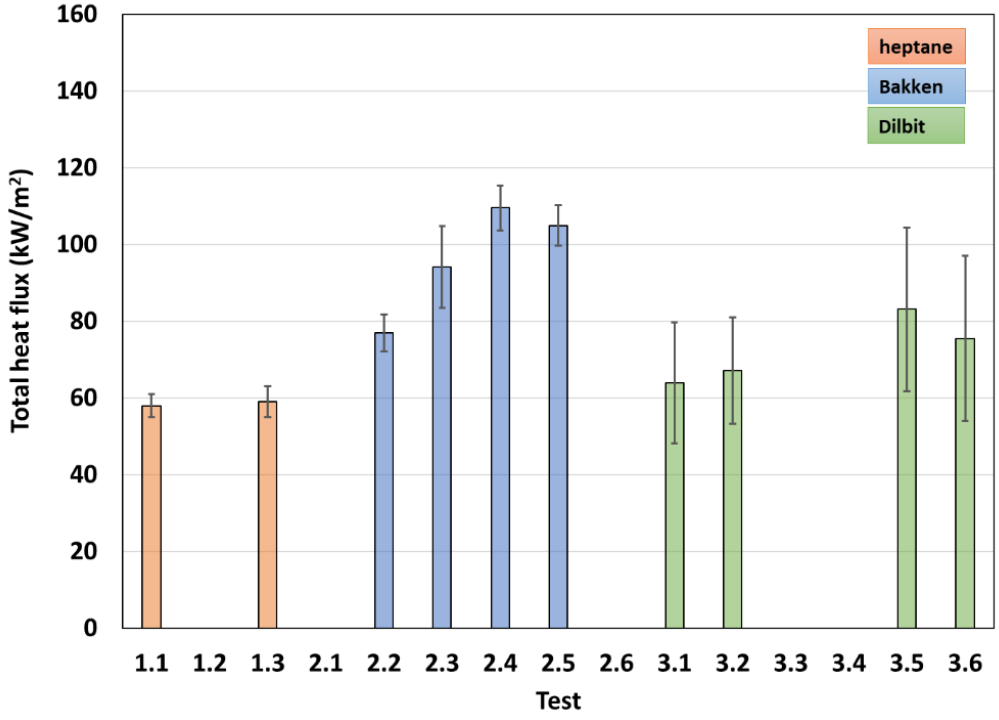

Figure 8-21: Calorimeter total heat flux averaged over time and all locations for all tests.

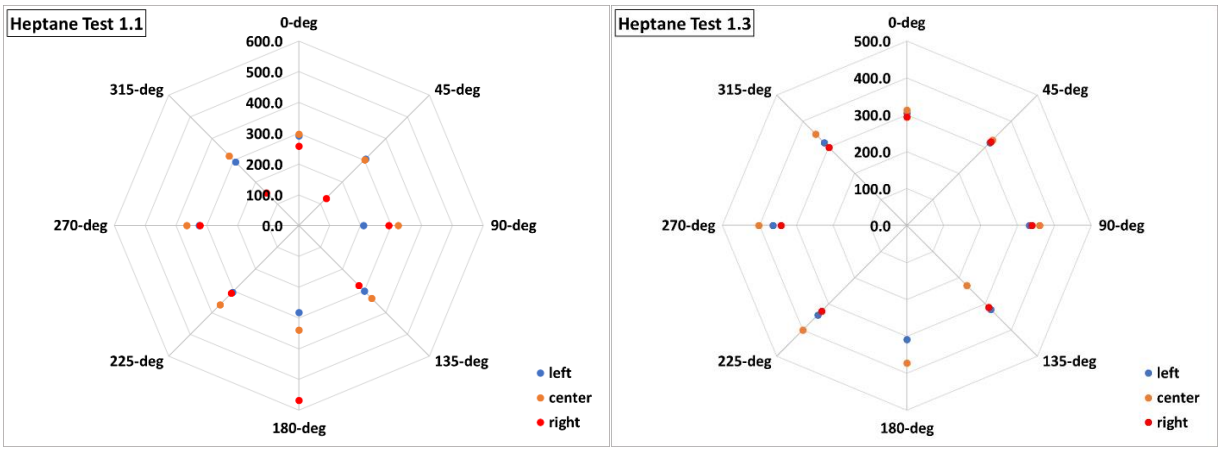

Figure 8-22: Calorimeter average temperatures at left, center, and right stations (inner cylinder) for heptane tests.

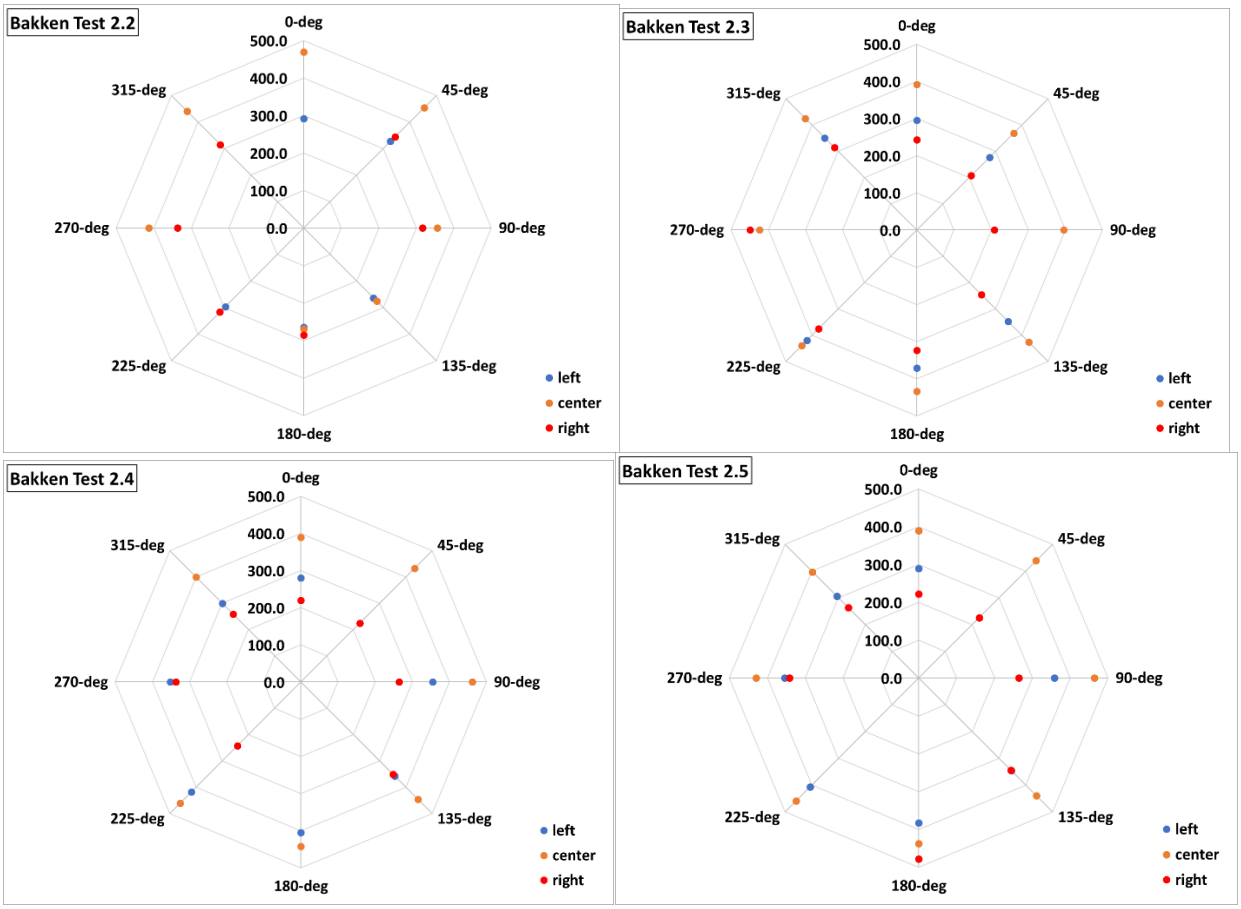

Figure 8-23: Calorimeter average temperatures at left, center, and right stations (inner cylinder) for Bakken tests.

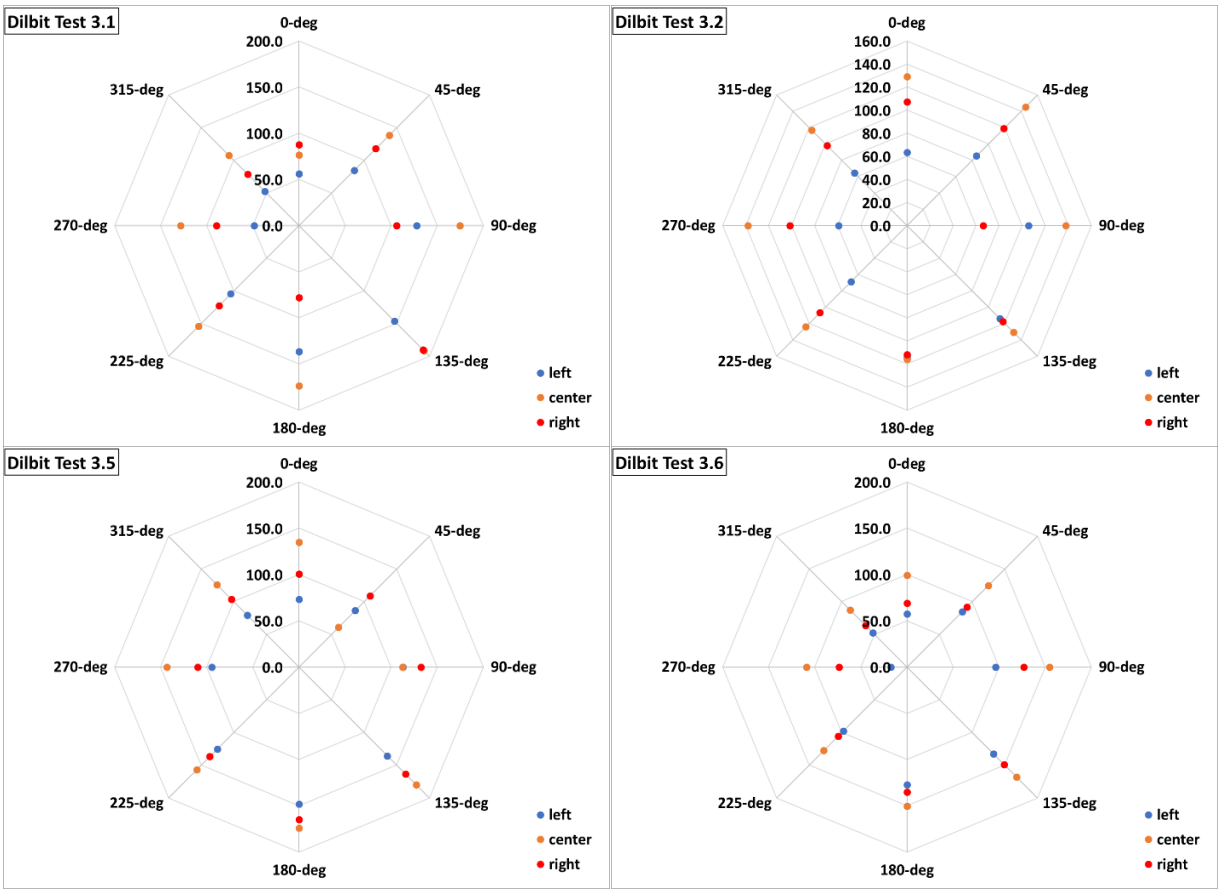

Figure 8-24: Calorimeter average temperatures at left, center, and right stations (inner cylinder) for Dilbit tests.

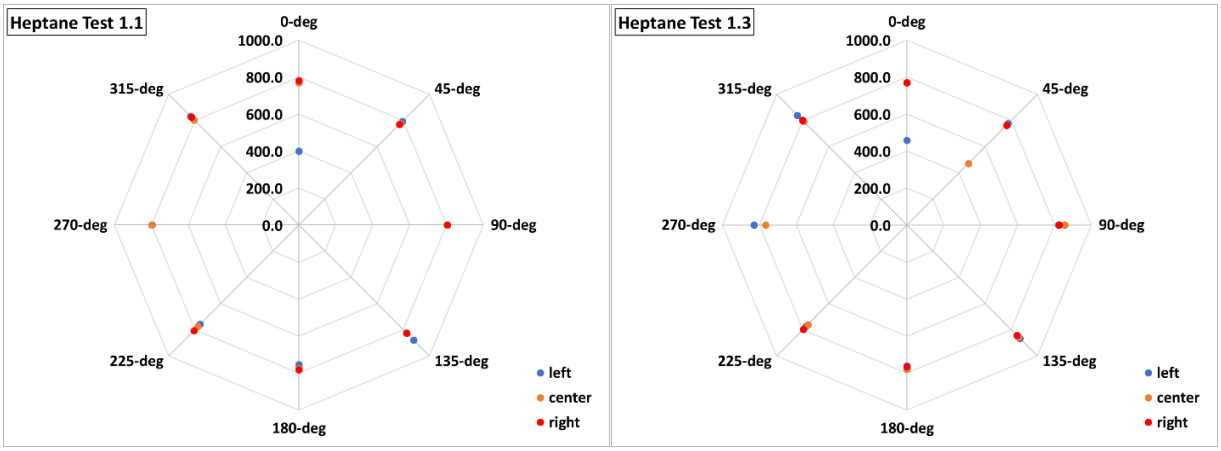

Figure 8-25: Calorimeter average temperatures at left, center, and right stations (outer cylinder) for heptane tests.

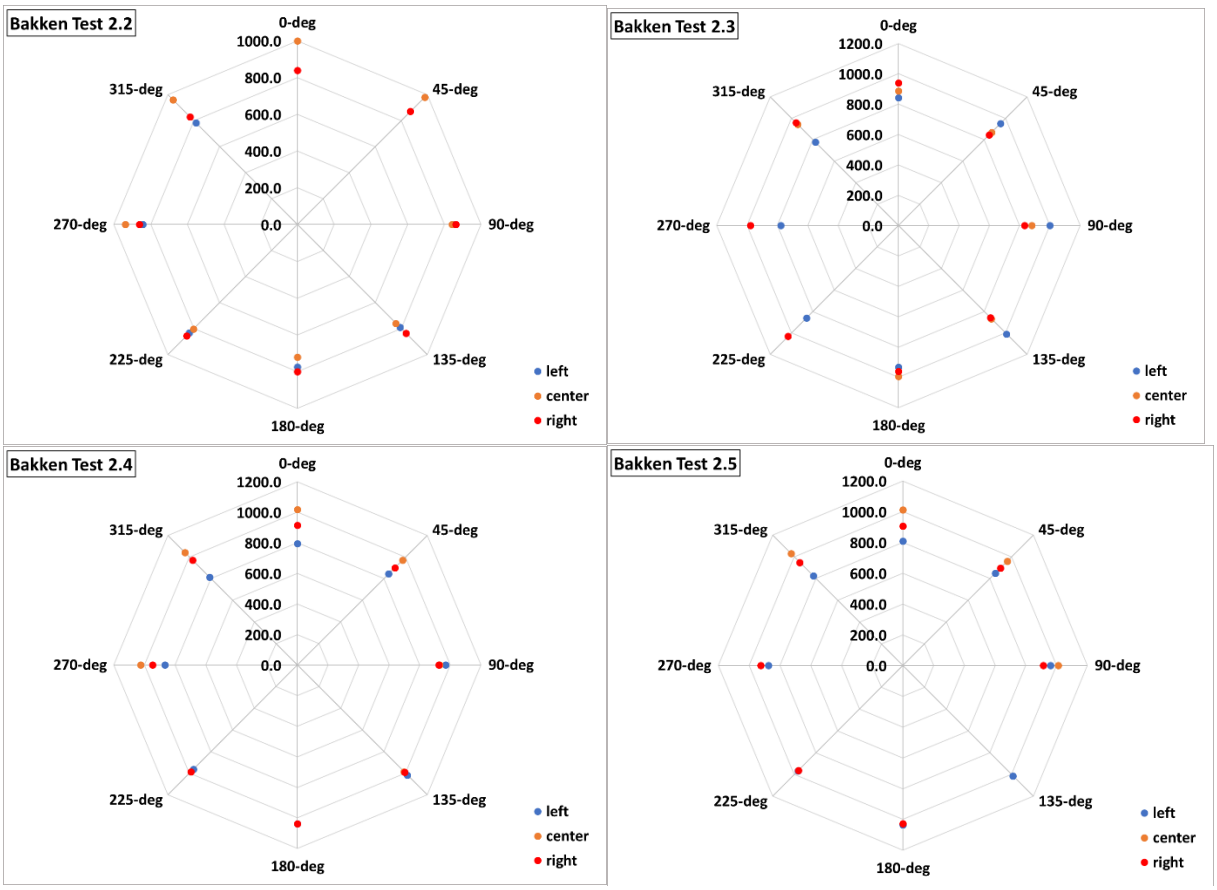

Figure 8-26: Calorimeter average temperatures at left, center, and right stations (outer cylinder) for Bakken tests.

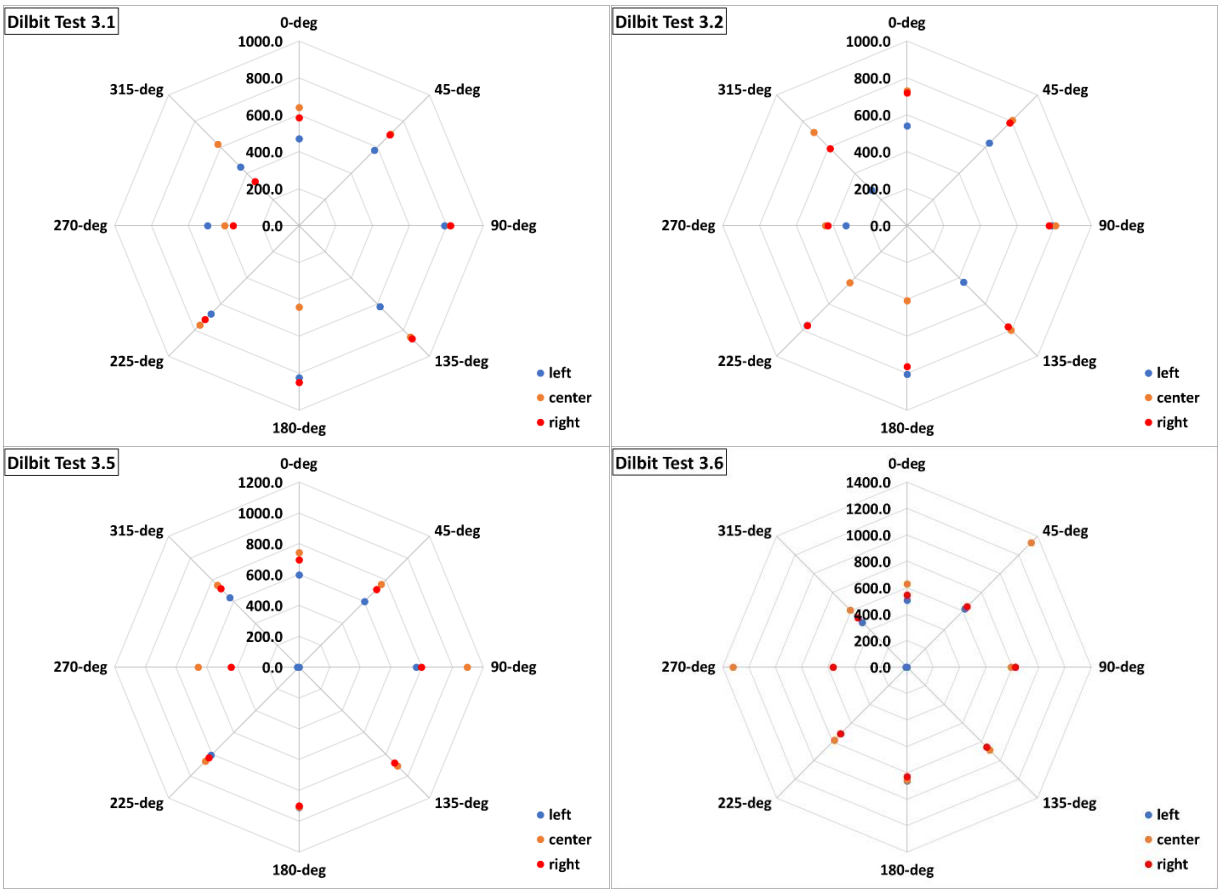

Figure 8-27: Calorimeter average temperatures at left, center, and right stations (outer cylinder) for Dilbit tests.

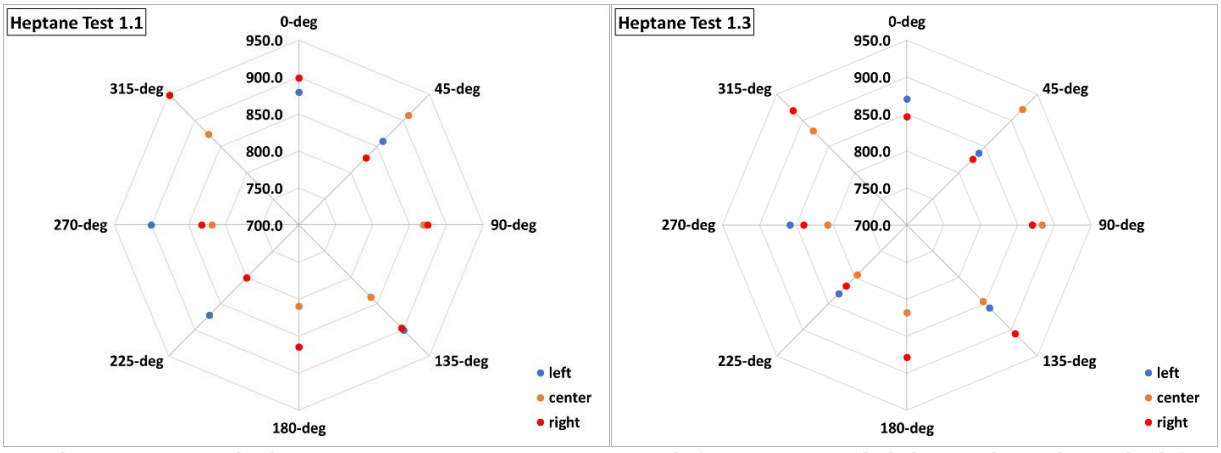

Figure 8-28: Calorimeter average temperatures at left, center, and right stations (exterior) for heptane tests.